VNIVERSITAT DE VALÈNCIA

Facultat de Farmàcia

Departamento de Farmacología

Programa de doctorado en BIOMEDICINA Y FARMACIA

Study on the effects of the adipose tissue-derived mesenchymal stem cell secretome on the innate inflammatory response

Tesis doctoral presentada por:
María del Carmen Carceller Zazo

Directores

Dra. María José Alcaraz Tormo
Dra. María Isabel Guillén Salazar
Dra. María Luisa Ferrándiz Manglano

Valencia, 2018

VNIVERSITAT DE VALÈNCIA

Facultat de Farmàcia -Departament de Farmacologia

Programa de doctorado en BIOMEDICINA Y FARMACIA

Dña. María José Alcaraz Tormo, Catedrática de la Universitat de València, **Dña. María Isabel Guillén Salazar**, Profesora Titular de la Universidad CEU-Cardenal-Herrera y **Dña. María Luisa Ferrándiz Manglano**, Catedrática de la Universitat de València

CERTIFICAN:

Que el trabajo presentado por la Licenciada María del Carmen Carceller Zazo, titulado "Study on the effects of the adipose tissue-derived mesenchymal stem cell secretome on the innate inflammatory response", para obtener el grado de Doctor, ha sido realizado en la Universitat de València en el Departamento de Farmacología, bajo nuestra dirección y asesoramiento.

Concluido el trabajo experimental y bibliográfico, autorizamos la presentación de la Tesis Doctoral, para que sea juzgada por el tribunal correspondiente.

Valencia, julio de 2018

Dra. Mª José Alcaraz Tormo Dra. Mª Isabel Guillén Salazar

Dra. Mª Luisa Ferrándiz Manglano

El presente trabajo se ha llevado a cabo dentro de los proyectos:

- Proyecto SAF2013-4874R concedido por MINECO: "Mecanismos celulares reguladores de la respuesta inflamatoria en patologías inflamatorias crónicas" 2014-2017.

- Proyecto PROMETEOII/2014/071 para grupos de investigación de excelencia, concedido por la Generalitat Valenciana: "Estrategias de protección frente a procesos inflamatorios y degenerativos" 2014-2017.

- Proyecto RETICEF RD12/0043/0013 concedido por el Instituto de Salud Carlos III: "Red de investigación en envejecimiento y fragilidad" 2013-2017.

El trabajo descrito en la presente Tesis se ha llevado a cabo en el Departamento de Farmacología, Facultad de Farmacia, Universidad de Valencia, bajo la dirección de la Dra. María José Alcaraz Tormo, la Dra. María Isabel Guillén Salazar, la Dra. María Luisa Ferrándiz Manglano. Carmen Carceller ha disfrutado de dos becas predoctorales del Subprograma *Atracció de Talent* de VLC-CAMPUS y de Formación de Profesorado Universitario (FPU) (FPU12/04512) otorgada por el Ministerio de Educación, Cultura y Deporte. Además, le fue concedida otra beca para la realización de una estancia breve con referencia EST14/00526 en el laboratorio del Pr. E.C.M. Mariman, bajo la supervisión del Dr. Johan Renes en el *Department of Human Biology NUTRIM School of Nutrition and Translational Research in Metabolism Faculty of Health, Medicine and Life Sciences in Maastricht (The Netherlands).*

Table of Contents

Summary

Adipose tissue-derived mesenchymal stem cells (MSC) have been shown to exert beneficial effects on some inflammatory conditions, which have been mainly related to the secretion of paracrine factors. Therefore, MSC have been investigated as potential therapeutic tools for the treatment of inflammatory and autoimmune diseases. The MSC secretome contains soluble factors and vesicular components known as extracellular vesicles (EV) which play an important role in different physiological processes. In this work, we have investigated the potential of mouse MSC conditioned medium (CM) to modulate the innate inflammatory response as well as the contribution of its components.

Our study has analyzed the effects of MSC and their CM on the *in vivo* innate inflammatory response induced by zymosan in the mouse air pouch model. These results indicate that MSC control the early response and this effect is mainly mediated by the secretome (CM) of these cells. MSC and CM significantly decreased cell migration, degranulation and the production of relevant inflammatory mediators. The effect on cell migration was related to the downregulation of chemoattractants such as LTB_4, MCP-1 and KC. In addition, MSC and CM significantly reduced the levels of pro-inflammatory mediators IL-1β, IL-6 and TNF-α at the early stage of the inflammatory response, which can be the consequence of the inhibition of nuclear factor-κB activation. MSC and CM also decreased the production of PGE_2, which may be dependent on the reduction in mPGES-1 expression.

We have studied and characterised the composition of the CM from MSC which contains soluble factors and EV (exosomes and microvesicles). Proteomic analysis indicated that apyrase is the most abundant protein in CM followed by phosphate-binding protein PstS and phosphate-import protein PhnD. In addition, the presence of chemokines such as KC, MCP-1 and MCP-5 was detected by a chemokine array.

Macrophages form the first line of defence as a component of the innate immune response. They are also the link between the innate and the adaptive response. The regulation of macrophage activation by lipopolysaccharide (LPS) is critical for controlling the initial phases of the immune response. Therefore, we have investigated the *in vitro* effects of CM and its components (soluble fraction and EV) in mouse peritoneal macrophages stimulated with LPS. CM regulates phagocytosis, cell migration and production of relevant inflammatory mediators.

CM and its EV-free fraction significantly reduced the production of IL-1β, TNF-α and NO in macrophages whereas the EV fraction was effective to a lower extent. We have also shown that apyrase may partly contribute to the anti-inflammatory effects of the soluble fraction while chemokines such as KC, MCP-1 and MCP-5 may be involved in the migration of neutrophils and monocytes observed in co-culture experiments with macrophages. Our data indicate that the soluble fraction plays a more important role than EV in mediating the anti-inflammatory effects of CM in mouse peritoneal macrophages.

Activation of macrophages by LPS involves the TLR4 which drives pro-inflammatory signalling. We have shown that the anti-inflammatory activity of CM in this *in vitro* model may be related, at least in part, to the downregulation of TLR4 expression leading to the reduction of TLR4 signalling.

Resum

S'ha demostrat que les cèl·lules mare mesenquimals derivades del teixit adipós (MSC) tenen efectes beneficiosos en algunes condicions inflamatòries, que s'han relacionat principalment amb la secreció de factors paracrins. Per tant, s'han investigat les MSC com a una poderosa eina terapèutica per al tractament de malalties inflamatòries i autoimmunitàries. El secretoma de les MSC conté factors solubles i components vesiculars coneguts com vesícules extracel·lulars (EV) que tenen un paper important en diferents processos fisiològics. En aquest treball, hem investigat el potencial del medi condicionat de les MSC de ratolí (CM) per modular la resposta inflamatòria innata, així com la contribució dels seus components.

En el nostre estudi hem analitzat els efectes de les MSC i el seu CM sobre la resposta inflamatòria innata *in vivo* induïda pel zimosan en el model de la bossa d'aire en ratolí. Aquests resultats indiquen que les MSC controlen la resposta primerenca i aquest efecte està principalment mediat pel secretoma (CM) d'aquestes cèl·lules. MSC i CM van disminuir significativament la migració cel·lular, la degranulació i la producció de mediadors inflamatoris rellevants. L'efecte sobre la migració cel·lular es va relacionar amb la reducció dels quimioattraients com LTB_4, MCP-1 i KC. A més, MSC i CM van reduir significativament els nivells de mediadors proinflamatoris IL-1β, IL-6 i TNF-α en la fase inicial de la resposta inflamatòria, que pot ser la conseqüència de la inhibició de l'activació del factor nuclear κB. MSC i CM també van reduir la producció de PGE_2, que pot dependre de la reducció de l'expressió de mPGES-1.

Hem estudiat i caracteritzat la composició del CM de les MSC que conté factors solubles i EV (exosomes i microvesícules). L'anàlisi proteòmic va indicar que l'apirasa és la proteïna més abundant en el CM, seguida de la proteïna PstS d'unió de fosfat i la proteïna PhnD d'importació de fosfat. A més, la presència de quimiocines com KC, MCP-1 i MCP-5 va ser detectada per un *array* de quimiocines.

Els macròfags formen la primera línia de defensa com a component de la resposta immune innata. També són el vincle entre la resposta innata i l'adaptació. La regulació de l'activació de macròfags per lipopolisacàrid (LPS) és fonamental per controlar les fases inicials de la resposta immune. Per tant, hem investigat els efectes *in vitro* del CM i els seus components (fracció soluble i EV) en macròfags peritoneals de ratolí estimulats amb LPS. CM regula la fagocitosi, la migració cel·lular i la producció de mediadors inflamatoris rellevants.

CM i la seua fracció sense EV van reduir significativament la producció de IL-1β, TNF-α i NO en macròfags, mentre que la fracció EV va ser efectiva en menor mesura. També hem demostrat que l'apirasa pot contribuir en part als efectes antiinflamatoris de la fracció soluble, mentre que les quimiocines com KC, MCP-1 i MCP-5 poden estar implicades en la migració de neutròfils i monòcits observats en experiments de cocultiu amb macròfags. Les nostres dades indiquen que la fracció soluble té un paper més important que les EV en la mediació dels efectes antiinflamatoris del CM en els macròfags peritoneals de ratolí.

TLR4 està implicat en l'activació dels macròfags per LPS, promovent la senyalització proinflamatòria Hem demostrat que l'activitat antiinflamatòria del CM en aquest model *in vitro* pot estar relacionada, almenys en part, amb la disminució de l'expressió TLR4 que condueix a la reducció de la senyalització TLR4.

Resumen

Se ha demostrado que las células madre mesenquimales derivadas de tejido adiposo (MSC) ejercen efectos beneficiosos sobre algunas afecciones inflamatorias, que se han relacionado principalmente con la secreción de factores paracrinos. Por lo tanto, se han investigado las MSC como posibles herramientas terapéuticas para el tratamiento de enfermedades inflamatorias y autoinmunes. El secretoma de las MSC contiene factores solubles y componentes vesiculares conocidos como vesículas extracelulares (EV) que juegan un papel importante en diferentes procesos fisiológicos. En este trabajo, hemos investigado el potencial del medio acondicionado (CM) de ratón de las MSC para modular la respuesta inflamatoria innata, así como la contribución de sus componentes.

Nuestro estudio ha analizado los efectos de las MSC y su CM en la respuesta inflamatoria innata *in vivo* inducida por zimosán en el modelo de bolsa de aire en ratón. Estos resultados indican que las MSC controlan la respuesta temprana y este efecto está mediado principalmente por el secretoma (CM) de estas células. Las MSC y su CM disminuyeron significativamente la migración celular, la desgranulación y la producción de mediadores inflamatorios relevantes. El efecto sobre la migración celular se relacionó con reducción de quimioatrayentes tales como LTB_4, MCP-1 y KC. Además, las MSC y su CM redujeron significativamente los niveles de mediadores proinflamatorios IL-1β, IL-6 y TNF-α en la etapa temprana de la respuesta inflamatoria, que puede ser la consecuencia de la inhibición de la activación del factor nuclear κB. Las MSC y su CM también disminuyeron la producción de PGE_2, que puede depender de la reducción en la expresión de mPGES-1.

Hemos estudiado y caracterizado la composición del CM de las MSC que contiene factores solubles y EV (exosomas y microvesículas). El análisis proteómico indicó que la apirasa es la proteína más abundante en el CM seguida por la proteína de unión a fosfato PstS y la proteína de importación de fosfato PhnD. Además, la presencia de

quimiocinas como KC, MCP-1 y MCP-5 fue detectada por un *array* de quimiocinas.

Los macrófagos forman la primera línea de defensa como un componente de la respuesta inmune innata. También son el vínculo entre la respuesta innata y la respuesta adaptativa. La regulación de la activación de macrófagos por lipopolisacárido (LPS) es crítica para controlar las fases iniciales de la respuesta inmune. Por lo tanto, hemos investigado los efectos *in vitro* del CM y sus componentes (fracción soluble y EV) en macrófagos peritoneales de ratón estimulados con LPS. El CM regula la fagocitosis, la migración celular y la producción de mediadores inflamatorios relevantes.

El CM y su fracción libre de EV redujeron significativamente la producción de IL-1β, TNF-α y NO en macrófagos, mientras que la fracción EV fue efectiva en menor medida. También hemos demostrado que la apirasa puede contribuir en parte a los efectos antiinflamatorios de la fracción soluble, mientras que las quimioquinas como KC, MCP-1 y MCP-5 pueden estar involucradas en la migración de neutrófilos y monocitos observados en experimentos de cocultivo con macrófagos. Nuestros datos indican que la fracción soluble juega un papel más importante que las EV en la mediación de los efectos antiinflamatorios de CM en los macrófagos peritoneales de ratón.

TLR4 está implicado en la activación de los macrófagos por LPS, promoviendo la señalización proinflamatoria. Hemos demostrado que la actividad antiinflamatoria del CM en este modelo *in vitro* puede estar relacionada, al menos en parte, con la disminución de la expresión de TLR4 que conduce a la reducción de la señalización de TLR4.

Abbreviations

ABC	Ammonium bicarbonate
ACN	Acetonitrile
APC	Allophycocyanin
ADP	Adenosine diphosphate
AMP	Adenosine monophosphate
bFGF	Basic fibroblast growth factor
BSA	Bovine serum albumin
CCL	C-C motif chemokine ligand
CD	Cluster of differentiation
CPGES	Cytosolic prostaglandin E synthase
CM	Conditioned medium
CoPP	Cobalt protoporphyrin
COX-2	Cyclooxygenase-2
CTACK	Cutaneous T cell-atracting chemokine
CXCL	C-X-C motif chemokine ligand
DAMP	Damage-associated molecular pattern
DMEM	Dulbecco's modified Eagle's medium
DNA	Deoxyribonucleic acid
EDTA	Ethylenediaminetetraacetic acid
EGF	Epidermal growth factor
ELISA	Enzyme Linked Immuno Sorbent Assay
EV	Extracellular vesicles
Ex	Exosomes
FA	Formic Acid
FBS	Fetal bovine serum
FGF	Fibroblast growth factor
FITC	Fluorescein isothiocyanate
GCP	Granulocyte chemotactic protein
G-CSF	Granulocyte colony-stimulating factor
GM-CSF	Granulocyte macrophage colony-stimulating factor
GPCR	G protein-coupled receptor
HGF	Hepatocyte growth factor
HLA	Human leucocyte antigen
HOCl	Hypochlorous acid
HO-1	Heme oxygenase-1
IFN-γ	Interferon-*γ*
IGF-1	Insulin-like growth factor-1
IgG	Immunoglobulin G
IL	Interleukin
ILV	Intra-luminal vesicles

ISCT	International Society of Cellular Therapy
KC	Keratinoyte chemoattractant
KGF	Keratinocyte growth factor
LC-MS/MS	Liquid chromatography and tandem mass spectrometry
LTB_4	Leukotriene B_4
LPS	Lipopolysaccharide
MAP	Mouse air pouch
MAPK	Mitogen-activated protein kinases
MCP-1	Monocyte chemoattractant protein-1
MDC	Macrophage-derived chemokine
MHC	Major histocompatibility complex
MIG	Monokine induced by IFN-γ
MIP-2α	Macrophage inflammatory protein-2α
mPGES-1	Microsomal prostaglandin E_2 synthase-1
MPO	Mieloperoxydase
MSC	Mesenchymal stem cells
MTT	3-(4,5-dimethylthiazol-2-yl)-2,5 diphenyltetrazolium bromide
Mv	Microvesicles
MVB	Multi-vesicular bodies
NF-κB	Nuclear factor kappa-light-chain-enhancer of activated B cells
NGF	Nerve growth factor
NK	Natural killer
NO	Nitric oxide
P	Passage
PAI	Plasminogen activator inhibitor
PBS	Phosphate-buffered saline
PE	Phycoerythrin
PerCP	Peridinin-Chlorophyll protein
PF-4	Platelet factor-4
PGE_2	Prostaglandin E_2
PMN	Polymorphonuclear leukocytes
RANTES	Regulated upon activation normal T cell expressed and secreted
RIA	Radioimmunoassay
RNA	Ribonucleic acid
RPMI	Roswell Park Memorial Institute
SDF-1	Stromal cell-derived factor-1

SGBS	Simpson-Golabi-Behmel syndrome
TARC	Thymus and activation regulated chemokine
TECK	Thymus-expressed chemokine
TLR	Toll-like receptor
TNF-α	Tumor necrosis factor-α
TCA	Trichloroacetic acid
TFA	Trifluoroacetic acid
TGF-β	Transforming growth factor-β
Th1	T helper 1
Th2	T helper 2
Th17	T helper 17
TRPS	Tunable resistive pulse sensing
TSG-6	Tumor necrosis factor-inducible gene 6 protein
VEGF	Vascular endothelial growth factor

Introduction

1. Innate immunity

Innate immunity has a critical role in overall immunity, as the body's first line of defence against infection or tissue damage. It comes into play immediately or within hours and was firstly called non-specific immunity, as it was believed that the involved mechanisms were non-specific. Innate immunity was considered as a separate entity from the adaptive immunity. However, years later, it has been shown that the innate immune response shows a higher degree of specificity, recognising common conserved antigens expressed by pathogens or injured tissues (Akira *et al.,* 2006; Elliott *et al.,* 2014) and can discriminate between pathogens and self-tissues. Furthermore, the adaptive immune response (antigen-specific) is induced via the production of different regulatory mediators by the innate response. One of the most significant regulatory mechanisms is the self-limited inflammatory reaction. Initial or acute inflammation has a protective role since it amplifies the innate immune response and leads to a correct specific response. Stimuli induce activation of innate and/or adaptive immune cells to destroy foreign elements and injured tissue while simultaneously induce factors leading to resolution (**Figure 1**). However, when the mechanisms that control the resolution of acute inflammation fail, there is an excess of or inappropriate inflammatory response such as that which occurs during sepsis, autoimmune or chronic degenerative diseases (Khatami, 2008). The innate immune response is a multifactorial mechanism involving cells and molecules with functions and relationships not well understood.

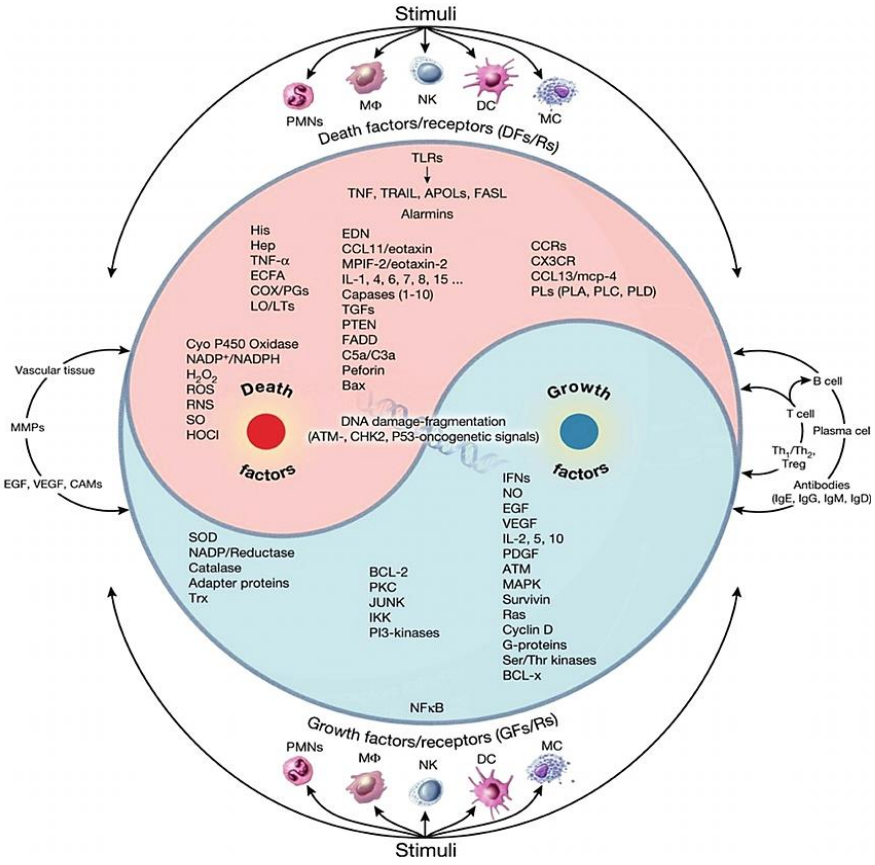

Figure 1. Graphic representation of 'yin' and 'yang' arms of acute inflammation. Activation of innate and/or adaptive immune cells is needed to destroy foreign elements and injured tissue while simultaneously pro-resolving mechanisms are induced (Khatami, 2008).

1.1. Inflammatory cells

1.1.1. Neutrophils

Granulocyte is the most abundant type of leukocytes, playing a pivotal role in the initial phase of the innate immune response as the first line of defence against pathogen invasion. There are three main granulocyte subsets including neutrophils, eosinophils and basophils, but the most dominant population are the neutrophils. During the acute inflammatory response, neutrophils are the first cells that come to the site of the problem responding to inflammatory cytokines and chemotactic agents produced by activated macrophages. Neutrophils come from the bloodstream in large waves as their functions are phagocytosis and death. However, most of the inflammatory effects produced by neutrophils are due to the release of intracellular granules content by a process called degranulation. The proteins contained in these granules have a microbicidal activity. These enzymes are contained in two types of granules inside the neutrophils: primary or azurophilic and secondary or specific granules. The first ones contain proteolytic enzymes, myeloperoxidase (MPO) among others, whereas the secondary granules contain lysozyme and collagenase (Schettler *et al*., 1991). Thus, MPO activity reflects leukocyte degranulation and is the most abundant pro-inflammatory enzyme stored in the primary granules of neutrophils (Schultz and Kaminker, 1962). The microbicidal activity of this peroxidase enzyme consists of an enzymatic reaction of hydrogen peroxide (H_2O_2) and Cl^- ions generating hypochlorous acid (HOCl) and other highly reactive species (Birben *et al.,* 2012; Heinecke*,* 1999) (**Figure 2**). HOCl is thought to be the most potent oxidant produced by neutrophils, modifying some cell components such as amino acids and lipids, leading to membrane destabilisation (Birben *et al.,* 2012; Hawkins and Davies*,* 1998a; Hawkins and Davies*,* 1998b).

Figure 2. Myeloperoxidase reaction

Besides their phagocytic functionality, neutrophils also act as antigen-presenting cells under pathological or inflammatory conditions, orchestrating adaptive immunity, since they can acquire surface expression of major histocompatibility complex (MHC) class II and costimulatory molecules as well as T cell stimulatory behaviour when cultured with selected cytokines (reviewed by Takashima and Yao, 2015). **Figure 3** shows defined steps in the acute inflammation time course: oedema, neutrophil infiltration, and then non-phlogistic monocyte/macrophage recruitment to inflammatory exudates. The reduction in neutrophil number coincides with the appearance of pro-resolving mediators such as lipoxins, resolvins, protectins and maresins.

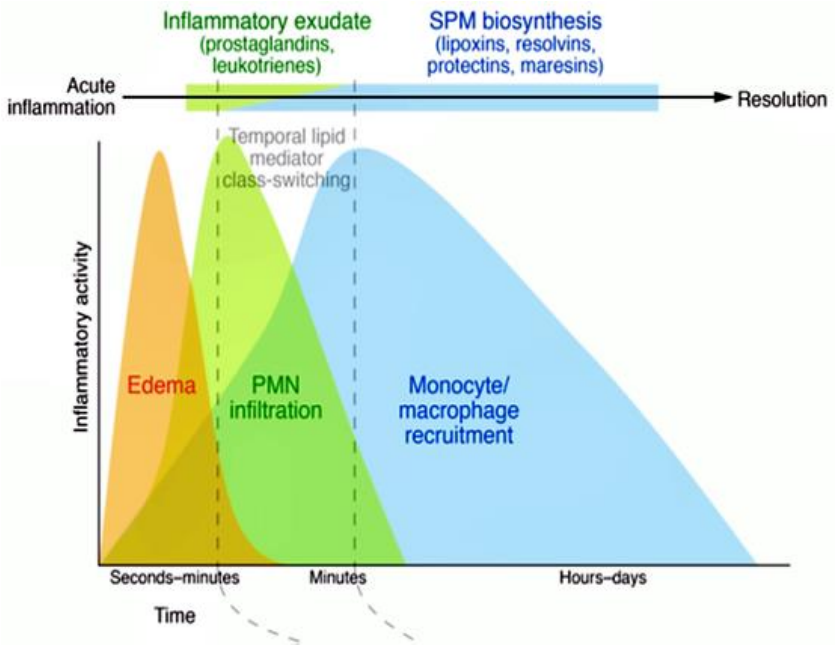

Figure 3. Innate cellular response. PMN: polimormonuclear leukocytes. SPM: specialized pro-resolving mediators. (Serhan and Levy, 2018).

1.1.2. Monocytes and macrophages

Monocytes represent 4% in mice and 10% in humans of the nucleated cells in the blood. There are also monocytes in the spleen and lungs that can be mobilised on demand (Swirski *et al*., 2009). During inflammation, there is a rapid tissue coating of monocytes to sites of injury, where they can differentiate into mononuclear phagocytes, macrophages and dendritic cells. However, most of the tissue macrophages do not derive from monocytes, but from embryonic precursors that maintain themselves in adults by self-renewal (Sheng *et al*., 2015). In addition, monocytes/macrophages are highly heterogenic cells with the ability to differentiate into an inflammatory or anti-inflammatory cell.

Macrophages were first discovered by Metchnikoff that described them as large phagocytic cells (reviewed by Arango Duque and Descoteaux, 2014). Macrophages are sentries of the immune system that mediate the transition from innate to adaptive immunity. They are in different tissues, and their primary function is to remove by phagocytosis foreign agents that enter the organism. Besides, they remove apoptotic cells and recycle nutrients by digesting waste products from tissues. Thus, they are essential for tissue homeostasis (Huber and Stingl, 1981). Macrophages also play a central role in inflammation. They are some of the first cells that interact with the foreign agents, initiating the immune response against these invaders. This process is due in part to the recognition of a part of the foreign agents through their toll-like and scavenger receptors, which have a broad ligand specificity for lipoproteins, lectins, proteins, oligonucleotides, polysaccharides, etc. They also express MHC class II in the membrane, thereby activating $CD4^+$ T lymphocytes. These lymphocytes release cytokines that activate B cells to produce antibodies that neutralise and assist in the destruction of the problem. Therefore, macrophages are cells that can also trigger the specific immune response.

Monocytes and tissue-resident macrophages recognise pathogen-associated molecular patterns (PAMP) through receptor binding (pattern recognition receptors (PRR)) (Akira *et al*., 2006; Bianchi, 2007). After the activation of PRRs, such as Toll-like receptors (TLR) (Kawai and Akira, 2010), inflammatory cytokines and lipid mediators are generated to provide essential signals for the recruitment of cells collaborating in the control of pathogens. The lipopolysaccharide of Gram-negative bacteria (LPS) is a classic PAMP widely studied in relation to macrophages. When this endotoxin is released, it binds to the LBP (LPS binding protein). Thus, the LPS / LBP complex binds to the surface PRR of macrophage, CD14. This LPS-binding protein is anchored to the cell surface by linkage to glycosylphosphatidylinositol (GPI) that lacks the cytoplasmic portion. It is known that TLR4 recognises LPS and transduces intracellular

signals to activate transcription factors, such as nuclear factor kappa-light-chain-enhancer of activated B cells (NF-κB) and mitogen-activated protein kinases (MAPK), which leads to the production of different inflammatory mediators (in particular, cytokines and chemokines (Prince *et al*., 2011)). A similar mechanism proceeds in the presence of damaged or dead cells which give rise to damage-associated molecular patterns (DAMP). (**Figure 4**).

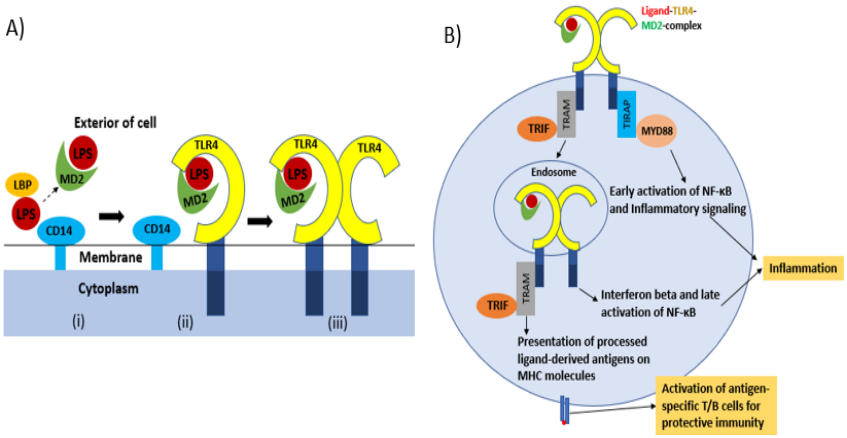

Figure 4. TLR receptor. A) Assembly of TLR4–MD2–LPS complex. The LPS is transferred to MD2 (i) Conjugation of LPS–MD2 with TLR4 (ii) then leads to dimerization of TLR4–MD2, and formation of TLR4–MD2–LPS complex (iii). **B)** After the recognition of ligand and assembly of TLR4-complex, co-receptors: TIRAP, MYD88, TRAM and TRIF, are recruited at the intracellular level for activation of TLR4-signaling resulting into antigen-specific immune responses (Awasthi, 2014).

In this section of the thesis, we have only made a brief reference to two specific types of cells that participate in innate immunity and therefore in the onset of immune inflammation. However, even in the case of cells that we could call "classical" in this context, not all the direct or indirect effects that monocytes/macrophages and neutrophils can produce in the first regulation of inflammation are still sufficiently well known. We must take into consideration the participation of many other cells of the immune system, as well as cells

that are components of the affected tissues and organs or even of pluripotent cells residing in these tissues. To this respect, mesenchymal stem cells (MSC) currently represent a very attractive field of study since on the one hand their presence has been demonstrated in most adult tissues, and on the other hand, their high immunomodulatory potential has been determined, which makes them candidate cells for the regulation of the inflammatory process.

1.2. Inflammatory mediators

1.2.1. Cytokines

Cytokines are small soluble proteins (~5–20 kDa) that play a relevant role in cell signalling in the innate and adaptive immune response. They are released by a wide range of cells, primarily by immune cells (Boyaka and McGhee, 2001). The intracellular signalling is initiated when cytokines bind to a specific cell surface receptor, inducing changes in cell function by regulation of several genes and transcription factors. Several cytokines are pleiotropic and share similar functions. These cytokines orchestrate different processes ranging from the regulation of local and systemic inflammation to cellular proliferation, metabolism, chemotaxis, and tissue repair. The primary function of cytokines is to regulate inflammation, and as such, play a vital role in the control of immune responses in health and disease. Thus, an excessive or imbalance production of cytokines and chemokines may lead to immunopathological situations, due to an uncontrolled immune response and disruption in cellular homeostasis.

Although cytokines can be produced by several cells such as polymorphonuclear leukocytes (PMN), endothelial and epithelial cells, adipocytes, and connective tissue, they are mainly produced by macrophages and lymphocytes. In macrophages, cytokines play an essential role. Depending on the subset of macrophages (classically and alternatively activated), the cytokines produced will be different as well as their functions (Biswas and Mantovani, 2010).

1.2.1.1. Pro-inflammatory cytokines

Macrophages secrete several cytokines including tumor necrosis factor-α (TNF-α), interleukin (IL)-1, IL-6, IL-8 and IL-12, when they are exposed to certain inflammatory stimuli (LPS). As previously explained, also activated lymphocytes, endothelial cells, and fibroblasts can produce these cytokines. However, macrophages and monocytes are the main sources of these cytokines. Macrophages release not only cytokines, but also chemokines, leukotrienes, prostaglandins, and complement. Cytokines may induce, in concert, local effects including increased vascular permeability and recruitment of inflammatory cells and systemic effects including fever and the production of acute inflammatory response proteins. When the production of these cytokines is not deregulated, the inflammatory response is beneficial for the host. Excessive production of IL-1β and TNF-α triggers an acute generalised inflammatory response characteristic of septic shock and multi-organ failure. TNF-α and IL-1β are endogenous pyrogens that are produced and released at the early stages of the immune response to lesions, stress and infections (Beutler, 1999).

TNF-α, a 185-amino acid glycoprotein, was first thought to induce necrosis in certain tumors (Carswell *et al*., 1975). It is one of the main cytokines responsible for inflammation. Whereas in the liver stimulates the acute inflammatory response by elevating the synthesis of C-reactive protein and other mediators, in the hypothalamus stimulates the release of the corticotropic releasing hormone, suppressing appetite, and inducing fever. Additionally, TNF-α induces vasodilation and enhances permeability, being propitious for lymphocyte, neutrophil, and monocyte infiltration. It regulates the release of chemokines and therefore helps to recruit these immune cells to the inflammation site. The expression of chemotactic mediators responsible for the recruitment of neutrophils is induced by TNF-α, in concert with IL-17 (Griffin *et al*., 2012). Furthermore, it increases the expression of cell adhesion molecules (Vieira *et al.,* 2009) that facilitate diapedesis. Since TNF-α induces the inflammatory

response, excess amounts of it have been found to play pathological roles in rheumatoid arthritis, inflammatory bowel disease, asthma, psoriasis, cancer, infectious diseases, and other autoimmune pathologies. Some of these ailments are currently co-treated with monoclonal antibodies that neutralise this cytokine (Sozzani *et al*., 2014). Macrophages secrete TNF-α to the extracellular space via the constitutive secretion pathway, and its trafficking is the best understood of all cytokines. The expression of vesicle trafficking proteins that regulate TNF-α trafficking was found to be increased by LPS (Stow and Murray, 2013; Murray *et al*., 2005; Pagan *et al*., 2003). Interestingly, it was shown that the secretion of TNF-α to the extracellular milieu is not only produced at the plasma membrane but also in a polarised manner at the phagocytic cup (Murray *et al*., 2005), releasing cytokines at the same time that they phagocytose microbial invaders more efficiently.

Another cytokine involved in the early stages of the immune response is **IL-1**. It is a cytokine that has three isoforms: IL-1α, IL-1β and IL-1Ra. IL-1α and IL-1β are strongly pro-inflammatory, perform many of the same functions and bind to the IL-1 receptor (IL-1R). However, there is only 25% amino acid homology between them. IL-1β is chiefly produced by monocytes and macrophages. However, natural killer (NK) cells, B cells, dendritic cells, fibroblasts, epithelial cells, etc. also release this cytokine. IL-1β stimulates the production of acute phase proteins from the liver and acts on the central nervous system to induce fever and prostaglandin secretion during inflammation. IL1-β induces granulocyte chemotaxis, enhancement of the expansion and differentiation of CD4 T cells (Ben-Sasson *et al*., 2009), and the expression of cell adhesion molecules on leukocytes and endothelial cells. Additionally, IL-1β enhances the expression of genes that produce it (Carmi *et al*., 2009). IL-1Ra competing for the same receptor regulates the pro-inflammatory action of IL-1α and IL-1β. When IL-1Ra binds to the IL-1R, it does not induce the pro-inflammatory signalling program mediated by IL-1α and IL-1β.

IL-1β is synthesized as pro-IL-1β, and it must be cleaved by inflammasome-activated caspase-1 or other proteases. Once IL-1β is activated there are different types of secretion, playing the autophagy a significant role in the release of this cytokine and others such as IL-18 (Dupont *et al*., 2011; Jiang *et al*., 2013). Autophagy is characterised by the formation of double-membrane vesicles, which capture and transport cytoplasmic material to acidic compartments where the material is degraded by hydrolytic enzymes (Ravikumar *et al*., 2009). In peritoneal macrophages, it has been shown that IL-1β is transported to the extracellular milieu via membrane transporters, such as ATP-binding cassette (ABC) transporters (Brough and Rothwell, 2007; Marty *et al*., 2005). Furthermore, exocytosis of P2X7R-positive multivesicular bodies containing exosomes has also been shown to be involved in the secretion of this cytokine (Qu *et al*., 2007). The different manners of IL-1 release in macrophages help to respond rapidly to inflammatory stimuli. IL-18 is a member of the IL-1 family and, also an inducer of interferon (IFN)-γ production. It synergizes with IL-12 to activate T cells and NK cells. Unlike IL-1β, IL-18 is not a pyrogen, and can even attenuate IL-1β-induced fever (Gatti *et al*., 2002). Lack of fever induction may be the consequence of the different signalling pathway used by IL-18 (MAPK p38 pathway), instead of NF-κB pathway, which is used by IL-1β (Lee *et al*., 2004).

Like TNF-α and IL-1β, **IL-6** is an endogenous pyrogen that promotes fever and the liver production of acute phase proteins. IL-6 is a pleiotropic cytokine that has both pro-inflammatory and anti-inflammatory functions that affect different processes ranging from immunity to tissue repair and metabolism. It exerts effects on B cells and cytotoxic T cells, promoting their differentiation into plasma cells and activating them, respectively. IL-6 also regulates bone homeostasis. As other pro-inflammatory cytokines, IL-6 is involved in several diseases such as Crohn's disease and rheumatoid arthritis (Nishimoto and Kishimoto, 2004). Pro-inflammatory properties are elicited when IL-6 signals in trans via soluble IL-6 receptors binding to gp130, which is ubiquitous in all cells, whereas the anti-inflammatory

properties are provoked when IL-6 signals through the classical pathway, which occurs via the IL-6 receptor that only a few cells express. IL-6 trans-signalling leads to recruitment of monocytes to the inflammation site (Hurst *et al.,* 2001), promotes the maintenance of T helper (Th) 17 cells, and inhibits T cell apoptosis and development of lymphocytes T regs (Scheller *et al.,* 2011). IL-6 canonical signalling also mediates apoptosis inhibition and the regeneration of intestinal epithelial cells (Scheller *et al.,* 2011).

1.2.1.2. Anti-inflammatory cytokines

Inflammation is regulated by several mechanisms. Some of these mechanisms are the inhibitors and antagonists, including anti-inflammatory cytokines such as IL-10 and transforming growth factor (TGF)-βs, among others.

IL-10 is a 35 kD cytokine produced by activated macrophages, B cells, and T cells which was firstly discovered in 1989 (Mosser and Zhang, 2008). It is involved in different processes such as inhibition of macrophage activation and production of TNF-α, IL-1β, IL-6, IL-8, IL-12, Granulocyte Macrophage Colony-Stimulating Factor (GM-CSF), or IFN-γ (by Th1 and NK cells), and induction of the growth, differentiation, and secretion of immunoglobulins (Ig)Gs by B cells (Defrance *et al*., 1992; Rousset *et al*., 1992; Fiorentino *et al*., 1991). IL-10 inhibits MHC-II expression in activated macrophages, suppressing antigen presentation (Chadban *et al*., 1998) and therefore diminishes their microbicidal activity and their capacity to respond to IFN-γ (Oswald *et al*., 1992; Cunha *et al*., 1992). When IL-10 is blocked, increases the levels of TNF-α and IL-6 as shown in experiments in murine models. Additionally, low levels of IL-10 promotes the development of gastrointestinal pathologies such as inflammatory bowel disease. In contrast, when IL-10 is exogenously added, survival is improved, and the levels of inflammatory cytokines are reduced (Varzaneh *et al*., 2014).

TGF-βs are regulatory molecules with pleiotropic effects on multiple cell types. TGF-βs are implicated in hematopoiesis and have a crucial role in embryogenesis, tissue regeneration, and cell proliferation and differentiation. They are involved in many biological processes, such as development, carcinogenesis, fibrosis, wound healing, and immune responses. Although TGF-βs positively regulates immune responses by recruiting leukocytes at the initial phase, promoting T cell survival, and inducing IgA class switching in B cells, their dominant role in the immune system is to induce tolerance, as well as to contain and resolve inflammation. TGF-βs, as IL-10, act on different target cells suppressing Th1 and Th2 cells and decreasing the inflammatory effects produced by cytokines TNF-α, IL-1β, IL-2 and IL-12, among others (Sanjabi *et al*., 2017).

1.2.2. Chemokines

Chemokines are a group of small proteins (8-12 kDa) with chemoattractive properties. They are involved in different processes like regulation of inflammation, cell differentiation, migration of immune cells, angiogenesis, antimicrobial activity, antitumor immunity and tumorigenesis, as well as the innate and adaptive immune responses. To date, there are more than 50 chemokines and 18 chemokine receptors identified. These molecules are classified into four families (CC, CXC, C, and CX3C) based on the way the first two conserved cysteine residues are arranged, creating a structural motif (Bachelerie *et al*., 2014a; Bachelerie *et al*., 2014b). Chemokines bind to receptors that are members of the G protein-coupled receptor (GPCR) family, activating the cells through the stimulation of signal transduction pathways inside the cell (Zhang and LiWang, 2014).

Chemokines are secreted as a response to pro-inflammatory stimuli with the aim of attracting and activating neutrophils, monocytes, lymphocytes and other effector cells to the site of infection. These chemokines are often induced by pro-inflammatory cytokines such as TNF-α, IL-6, and IL-1β, as mentioned above. Cells that are attracted by chemokines migrate toward the source of that

mediator. The main chemokines released by macrophages are keratinocyte-derived chemokine (KC)/ C-X-C motif chemokine ligand (CXCL)1 (mouse), IL-8/CXCL8 (human), macrophage inflammatory protein-2α (MIP-2α)/CXCL2, regulated upon activation normal T cell expressed and secreted (RANTES)/ C-C motif chemokine ligand (CCL)5, monokine induced by IFN-γ (MIG)/CXCL9, or IFN-γ-induced protein (IP) 10/CXCL10 and IP9/CXCL11.

Both **CXCL1** and **CXCL2** share 90% amino acid similarity and are released by monocytes and macrophages recruiting neutrophils and hematopoietic stem cells (Moser *et al*., 1990; Pelus and Fukuda, 2006). These chemokines promote the angiogenesis and development of tumors such as melanomas (Addison *et al*., 2000). Similarly to CXCL1 and CXCL2, the chemokine **CXCL8** is a chemoattractant for neutrophils inducing degranulation and morphological changes (Gouwy *et al*.,2004; Starckx *et al*., 2002). Besides, other cells such as keratinocytes, endothelial cells, eosinophils, and basophils are recruited by this chemokine which plays a role in inflammatory diseases such as psoriasis, Crohn's disease, and cancer (Van Damme *et al*., 2004; Gijsbers *et al*., 2004). On the other hand, **CCL5** is a chemoattractant for T cells, basophils, eosinophils, and dendritic cells to the site of inflammation. Additionally, it promotes tumorigenesis and metastasis (Donlon *et al*., 1990). Similarly, to **CXCL9** and **CXCL10**, **CXCL11** is interferon-inducible and also mediates T cell recruitment, although more potently than CXCL9 and CXCL10 (Keeley *et al*., 2008; Rosenblum *et al*., 2010; Cole *et al*., 1998).

1.2.3. Eicosanoids: Prostaglandin E_2 and Leukotriene B_4

Prostaglandins (PGs) and leukotrienes (LTs) are two classes of lipid mediators derived from the arachidonic acid metabolism (Wang and Dubois, 2010). In particular, PGE_2 and leukotriene (LT) B_4 are some of the eicosanoids involved in the regulation of the immune system.

PGs are generated through the oxidation of arachidonic acid by cyclooxygenase (COX) enzymes, COX-1 and COX-2 (Funk, 2001). Whereas COX-2 is induced by different stimuli (Crofford, 1997), COX-1 is constitutively expressed in most mammalian cells. COX enzyme first oxidises arachidonic acid to form PGG_2. Secondly, COX reduces PGG_2 to form PGH_2 which can be modified to produce five different PGs. One of them is **PGE_2** which is the principal metabolic product of COX-2 activity acting in concert with other enzymes such as cytosolic PGE synthase (cPGES), microsomal PGE synthase-1 (mPGES-1), or microsomal PGES-2 (mPGES-2). It is described that cPGES and mPGES-2 maintain the physiological levels of PGE_2, whereas mPGES-1 produces PGE_2 levels when activated by a wide array of stimuli including pathogen recognition. Upon intracellular production, PGE_2 is released to the extracellular compartment.

PGE_2 and LTB_4 are some of the eicosanoids involved in the regulation of the immune system (Wang and Dubois, 2010). It has been shown that PGE_2 plays both pro- and anti-inflammatory roles. For example, PGE_2 can mediate endothelial permeability to promote inflammatory cell recruitment (Omori *et al*., 2014); yet actions on inflammatory cells themselves are often inhibitory (**Figure 5**)**.**

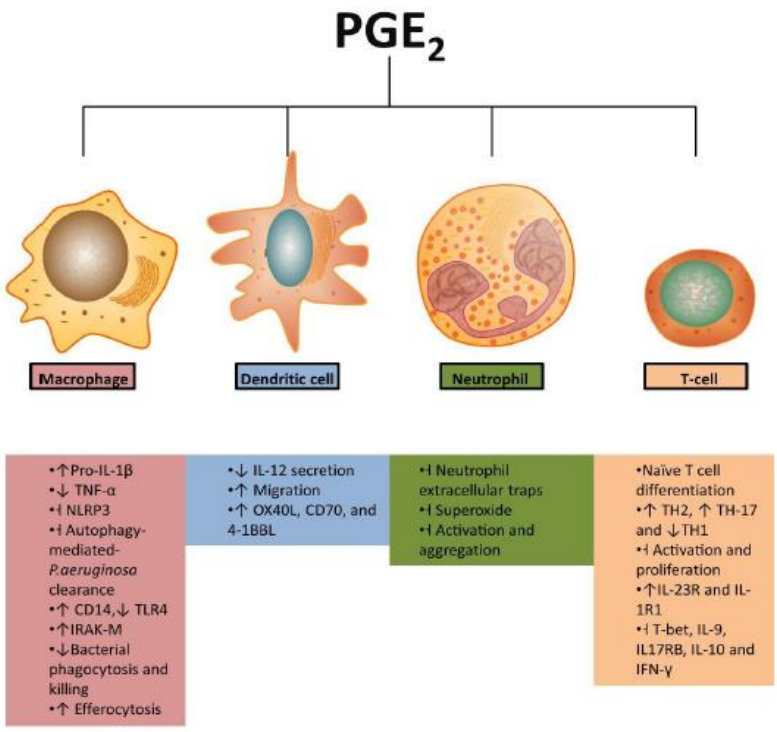

Figure 5. PGE_2 effects on immune cells (Martínez-Colon and Moore, 2018).

LTs are generated from arachidonic acid through the sequential action of two enzymes, cytosolic phospholipase A_2 and 5-lipoxygenase (5-LO), which is expressed in all cells of myeloid origin. After translocation of 5-LO to the nuclear membrane, LTA_4 is formed and then it can be converted either to **LTB_4** through the action of LTA_4 hydrolase (Samuelsson and Funk, 1989) or to LTC_4 by LTC_4 synthase. Although LTB_4 was first identified in neutrophils (Ford-Hutchinson *et al*., 1980), it is produced by other cells (James *et al*., 2006; Jame *et al*., 2007). Initially, LTB_4 was identified due to its involvement in the recruitment of neutrophils. However, it has been shown that its chemoattractant properties affect other inflammatory cells in the early phase of the immune response. LTB_4 enhances the release of cytokines IL-1 (α/β) and IL-6 and the chemokine monocyte

chemoattractant protein (MCP)-1 by monocytes, and the production of IL-8 by neutrophils (Rola-Pleszczynski and Lemaire, 1985; Huang *et al*., 2004; Gaudreault *et al*., 2012; Kuhns *et al*., 2001). However, aberrant levels of LTB_4 can lead to negative effects on host responses and may be pathogenic in inflammatory diseases.

2. Mesenchymal stem cells

Stem cells are a class of undifferentiated cells capable of self-renewal continuously in an almost unlimited manner, to form clonal cell populations. Remarkably, stem cells can differentiate into multiple cell lineages (Graf, 2002; Watt and Hogan, 2000). These unique properties provide an attractive therapeutic potential in regenerative medicine and cellular therapy for the treatment of several diseases, such as Alzheimer's disease, Crohn's disease, cardiovascular diseases, among others. Stem cells can be divided into three different categories: embryonic stem cells, induced pluripotent stem cells, and adult stem cells.

MSC, also known as multipotent mesenchymal stromal cells, are a heterogeneous population of adult stem cells characterised by a fibroblastic phenotype, plastic adherence and a high self-renewal potential. They derive from the mesodermal embryonic layer, being able to differentiate into osteoblasts, chondrocytes and adipose tissue. These cells have been the focus in regenerative medicine for their immunomodulatory properties, homing ability to the site of injury, multipotent differentiation capacity, ease of expansion in cell culture and the production of bioactive factors affecting numerous physiological or pathological processes.

These cells were initially discovered in the bone marrow by soviet biologist Aleksandr Friedenstein and colleagues in the 1960s (reviewed in Friedenstein, 1990). However, they were officially named as mesenchymal stem cells years later by Caplan (1991). Although they

were initially isolated from the bone marrow, they have been reported to be present in a wide range of tissues such as adipose tissue (Zuk *et al*., 2001), amniotic fluid (In't Anker *et al*., 2003), cord blood (Erices *et al*., 2000), fetal blood and liver (Campagnoli *et al*., 2001), menstrual fluid (Meng *et al*., 2007), and in the synovial membrane (De Bari *et al*., 2001).

The defining characteristics of MSC were inconsistent among investigators since there were not universally accepted criteria to define MSC. Consequently, the International Society of Cellular Therapy (ISCT) proposed minimum criteria to identify MSC (Dominici *et al*., 2006). One of these criteria is that cells must be adherent to plastic under standard culture conditions. In addition, they must express a specific set of cluster of differentiation (CD) molecules, such as CD105, CD73, and CD90, whereas they must lack the expression of CD45, CD34, CD14, CD11b, CD79 alpha or CD19 and human leukocyte antigen (HLA)-DR surface molecules. Furthermore, they must demonstrate *in vitro* differentiation potential into a variety of cell types from the mesoderm including adipocytes, chondrocytes and osteoblasts, but not hematopoietic cells. However, it has been described that MSC are also able to differentiate into cells from the other two primary germ layers (ectodermic and endodermic lineages) including neural cells, cardiomyocytes, hepatocytes, pancreatic β-cells and vascular endothelial cells (Uccelli *et al*., 2008; Frese *et al*., 2016) (**Figure 6**).

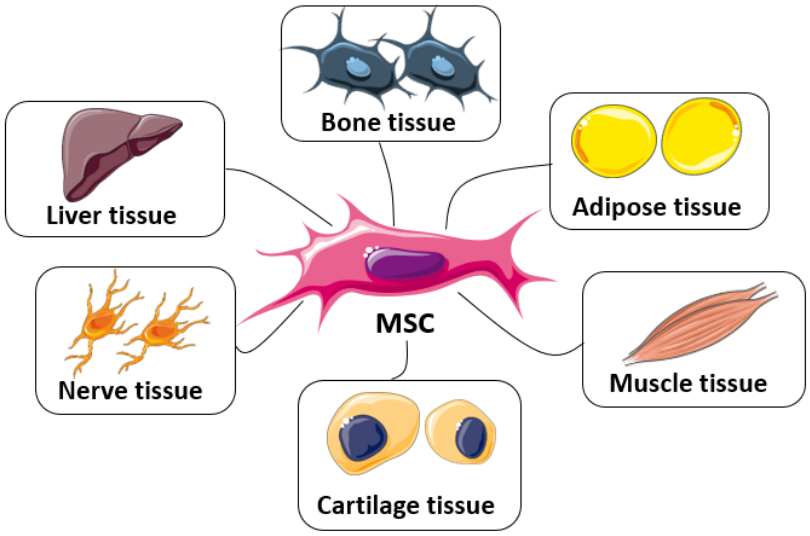

Figure 6. Differentiation of mesenchymal stem cells into different types of cells.

2.1. Adipose tissue-derived mesenchymal stem cells

Adipose tissue-derived MSC offer advantages over MSC from bone marrow or other sources since they can be obtained more easily and in much larger amounts. For example, a quantity of 100 ml of bone marrow transplantation contains approximately 6 x 10^8 nucleated cells, of which only 0.001-0.01% are MSC. However, in the adipose tissue, there are approximately 0.5-2.0 x 10^6 cells/gram of adipose tissue from which 1-10% MSC can be obtained (Varma *et al*., 2007).

In addition, according to their tissue of origin, MSC isolated from bone marrow and adipose tissue have specific differences at the transcriptional and proteomic levels. MSC of adipose tissue expresses higher levels of insulin-like growth factor-1 (IGF-1), vascular endothelial growth factor (VEGF)-D and IL-8 compared to MSC from bone marrow. However, other factors such as nerve growth factor (NGF), VEGF-A, basic fibroblast growth factor (bFGF) and angiogenin

are expressed at comparable levels between them. They may also show differences in their angiogenic capacity.

In a comparative study by Ivanova-Todorova *et al*. 2009, it was demonstrated that human MSC from adipose tissue have greater anti-inflammatory capacity on dendritic cells derived from monocytes compared to human MSC from bone marrow. Besides, adipose tissue-derived MSC significantly reduced cell surface markers (CD80, CD83, CD86) of dendritic cells and increased the anti-inflammatory cytokine IL-10, to a greater extent than bone marrow MSC. In other studies, MSC from adipose tissue potentiated the immunosuppressive effects of cyclosporin A through the production of Jagged-1, which suppresses the NF-κB pathway in T lymphocytes (Shi *et al*., 2011). In addition, the infusion of MSC from adipose tissue, in a murine model of experimental colitis, decreased the level of inflammatory cytokines (TNF-α, IFN-γ, IL-6, IL-1β and IL-12) and increased the level of anti-inflammatory IL-10 and IL-10-secreting regulatory T cells (González-Rey *et al*., 2009).

In the present decade, the number of clinical trials using MSC from adipose tissue has increased rapidly, from 18 to more than 150 studies (www.clinicaltrials.gov). These clinical trials have addressed a wide range of conditions, including fistula, musculoskeletal disorders, ischemia, soft tissue damage, graft-versus-host disease, diabetes, lipodystrophy, etc. (Nordberg and Loboa, 2015). In this context, MSC have shown beneficial effects in several of these clinical trials, such as in chronic graft-versus-host disease (Jurado *et al*., 2017), Crohn's disease (García-Olmo *et al*., 2005 and 2009) and multiple sclerosis (Riordan *et al*., 2009).

2.1.1. Secretome from adipose tissue-derived mesenchymal stem cells

MSC are present in multiple tissues. However, the overall quantity in the organism is scant, and great amounts of MSC are needed to be used as cell therapy. Thus, MSC need to proliferate *in vitro* for more than eight weeks before implantation. Also, the optimal culture conditions are influenced by the patient's age and clinical characteristics (Sotiropoulou *et al*., 2006; Duggal and Brinchmann, 2011) and implanted MSC do not survive for long. Although the therapeutic effects of MSC were first thought to be related to their differentiation and engrafting capacities, several studies have shown that the main effects of MSC are probably mediated by paracrine mechanisms (Maguire, 2013). Therefore, recent studies have brought attention to the wide array of bioactive factors produced by MSC, which could be responsible for the regulation of several physiological processes (Madrigal *et al*., 2014). These factors secreted by the MSC to the extracellular space are known as secretome or conditioned medium (CM) and regulate the communication between cells. In fact, it has been reported that the secretome from MSC provides several advantages over the cell-based therapy such as manufacturing, stability during extended storage, handling, economic aspects, easy- and ready-to-use product in clinical application, low immunogenicity, and their potential as a ready-to-go biological therapeutic agent (Konala *et al*., 2016). Nevertheless, regulatory requirements for manufacturing and quality control will be necessary to establish the safety and efficacy profile of these products.

The secretome contains soluble and vesicular components including a diverse range of proteins, lipids, free nucleic acids, cytokines, chemokines, angiogenic factors, growth factors and extracellular vesicles (EV) (Gnecchi *et al*., 2016). In 1987, the term exosome was first used to describe small membrane vesicles formed by vesiculation of intracellular endosomes and released by exocytosis

(Johnstone *et al*., 1987). It took more than 30 years from the first discoveries to realise that these vesicles were not merely cellular dust or a way to remove unwanted components from the cells. They were further recognised as mediators of intercellular communication (Raposo *et al*., 1996; Zitvogel *et al*., 1998) involved in immune response induction and other functions, acting as a cargo vehicle for the transport of proteins, nucleic acids between cells. The composition of EV mirrors the genetic and proteomic composition of the secreting cells.

Depending on their biogenesis and size, EV are classified into three main classes: apoptotic bodies, microvesicles (Mv) (also known as microparticles or ectosomes) and exosomes (Ex). EV differ in size, Ex are in the range of 50-150 nm, whereas Mv are in the range of 100-1,000 nm and apoptotic bodies have a larger diameter (50–5,000 nm) (Tkach *et al*., 2017). The biogenesis and secretion of EV have been extensively reviewed by Colombo and colleagues (2014). Apoptotic bodies are released as blebs of cells undergoing apoptosis whereas Mv originate from the outward budding and fission of the plasma membrane. By contrast, Ex have an endocytic origin and are generated by the invagination or reverse budding of the peripheral membrane of the endosomes, forming intra-luminal vesicles (ILV) inside the endosomes, which are then termed multi-vesicular bodies (MVB) (**Figure 7**).

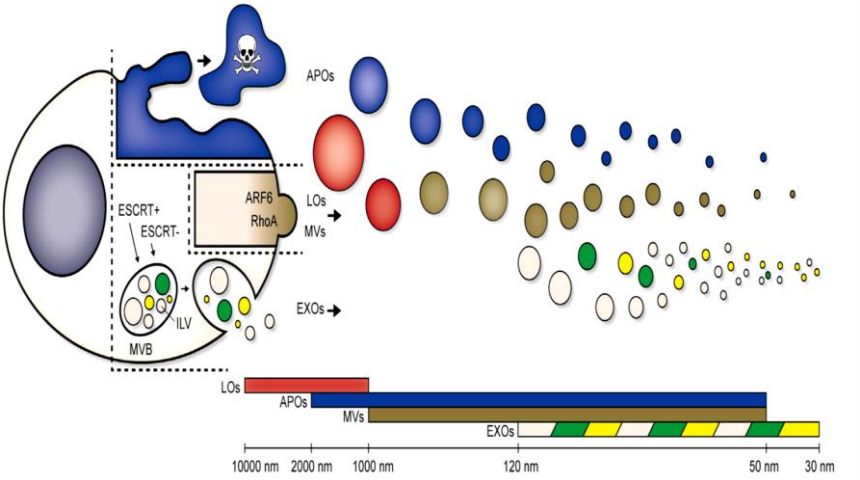

Figure 7. Classification of EV (Willms *et al.*, 2018)

These MVB can follow either the secretory or lysosomal pathways. In the secretory pathway, MVB fuse with the cell membrane, which results in the release of ILV as Ex into the extracellular space by exocytosis and incorporation of the peripheral membrane of the MVB into the plasma membrane. In the lysosomal pathway, MVB fuse with lysosomes releasing ILV in the lysosomal lumen that contain hydrolases, ensuring the degradation of their content.

The composition inside Ex is similar to the cell they are originated from. These vesicles contain different molecules with biological properties including a subset of lipids (i.e. cholesterol, sphingomyelin, and hexosylceramides), nucleic acids (Ribonucleic acid (RNA) subtypes: i.e. messenger (m)RNA, micro (mi)RNA, transfer (t)RNA, ribosomal (r)RNA, small interfering (si)RNA, long non-coding (lnc)RNA and deoxyribonucleic acid (DNA) subtypes: i.e. mitochondrial (mt)DNA, single-stranded (ss)DNA, double-stranded (ds)DNA) and proteins (both endosome-associated proteins, tetraspanins, and lipid raft-associated

proteins as well as discrete protein cargo) that are derived from the parent cell (**Figure 8**).

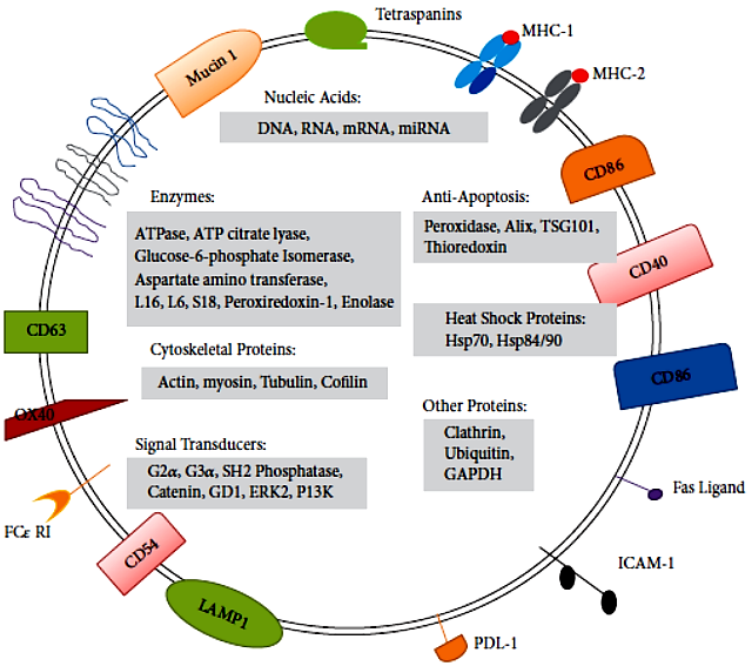

Figure 8. Exosome (Mortaz *et al*., 2018)

There are several manners of isolation and characterisation of the EV: size-based separation (differential centrifugation and ultrafiltration), density-based separation (sucrose and OptiPrepTM gradients), immuno-affinity, and polyethylene glycol precipitation (Théry *et al*., 2006; Lobb *et al*., 2015; Lener *et al*., 2015). The most common isolation procedure is by differential ultracentrifugation. Large vesicles, MV, are pelleted at low-speed centrifugation (2,000 x g), whereas the small vesicles, Ex of less than 150 nm of diameter, are pelleted at high-speed ultracentrifugation (100,000 x g-120,000 x g) (Kowal *et al*., 2016). It should be noted, however, that none of these methods can reliably separate EV subgroups. It is complicated to

separate pure populations of Mv and Ex as sizes overlap. Hence, in recent articles, this standard/traditional classification into three main classes of EV has started to be changed to large vesicles and small vesicles (Kowal *et al*., 2016; Tkach *et al*., 2017).

Isolation of pure population of EV is major technical challenge. The International Society for Extracellular Vesicles described in 2014 the minimal requirements for the definition of EV and some proteins expected to be present in these vesicular components (Lötvall *et al*., 2014; **Table 1**). A recent in-depth proteomic analysis of MSC-derived EV has shown that MSC can package as much as one-third of their protein content within EV. MSC have shown to deliver cytoplasmic material to other cells using nanotubules and EV (Sinclair *et al*., 2016). For instance, Matula *et al*. (2016) reported the bidirectional transfer of cellular material between MSC and peripheral T cells using tunnelling nanotubules and EV.

1. Transmembrane or lipid-bound extracellular proteins	2. Cytosolic proteins	3. Intracellular proteins	4. Extracellular proteins
Argues presence of a membrane in the isolate	With membrane- or receptor-binding capacity	Associated with compartments other than plasma membrane or endosomes	Binding specifically or non-specifically to membranes, co-isolating with EVs
Present or enriched in EVs/exosomes	Present or enriched in EVs/exosomes	Absent or under-represented in EVs/exosomes, but present in other types of EVs	Variable association with EVs
Examples: Tetraspanins (*CD9*, *CD63*, *CD81*) Integrins (*ITG*—**) or cell adhesion molecules (*CAM*—*) Growth factor receptors Heterotrimeric G proteins (*GNA*—**) Phosphatidylserine-binding *MFGE8*/lactadherin	Examples: Endosome or membrane-binding proteins (*TSG101*, annexins=*ANXA*—*, Rabs=*RAB*—*) Signal transduction or scaffolding proteins (syntenin)	Examples: Endoplasmic reticulum (Grp94=*HSP90B1*, calnexin=*CANX*) Golgi (*GM130*) Mitochondria (cytochrome C=*CYC1*) Nucleus (histones=*HIST*—*H*—*) Argonaute/RISC complex (*AGO*—*)	Examples: Acetylcholinesterase (*ACHE*) Serum albumin Extracellular matrix (fibronectin=*FN1*, collagen=*COL*—*A*—*) Soluble secreted proteins (cytokines, growth factors, matrix metalloproteinases =*MMP*—*)

At least one protein of each category 1, 2 and 3 should be quantified in the EV preparations. EV association of proteins of category 4 should be demonstrated by other means.

*Italics: official gene names;
**denotes different possible family members.

Table 1. Different categories of proteins and their expected presence in EV isolates, including some examples (non-exclusive) (Lötval *et al.*, 2014).

2.1.2. Therapeutic applications of MSC-derived secretome

Clinical and basic science studies have demonstrated the anti-microbial, anti-fibrotic and pro-regenerative activity of the CM from adipose tissue-derived MSC which can regulate processes such as angiogenesis, cell proliferation and differentiation, immune modulation, wound healing, bone regeneration, kidney and cardiac regeneration, etc. (Maguire, 2013; Haynesworth *et al*., 1996; Tögel *et al*., 2005; Gnecchi *et al*., 2006; Timmers *et al*., 2007).

According to several studies, it has been suggested that the paracrine factors linked to the cytoprotective effect of MSC on ischemic cardiomyocytes for cardiac regeneration are VEGF, hepatocyte growth factor (HGF), fibroblast growth factor (FGF), IGF-1, and thymosin β4 (TB4) (Gnecchi *et al*., 2008). VEGF-A has been found to be responsible for angiogenesis, and angiopoietin 1 has a role in neo-vessel maturation, contributing to wound healing (Khubutiya *et al*., 2014). Furthermore, other factors such as HGF, VEGF, stromal cell-derived factor-1 (SDF-1), keratinocyte growth factor (KGF), FGF, placental growth factor (PGF), MCP-1, and IGF-1 have shown proliferative and regenerative effects (Kuraitis *et al*., 2012). The anti-inflammatory effects exerted by MSC have been attributed to the production of anti-inflammatory cytokines (IL-10, TSG-6) and reduction of pro-inflammatory factors (IL-1α, IL-1β, IL-6, IL-17, IFN-γ, granulocyte colony-stimulating factor (G-CSF), GM-CSF, MIP-2α, MCP-1) (Khubutiya *et al*., 2014).

Different studies have shown the suppression of the immune response by MSC from adipose tissue. According to Ivanova-Todorova and colleagues (2009), MSC from adipose tissue have shown to be better suppressors of the immune response in comparison to MSC from bone marrow, as mentioned above (Ivanova-Todorova *et al*., 2009). Although EV produced by different cell types can play an essential role in the regulation of immunity and inflammation (Robbins

et al., 2016), little is known of the anti-inflammatory and immunomodulatory effects of EV secreted by adipose tissue-derived MSC. It has been reported that Ex from human adipose tissue-derived MSC can exert an inhibitory effect in the differentiation and activation of T cells (Blázquez *et al*., 2014).

The secretome of adipose tissue-derived MSC is active on the immune response, not only under standard conditions but also in the context of a pro-inflammatory stimulus. DelaRosa and their colleagues (2009) reported that the secretome from adipose tissue-derived MSC (previously activated by IFN-γ) had immunosuppressive properties as shown by the decrease of the proliferation of peripheral blood mononuclear cells and the modulation of HGF, PGE_2, TGF-β1, indoleamine 2,3-dioxygenase, nitric oxide (NO), and IL-10 (DelaRosa *et al*., 2009). **Figure 9** provides a summary of possible mechanisms of action of MSC and their secretome in the regulation of immune cells (Singer and Caplan, 2011).

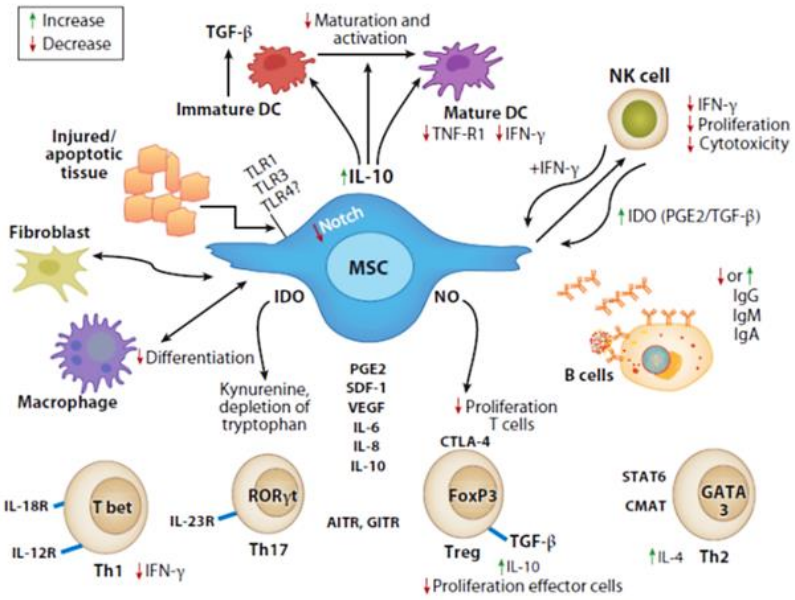

Figure 9. Mechanisms of immunomodulation by MSC and their secretome (Singer and Caplan, 2011).

It has also been described that the secretome can be modified by preconditioning the MSC to obtain a tailor-made secretome profile and promote a better biological response from MSC. For instance, a study by Ti and colleagues (2015) showed that treating MSC with LPS modulates the abundance of miR-let-7b in MSC-derived Ex which in turn enhances wound healing and decreases inflammation via signalling to macrophages. Kilroy and colleagues (2007) showed the protein secretion profile by adipose tissue-derived MSC after LPS-stimulation for 24 h. The secreted proteins were hematopoietic factors such as G-CSF, GM-CSF, macrophage colony-stimulating factor (M-CSF) and pro-inflammatory factors such as IL-6, IL-8, IL-7, IL-11 and TNF-α. The concentration of most of these factors in the secretome increased in a time-dependent manner. TNF-α displayed a slightly different temporal expression pattern by reaching its peak concentration at 8 h and then decreasing by 24 h. This study also

analysed the effect of exogenous epidermal growth factor (EGF) and bFGF on the adipose tissue-derived MSC secretome. EGF and bFGF exposure led to an increase in HGF secretion by these cells.

A more recent study by Lee and colleagues (2010) used more sensitive detection protocols along with bioanalytical tools to comprehensively characterise the adipose tissue-derived MSC secretome response to TNF-α exposure. 187 proteins were detected, and 118 were up-regulated due to TNF-α exposure. The up-regulated proteins included IL-6, IL-8/CXCL 8, MIP-2α/CXCL2, CXCL5, granulocyte chemotactic protein-2 (GCP-2/CXCL6, CXCL10, MCP-1/CCL2, complement proteins B, C1s, C1γ, and D, plasminogen activator inhibitor (PAI)-1, PAI-2, cathepsin A, B, C, F, K, O, and S, pentraxin 3.

Aims of the study

Adipose tissue-derived mesenchymal stem cells have shown beneficial effects on several inflammatory diseases, mainly due to their paracrine activity. The conditioned medium of these cells contains soluble factors and vesicular components known as extracellular vesicles. Extracellular vesicles participate in various physiological processes and have important roles in immune regulation. Furthermore, they have been tested as potential therapeutic tools for the treatment of inflammatory and autoimmune diseases. In this context, we wanted to investigate whether the secretome of mouse adipose tissue-derived mesenchymal stem cells modulates the innate inflammatory response as well as the contribution of its components. Therefore, our objectives in this thesis are:

1. Compare the effects of mouse adipose tissue-derived mesenchymal stem cells and their conditioned medium on the *in vivo* innate inflammatory response induced by zymosan in the mouse air pouch model.

2. Study the protein composition of this conditioned medium, isolate and characterise their vesicular components (extracellular vesicles), mainly exosomes and microvesicles.

3. Determine the effects of the soluble fraction and extracellular vesicles of the conditioned medium from mouse adipose tissue-derived mesenchymal stem cells on the innate inflammatory response (phagocytosis, migration and production of pro-inflammatory mediators) using an *in vitro* model: mouse peritoneal macrophages stimulated with LPS.

Material and methods

1. ISOLATION AND CULTURE OF CELLS FROM MOUSE

Mesenchymal stem cells (MSC), neutrophils, monocytes and macrophages were isolated from CD1 male mice of 8-10 weeks of age. Mice were maintained at 21˚C ± 2˚C on a 12-h light/dark cycle with feed and water *ad libitum*. All the animal experiments were approved by the Institutional Animal Care and Use Committee of the University of Valencia, Spain.

1.1. Mesenchymal stem cells from adipose tissue

To obtain mouse MSC from adipose tissue, perigonadal and inguinal fat pads were both isolated separately from CD1 male mice. Next, adipose tissue was minced and digested with 1 mg/ml of type IA collagenase (Sigma-Aldrich®) in Roswell Park Memorial Institute (RPMI) medium (Gibco®) supplemented with penicillin (100 U/ml) and streptomycin (100 µg/ml) (1% penicillin/streptomycin) (Sigma-Aldrich®) at 37˚C for 1 h and then centrifuged at 500 x g for 10 min at 17˚C. After removal of the supernatant, pellet (stromal vascular fraction) was resuspended in RPMI medium supplemented with 10% fetal bovine serum (FBS) (Biowest SAS), 1% penicillin/streptomycin and filtered through a 70 µm membrane. Cells were seeded onto cell culture flasks and maintained at standard culture conditions (5% CO_2 enriched atmosphere at 37˚C). 24 h later non-adherent cells were removed and RPMI medium was changed with Dulbecco's modified Eagle's medium (DMEM) HAM's F-12 medium (Sigma-Aldrich®) containing 15% FBS, 1% penicillin/streptomycin (**Figure 10**). Medium was replaced every 2 to 3 days. Cells were observed using a Leica DM IL LED (Leica Microsystems) microscope (**Figure 11**).

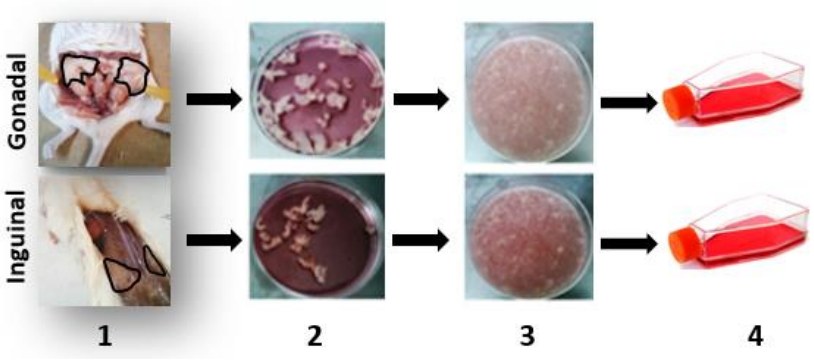

Figure 10. Isolation of MSC from gonadal and inguinal adipose tissue from CD1 male mice. Gonadal and inguinal fat pads were isolated (1), minced (2), digested with collagenase (3) and the cell pellet was seeded on 75 cm^2 cell culture flasks (4).

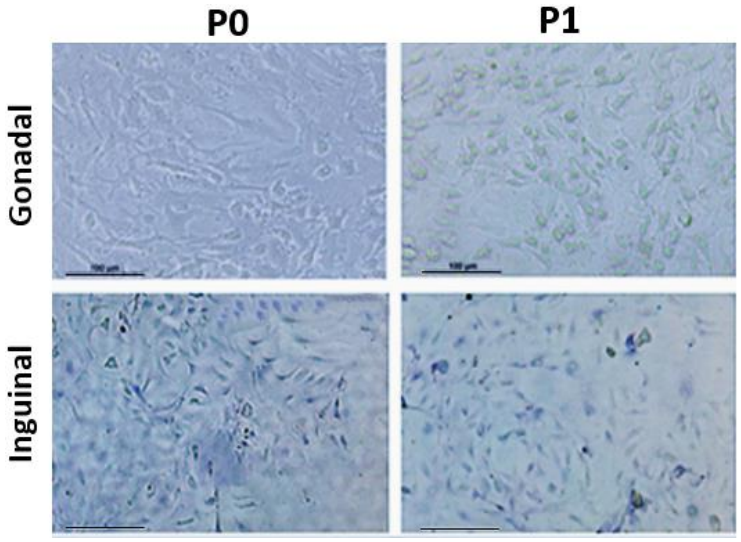

Figure 11. Representative mouse adipose tissue-derived MSC culture images at passage (P)0 and P1 from gonadal and inguinal fat pads. Cells were cultured in DMEM/Ham's F-12 supplemented with 15% FBS and 1% penicillin/streptomycin. Scale bar: 100 µm.

To characterise phenotypically mouse MSC by flow cytometry (Becton Dickinson LSRFortessa™), positive markers anti-CD105-Phycoerythrin (PE) (eBioscience™, San Diego, CA, USA) and anti-CD29-Peridinin-Chlorophyll protein (PerCP)-eFluor™ 710 (eBioscience™)

and negative markers anti-CD11b-Allophycocyanin (APC) (eBioscience™) and anti-CD45-Fluorescein isothiocyanate (FITC) (eBioscience™) were used. When cultured MSC in 75 cm^2 flasks were confluent, they were rinsed with phosphate-buffered saline (PBS) (Gibco®) and collected by trypsinization (Trypsin-EDTA solution 0.25%, Gibco®). After several washes with PBS, 1 x 10^6 cells suspended in 100 µl of PBS were added into different tubes. Then, cells were incubated with the corresponding fluorochrome-conjugated antibodies (CD29, CD105, CD11b and CD45) for 30 min at 4˚C. A control tube without incubated antibody was used to measure the autofluorescence from the cells. To determine the cell viability propidium iodide was used. Following the incubation, cells were washed with PBS and finally resuspended in 500 µl of PBS/tube and determined by flow cytometry (Becton Dickinson LSRFortessa™).

To obtain the conditioned medium (CM) from adipose tissue-derived MSC, the supernatant of the cultured MSC was collected every 48-72 h and was then centrifuged at 300 x g for 10 min at 4˚C and the supernatant stored at -80˚C until use. Experiments were performed using this CM obtained from MSC at passage (P) 1.

1.2. Mesenchymal stem cells from bone marrow

To obtain mouse MSC from bone marrow, femur and tibia were isolated from CD1 male mice and bone marrow was obtained by flushing through a syringe with a 25 G needle (0.5 mm x 16 mm). Cell suspension was filtered through a 70 µm filter to remove muscle, any bone spicules and cell clumps. Then, cell suspension was centrifuged at 500 x g for 5 min at room temperature. The yield and viability of cells were determined by Trypan blue exclusion and cells were counted on a hemocytometer (Neubauer chamber). Cell pellet was resuspended in RPMI medium with 10% FBS and 1% of penicillin/streptomycin, seeded onto flasks and incubated at 37˚C with 5 % CO_2 in a humidified chamber. After 24 h, non-adherent cells that accumulate on the surface of the flask were removed by changing the

medium with DMEM HAM's F-12 medium containing 15% FBS, 1% of penicillin/streptomycin. Medium was replaced every 2 to 3 days. Cells were observed using a Leica DM IL LED (Leica Microsystems) microscope. Since mouse bone marrow-derived MSC yield obtained was very low (data not shown), no phenotypic characterisation of MSC by flow cytometry and no further studies were performed. Thus, we decided to continue working with adipose tissue derived-MSC.

1.3. Macrophages

To isolate resident macrophages from the peritoneal cavity, a volume of 10 ml of PBS was injected into the peritoneal cavity. Peritoneal exudate cells were collected in a 50 ml conical tube and centrifuged at 500 x g, for 6 min. Then, the pellet was resuspended in a lysis buffer (Sigma®) for 30 seconds to eliminate erythrocytes. Cell pellet was rinsed with RPMI medium. Then, cells were seeded at 3 x 10^5 cells/well in 500 µl of RPMI supplemented with 10% FBS and 1% penicillin/streptomycin on a 24-well plate. Cells were maintained at standard culture conditions (5 % CO_2 enriched atmosphere at 37˚C). After 24 h medium was changed to DMEM HAM's F-12 medium with 10% FBS and 1% penicillin/streptomycin. Prior to the beginning of each experiment, medium from macrophages was replaced with DMEM HAM'S F-12 medium supplemented with 10% extracellular vesicles (EV)-depleted FBS and 1% penicillin/streptomycin.

Macrophages were characterised phenotypically by flow cytometry using positive markers anti-CD11b-APC and anti-F4/80-PerCP-Cy (Cyanine) 5.5 (**Figure 12**). First, cells were washed with PBS and collected from 24-well plates with Buffer I (500 ml of PBS, 2 ml of ethylenediamine tetraacetic acid 0.5 M, 8.5 ml of bovine serum albumin (BSA) from Sigma-Aldrich®, 442.4 µl of HCl 1 N). Then, 3 x 10^5 cells resuspended in 0.1 ml of Buffer I were pre-treated with Mouse Fc-block (BD, CD16/32 mAb (BD Pharmingen™); 1/100 dilution) for 5 min at 4˚C to block the binding sites of Fc receptors. Following the incubation with the corresponding fluorochrome-conjugated

antibodies for 20 min at 4˚C in darkness at the recommended concentrations following the manufacturers' instructions, cells were washed with Buffer I supplemented with 10% FBS. Finally, cells were resuspended in 0.5 ml PBS to be analyzed by flow cytometry (Becton Dickinson LSRFortessa™). We measured the percentage of positive cells and/or the intensity of fluorescence. To measure the expression of TLR4 (BioLegend®) and CD14 (eBioscience™) on the surface of macrophages, antibodies anti-TLR4-PE and anti-CD14-PE were used. An isotype was used as a control.

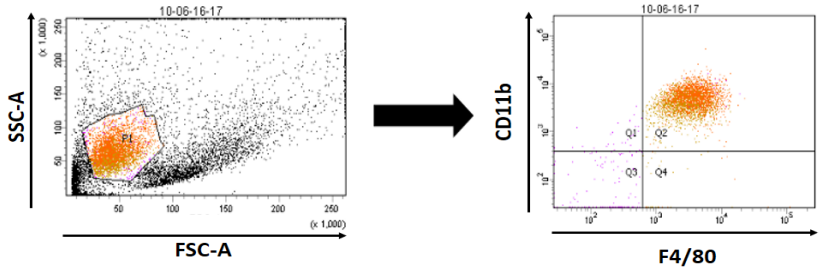

Figure 12. Phenotypic characterisation of resident peritoneal macrophages by flow cytometry. Resident peritoneal macrophages were characterised by positive markers CD11b-APC and F4/80-PerCP Cy5.5. Representative image of 4 independent experiments.

Macrophages are main cells in the innate inflammatory response. Since we wanted to evaluate the effects of CM, Extracellular vesicles (EV)-free CM and EV from MSC in the innate immune activity, we focused on studying the inflammatory response on mouse peritoneal macrophages. Furthermore, we assessed the phagocytic activity and the implication of macrophages in neutrophils and monocytes migration.

To induce an inflammatory response in macrophages, we stimulated the cells with lipopolysaccharide (LPS) (lipoglycans found in the outer membrane of Gram-negative bacteria). LPS binds sequentially to CD14 and TLR4/MD2 receptor triggering the production of proinflammatory mediators (Płóciennikowska *et al*., 2016).

1.4. Neutrophils

Neutrophils were isolated from CD1 male mouse femur and tibia bone marrow by flushing PBS through a 10 ml syringe and a 25 G needle (0.5 mm x 16 mm). The bone marrow suspension was filtered through a 70 µm filter. Then, the cell suspension was centrifuged at 1,900 rpm, for 5 min at 23˚C (Centrifuge 5810R Eppendorf®). Once bone marrow cells were obtained, neutrophils were isolated by immunomagnetic cell sorting (positive selection) using the antibody anti-Ly-6G-Gr1-FITC (eBioscience™) and anti-FITC conjugated with Microbeads according to the manufacturer's instructions (Miltenyi Biotec, Madrid, Spain) (**Figure 13**).

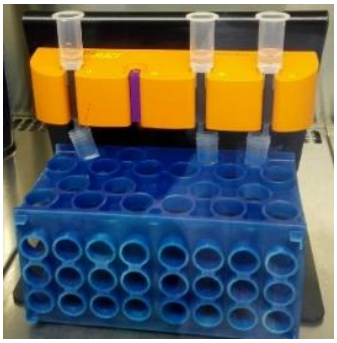

Figure 13. Immunomagnetic cell sorting for neutrophil isolation from mouse bone marrow.

Neutrophils were characterised phenotypically after isolation by immunomagnetic cell sorting. To that purpose, flow cytometry (Becton Dickinson LSRFortessa™) was used and cells were stained with positive markers anti-CD11b-APC and anti-Ly6G-FITC. Cells were characterised following the same method used in **section 1.3. Macrophages**.

1.5. Monocytes

To isolate monocytes**,** bone marrow from femurs and tibiae of mice were harvested in a conical tube by flushing PBS through a 10 ml syringe and a 25 G needle. After removing erythrocytes with lysis buffer, cells were plated on a 100-mm diameter tissue culture dish and incubated at 37 ˚C and 5 % CO_2 for 3 h. Then, cells were harvested with trypsin 0.25 % followed by several washes with DMEM HAM's F-12 medium and used to perform the migration assay with monocytes.

To characterise monocytes, cells were first washed with PBS. Then, they were pre-treated with Mouse Fc-block (BD, CD16/32 mAb (BD Pharmingen™); 1/100 dilution) for 5 min at 4˚C to block the binding sites of Fc receptors. Following the incubation with the corresponding fluorochrome-conjugated antibodies (positive markers anti-CD11b-APC and anti-Ly6C and negative marker anti-F4/80-PerCP-Cy5.5) for 20 min at 4˚C in darkness at the recommended concentrations regarding the manufacturers' instructions, cells were washed with Buffer I supplemented with 10% FBS. Finally, cells were resuspended in 0.5 ml PBS to be analysed by flow cytometry (Becton Dickinson LSRFortessa™). We measured the percentage of positive cells and/or the intensity of fluorescence.

2. MOUSE AIR POUCH MODEL (MAP)

To study the effects of the MSC and conditioned medium from MSC (CM) in the innate inflammatory response, we induced with zymosan an innate inflammatory process at two-time points (4 h and 18 h) using the air pouch model in CD1 male mice of 8-10 weeks of age. Mice were maintained at 21˚C ± 2˚C on a 12-h light/dark cycle with feed and water *ad libitum.* All the animal experiments were approved by the Institutional Animal Care and Use Committee of the University of Valencia, Spain.

The air pouch was produced on the back of the animal injecting subcutaneously 10 ml of sterile air through a 0.22 µm filter (day 0). Mice were re-injected in the same area with 5 ml of sterile air three days later (day 3) (**Figure 14**).

Figure 14. Air pouch model. Image of a CD1 male mouse with a dorsal air pouch.

Six days after the initial injection (day 6), 1 ml of saline buffer or 1 ml of 1% wt/vol zymosan (Sigma-Aldrich®) in saline buffer was injected into the air pouch subcutaneously. One hour later, MSC (2×10^6 MSC) in medium, CM or medium (500 µl) were injected into the air pouch. Different experimental groups were used, as indicated in Results: control medium (M) (DMEM HAM's F-12 medium containing 15% FBS and 1% penicillin/ streptomycin), control MSC (C), conditioned medium from MSC (CM), zymosan control (Z), zymosan with MSC (Z+C), zymosan with CM (Z+CM). All treatments were administered by injection into the air pouch (**Figure 15**). In addition, other control groups were used such as a group injected only with saline and a group injected with zymosan + saline. Some experiments assessed the effects of CM concentrated by lyophillization or by filtration, as indicated in Results.

At 4 h and at 18 h after the zymosan stimulation, mice were sacrificed by cervical dislocation and the exudate of the air pouch was collected. Cells in the exudate were determined with a Coulter counter. After centrifuging the exudates at 10,000 x g for 5 min at 4˚C,

supernatants were collected and frozen at -80˚C to measure the levels of cytokines (IL-1β, TNF-α, IL-6, IL-10, Tumor necrosis factor-inducible gene 6 protein (TSG-6)), chemokines (KC, Monocyte chemoattractant protein-1 (MCP-1)), eicosanoids (prostaglandin E_2 (PGE_2), leukotriene B_4 (LTB_4)) and myeloperoxidase (MPO) activity.

Cell pellets were lysed and centrifuged at 10,000 x g for 10 min at 4˚C. Supernatants were collected and protein concentration was evaluated by use of the DC protein reagent (BioRad). Proteins (30 µg) were separated with the use of sodium dodecyl sulfate-polyacrylamide gel electrophoresis (12.5%) and transferred to polyvinylidene difluoride (PVDF) membranes. Membranes were blocked with 5% non-fat dry milk and incubated with specific polyclonal antibodies against cyclooxygenase-2 (COX-2) (Millipore®) and microsomal prostaglandin E_2 synthase-1 (mPGES-1) (Cayman Chemical) for 2 h at room temperature or overnight at 4˚C, respectively. β-Actin (Sigma-Aldrich®) was used as protein loading control. Finally, membranes were incubated with peroxidase-conjugated polyclonal goat anti-rabbit immunoglobulin (Ig)G (Dako), and the immunoreactive bands were visualized by means of enhanced chemiluminescence (ECL™, GE Healthcare) through the use of an AutoChemi image analyzer (UVP Inc). Band intensity was analyzed by use of optical densitometry with the use of ImageJ analysis software (National Institutes of Health, USA). Band densities were corrected for background, and protein levels were normalized against β-actin.

The MAP model was also used to study the effects of cobalt protoporphyrin IX (CoPP)-treated MSC and their CM in the innate inflammatory response at the 18 h time-point of the zymosan inflamed air-pouch model. CoPP is a well-known heme oxygenase-1 (HO-1) inducer. MSC were first seeded onto 75 cm^2 flasks with 15 ml of culture medium (DMEM HAM's F-12 supplemented with 15% FBS and 1% penicillin/streptomycin). After reaching confluence, cells were incubated with CoPP at a final concentration of 10 µM for 48 h. CoPP-treated MSC (2 x 10^6 MSC) (C_{CoPP}) in medium and 500 µl of their

CM (CM_{CoPP}) were separately injected into the air pouch of mice in the presence or absence of zymosan. Control groups such as control zymosan (Z), control medium (M), control MSC (without CoPP) (C), control CM (without CoPP) (CM) were used (**Table 2**).

Control groups without zymosan	**Groups with zymosan**
M (culture medium)	Z Zymosan
C (2×10^6 MSC)	Z+C (2×10^6 MSC)
C_{CoPP} (2×10^6 MSC incubated with CoPP)	Z+C_{CoPP} (2×10^6 MSC incubated with CoPP)
CM	Z+CM
CM_{CoPP} (CM from MSC incubated with CoPP)	Z+CM_{CoPP} (CM from MSC incubated with CoPP)

Table 2. Experimental groups of MAP model (for CoPP-treated MSC)

Mice were sacrificed by cervical dislocation 18 h after zymosan administration and the exudate from the air pouch was collected. Cells in the exudate were determined with a Coulter counter. Cells were centrifuged at 10,000 for 5 min at 4˚C and supernatants were collected and frozen at -80˚C to measure the levels of cytokines (IL-1β, TNF-α), chemokines (KC), eicosanoids (PGE_2), nitrite and MPO activity. Cell pellets were lysed and centrifuged at 10,000 x g for 10 min at 4˚C. Supernatants were collected and protein concentration was evaluated by use of the DC protein reagent (BioRad). Proteins were separated and visualized similarly as described above to determine HO-1 expression. The incubation of the antibody against HO-1 (Enzo life Science) was overnight at 4˚C.

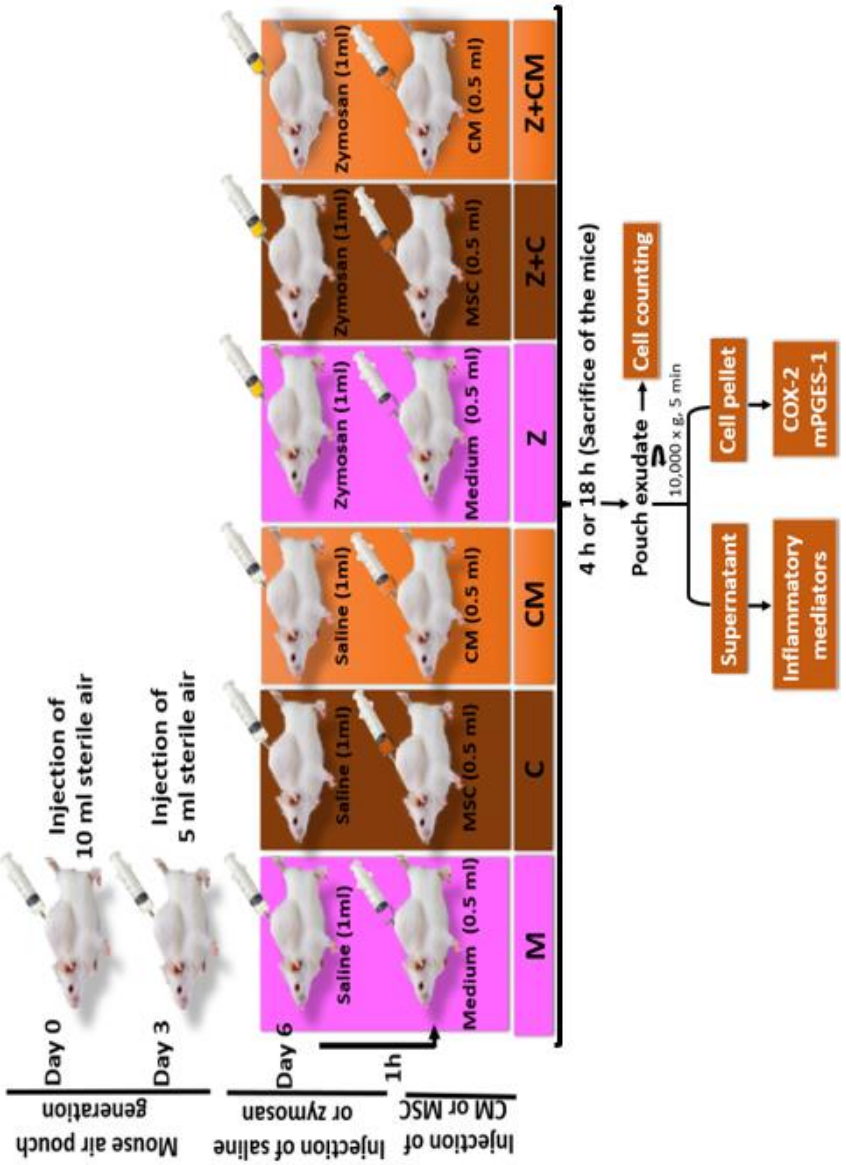

Figure 15. Experimental design of the MAP model. Experimental groups included control medium (M), control MSC (C), conditioned medium (CM), zymosan control (Z), zymosan treated with MSC (Z+C) and zymosan treated with CM (Z+CM). Z indicates 1% zymosan in saline; MSC, 2 x 10^6 cells in medium; Medium: DMEM HAM's F-12 medium (Sigma-Aldrich®) containing 15% FBS, 1% penicillin/streptomycin

3. CONDITIONED MEDIUM FROM ADIPOSE TISSUE-DERIVED MSC

3.1. Proteomic analysis

3.1.1. Albumin depletion and electrophoresis of the samples

FBS contains several growth factors, proteins and other components. Serum albumin is a highly abundant protein in FBS. To detect and analyse less abundant proteins, removal of this highly abundant protein is necessary. Since CM obtained from MSC and complete DMEM HAM's F-12 medium contained 15% FBS, they were first albumin-depleted in a cibacron blue affinity column (**Figure 16**) that specifically retains this protein using the affinity chromatography kit (Zeulab) according to manufacturer's instructions.

Figure 16. Albumin depletion from the sample. To deplete specifically the albumin from the CM samples, a cibacron blue affinity column was used.

After removing the albumin from the samples, trichloroacetic acid (TCA) (10% final concentration) was used to precipitate the proteins overnight at 5˚C. Then, the supernatant was discarded by centrifugation at 14,000 x g, at 5˚C for 1 h and the pellet was rinsed

with acetone (-20˚C). The supernatant was removed by centrifugation as previously described. Next, pellet was air dried and resuspended in 50 µL of 0.5 M ammonium bicarbonate (ABC) by sonication and vigorous shaking. Protein concentration was determined at 280 nm by a Nanodrop and then 25 µg and 50 µg of protein of each sample were loaded by duplicate in 1D polyacrylamide gel electrophoresis (PAGE) gels to verify the albumin removal. Two different gels were used: a commercial gel (Any KD of Bio-Rad of 0.5 mm) and a gel of 12% acrylamide and a width of 1.5 mm. Then, the samples used to determine the amount of proteins were from the lane with 50 µg of loaded protein.

Before determining the amount of protein by liquid chromatography and tandem mass spectrometry (LC-MS/MS), samples (lane 50 µg) were digested with sequencing grade trypsin (Promega) as described elsewhere (Shevchenko *et al*., 1996). 300 ng of trypsin in 150 µL of ABC solution was used for each sample. The digestion was stopped with trifluoroacetic acid (TFA) (1% final concentration), a double extraction with acetonitrile (ACN) was done and all the peptide solutions were dried in a rotatory evaporator. The top and down peptide digested solutions were combined and dried. The final mixture was resuspended with 7 µL of 2% ACN; 0.1% TFA.

3.1.2. Liquid chromatography and tandem mass spectrometry (LC–MS/MS)

5 µl of each sample were loaded onto a trap column (NanoLC Column, 3 µ C18-CL, 350 µm x 0.5 mm; Eksigent) and desalted with 0.1% TFA at 3 µl/min during 5 min.

The peptides were then loaded onto an analytical column (LC Column, 3 µm C18-CL, 75 µm x 12 cm, Nikkyo) equilibrated in 5% acetonitrile 0.1% formic acid (FA). Elution was carried out with a linear gradient of 5% to 35% B in A for 120 min. (A: 0.1% FA; B: ACN, 0.1% FA)

at a flow rate of 300 nl/min. Peptides were analysed in a mass spectrometer nanoESI qQTOF (5600 TripleTOF, ABSCIEX).

Eluted peptides were ionized applying 2.8 kV to the spray emitter. Analysis was carried out in a data-dependent mode. Survey MS1 scans were acquired from 350–1250 m/z for 250 ms. The quadrupole resolution was set to 'UNIT' for MS2 experiments, which were acquired 100–1500 m/z for 25 ms in 'high sensitivity' mode. Following switch criteria were used: charge: 2+ to 5+; minimum intensity; 70 counts per second (cps). Up to 50 ions were selected for fragmentation after each survey scan. Dynamic exclusion was set to 15 s. The system sensitivity was controlled with 2 fmol of 6 proteins (LC Packings).

Sample processing and protein quantification of each sample were performed by liquid chromatography and tandem mass spectrometry (LC-MS/MS) in the Central Service for Experimental Research (SCSIE, University of Valencia).

3.2. Chemokines array

An array is a membrane-based sandwich immunoassay where a collection of capture antibodies is spotted and fixed on a membrane and the interaction between the antibody and its target antigen is detected.

The array used to determine chemokines was the Mouse chemokine Array C1 from RayBiotech that measures up to 25 chemokines in a single assay (**Figure 17**). The chemokines analysed in these membranes were:

6 Ckine (C-C motif chemokine ligand(CCL)21), B lymphocyte chemoattractant (BLC) (C-X-C motif chemokine ligand (CXCL)13), cutaneous T cell-attracting chemokine (CTACK) (CCL27), CXCL16, Eotaxin-1 (CCL11), Eotaxin-2 (CCL24), Fractalkine (CX3CL1), Interferon-inducible T-cell alpha chemoattractant (I-TAC) (CXCL11), keratinocyte-

derived cytokine (KC) (CXCL1), LPS-inducible CXC chemokine (LIX) (CXCL5), monocyte chemoattractant protein (MCP)-1 (CCL2), MCP-5, macrophage-derived chemokine (MDC) (CCL22), monokine induced by gamma interferon (MIG) (CXCL9), macrophage inflammatory protein (MIP)-1 α (CCL3), MIP-1γ, MIP-2 (CXCL2), MIP-3β (CCL19), MIP-3α (CCL20), platelet factor-4 (PF-4) (CXCL4), regulated upon activation normal T cell expressed and secreted (RANTES) (CCL5), stromal-derived factor-1 (SDF-1) (CXCL12), thymus and activation regulated chemokine (TARC) (CCL17), I-309 (T cell activation gene-3, TCA-3) (CCL1) and thymus-expressed chemokine (TECK) (CCL25).

	A	B	C	D	E	F	G	H
1	POS	POS	NEG	NEG	6Ckine (CCL21)	BLC (CXCL13)	CTACK (CCL27)	CXCL16
2								
3	Eotaxin-1 (CCL11)	Eotaxin-2 (CCL24)	Fractalkine (CX3CL1)	I-TAC (CXCL11)	KC (CXCL1)	LIX	MCP-1 (CCL2)	MCP-5
4								
5	MDC (CCL22)	MIG (CXCL9)	MIP-1 alpha (CCL3)	MIP-1 gamma	MIP-2	MIP-3 beta (CCL19)	MIP-3 alpha (CCL20)	PF-4 (CXCL4)
6								
7	RANTES (CCL5)	SDF-1 (CXCL12)	TARC (CCL17)	I-309 (TCA-3/CCL1)	TECK (CCL25)	BLANK	BLANK	POS
8								

Figure 17. Mouse chemokine Array C1 from RayBiotech. Detection of 25 chemokines.

The array was used to evaluate the chemokines present in the CM obtained from MSC. The array was performed according to the manufacturer's instructions (**Figure 18**).

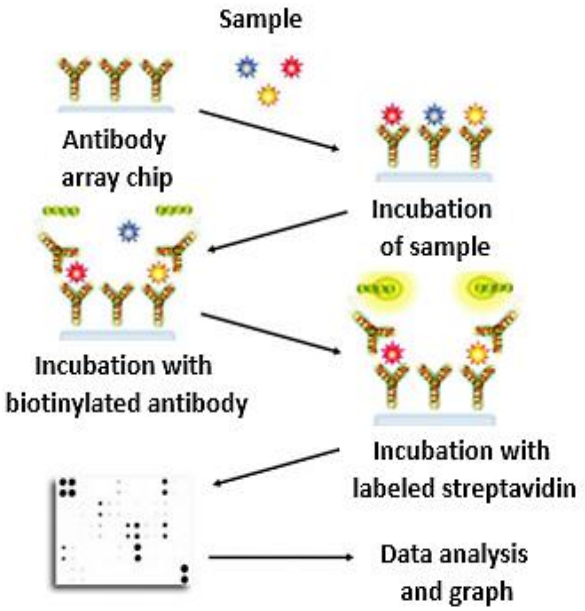

Figure 18. Array description. Capture antibodies spotted and fixed on a membrane. When the sample is added onto the membrane, the target antigens bind with the corresponding antibodies. After the two incubations with biotinylated antibody and with labelled streptavidin, respectively, data can be analysed.

3.3. Isolation and characterisation of extracellular vesicles

3.3.1. Extracellular vesicles

There are different procedures to isolate EV based on their biophysical and biochemical properties. Differential centrifugation combined with size filtration is a well-established and commonly used method to isolate EV (Coumans *et al*., 2017).

First, MSC were seeded onto 175 cm^2 flasks with 30 ml of medium DMEM HAM's F-12, 15% EV-depleted FBS, 1% penicillin/streptomycin. EV-depleted FBS was previously generated by 100,000 x g

centrifugation, for 18 h at 4˚C and then the supernatant was collected and stored at -80˚C until use.

The method used to isolate both types of EV, large and small ones, (Mv and Ex, respectively) from CM obtained from MSC was differential centrifugation combined with size filtration based on the size and density of EV increasing sequentially the centrifugal force (from 12,600 x g to 100,000-120,000 x g) to pellet the EV and decreasing the size of the pore from the filter to avoid contamination of vesicles from different sizes. CM obtained from MSC was collected at 48-72h at P1 and centrifuged at 300 x g for 10 min at 4˚C to remove cells. After filtering the supernatant through a 5 µm filter (Millipore) by hydrostatic pressure, it was centrifuged at 2,000 x g for 10 min to pellet the apoptotic bodies, that were washed with PBS, resuspended in 600 µl and centrifuged again at 2,000 x g for 10 min. Finally, the pellet was resuspended in 15 µl of PBS and stored at 4˚C for further analysis. Then, the supernatant that contained the Mv and Ex was filtered through a 0.8 µm filter (Millipore) by hydrostatic pressure and centrifuged at 12,600 x g for 30 min to pellet the Mv. This pellet was washed several times with PBS and centrifuged as previously described. Finally, it was resuspended in 15 µl in PBS. To obtain the Ex, supernatant was filtered through a 0.22 µm filter and then ultracentrifuged at 100,000 x g for 70 min (Beckman Coulter). The pellet (with Ex) was washed several times with PBS and finally resuspended in 15 µl of PBS. The supernatant after the first ultracentrifugation (EV-free CM) was stored at -80˚C for further experiments (**Figure 19**).

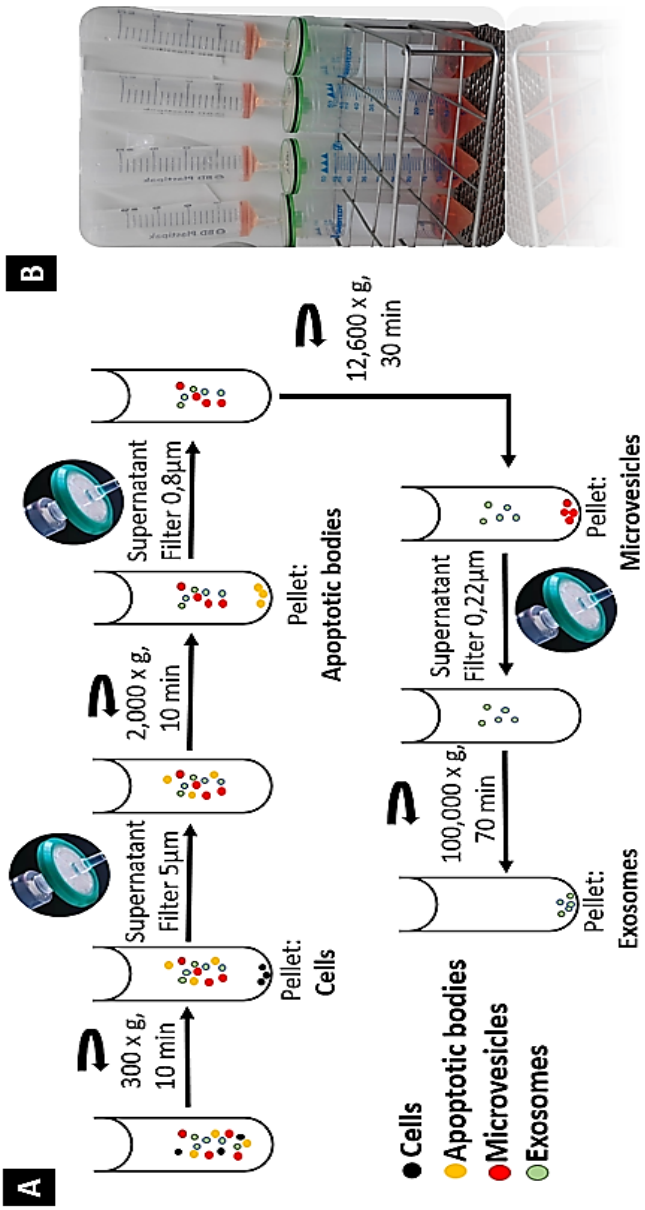

Figure 19. Representative scheme of the EV isolation (A) and an image of the instruments used (B). Differential centrifugation combined with size filtration was the method used to isolate the EV.

3.3.2. Tunable resistive pulse sensing (qNano system)

There is no reliable method to characterise EV. For this reason, we need to use at least two different methods to characterise them in a proper manner. For this purpose we used tunable resistive pulse sensing (TRPS) technology and transmission electron microscopy.

Size distribution and concentration of EV were determined by TRPS (qNano system from Izon). This consists of two fluid cells that are separated by a non-conductive elastic membrane with a nanopore that can measure the size and concentration of single particles suspended in an electrolyte by applying a voltage. The particles (for example, MV or Ex) suspended in electrolyte (PBS filtered through a 0.22 µm filter) are applied to the upper fluid cell, whereas the lower fluid cell is filled with the electrolyte free from particles (particle-free electrolyte). After applying a voltage and pressure, Mv or Ex are driven through the nanopore producing an alteration of the electric current also called resistive pulse or "blockade" signal that is detected and measured by the application software. The size distribution of the particles (volume of each particle) is determined with the blockade magnitude (resistive pulse), whereas the particle concentration is determined with the blockade frequency. To calculate the surface charge of each particle, blockade duration is used. This blockade duration changes with the velocity of the particle (**Figure 20**).

To determine the size distribution and the concentration of Mv or Ex (unknown sample), single calibration sample with particles of known concentration and particle size were used. To measure the concentration and size distribution of Mv and Ex, a nanopore NP300 and NP150 were used, respectively and carboxylated polystyrene particle standards CPC400 and CPC200 (Bonsai) were diluted in PBS (+0.03% w/v Tween 20 in case of Ex).

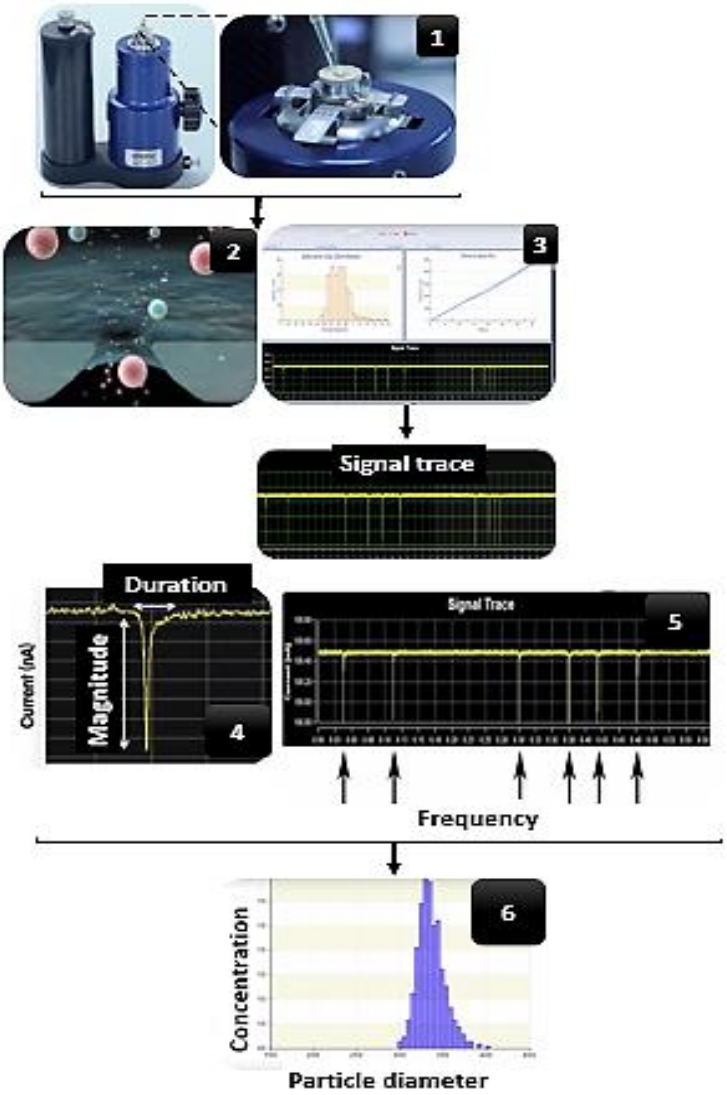

Figure 20. Representative scheme of TRPS (qNano system). A suspension with Mv or Ex is applied to the upper fluid cell (1). Then, Mv and Ex are driven through the nanopore after applying determined voltage and pressure (2) and detected and measured by the application software (3). The magnitude of the current is used to determine the size distribution of the particles (volume of each particle) (4). The blockade duration is used to calculate the surface charge of each particle (4). The blockade frequency is used to determine the particle concentration (5). Finally, results of concentration and size distribution (particle diameter) are represented (6).

3.3.3. Transmission electron microscopy of EV preparations

To determine the presence of Mv and Ex and characterise their morphology and size, pellets were fixed in Karnovsky's solution (Doughty *et al.*, 1997). After rinsing the samples with PBS and post-fixed in osmium tetroxide, they were dehydrated in graded ethanol and embedded in LR-White resin. Following overnight polymerization of samples at 60˚C, resin blocks were cut with the ultramicrotome Ultracut UC6 Leica. The ultrathin sections (60 nm) obtained were contrasted with uranyl acetate and lead citrate and observed using Jeol JEM-1010 transmission electron microscope at 80 kV (**Figure 21**).

Figure 21. Transmission electron microscopy. Preparing the sample and mounting it (red arrow) in the holder (upper image). Transmission electron microscopy (bottom image).

4. MTT assay

The 3-(4,5-dimethylthiazol-2-yl)-2,5 diphenyltetrazolium bromide (MTT) assay consists of the reduction of MTT to its insoluble formazan by the succinate dehydrogenase enzyme from the mitochondria in living cells turning the yellow colour from MTT into purple colour (formazan) (**Figure 22**).

To determine the viability of the macrophages treated with EV, EV-free CM and CM in presence or absence of LPS (1 µg/µl) for 20 h, the cells were incubated with MTT (200 µg/ml) for 90 min at 37˚C in the dark. Then, after removing the medium, cells were solubilized in dimethyl sulfoxide (150 µL) to quantitate formazan at 490 nm in the spectrophotometer VICTOR 2TM V 1420 multilabel counter (Perkin Elmer, Madrid, Spain). The value of the absorbance is proportional to the number of viable cells present. Viability of untreated and unstimulated cells was considered as 100%. Results from other treated and stimulated cells were calculated regarding the viability of the untreated and unstimulated cells.

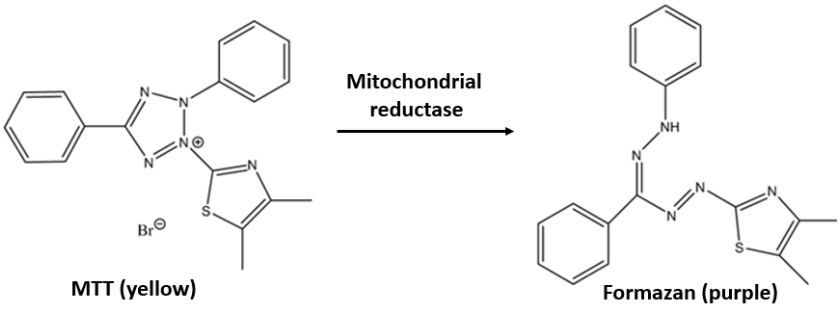

Figure 22. Reduction of MTT to formazan.

5. Enzyme Linked Immuno Sorbent Assay (ELISA)

Several cytokines were measured by enzyme-linked immunosorbent assay (ELISA) in different experiments according to the manufacturer's instructions using the Victor^2 Wallac, 1420 multilabel Counter:

- MAP assay: the cytokines measured in the supernatant of the exudate were IL-1β, TNF-α, IL-6, KC, IL-10, TSG-6 and MCP-1.
- Macrophages and chemotaxis assay: the cytokines measured in the supernatant were IL-1β, TNF-α, KC, MCP-1 and MCP-5.

Cytokine	Company	Range detection or Sensitivity
IL-1β	R&D Systems®	15.6 to 1000 pg/ml
TNF-α	R&D Systems®	31.2 to 2000 pg/ml
IL-6	eBioscience™ Inc.	4.0 pg/ml
IL-10	eBioscience™ Inc.	5.0 pg/ml
TSG-6	Antibodiesonline	62.5 to 4000 pg/ml
KC	PromoKine	8.0 pg/ml
MCP-1	RayBiotech	2.74 to 2000 pg/ml
MCP-5	eBioscience™ Inc.	1.58 pg/ml

Table 3. Cytokines measured by ELISA.

6. Determination of eicosanoids by radioimmunoassay

Radioimmunoassay (RIA) was used to determine the concentration of PGE_2 and LTB_4 in the supernatant of the exudates in

the MAP assay and in the supernatant of cultured peritoneal macrophages with the radioactive labelled with tritium ^{3}H-PGE_2 ([5,6,8,9,11,12,14,15, (n)-^{3}H] PGE_2 from GE Healthcare Life Sciences, Barcelona, Spain) or ^{3}H-LTB_4 [5,6,8,9,11,12,14,15 ^{3}H(N)] LTB_4 from PerkinElmer, Boston, MA, USA (Moroney *et al*., 1988). This technique detects the radioactivity (β emissions) from the samples with an unknown eicosanoid concentration and is based on the competitive binding, where a radioactive antigen (a known concentration of radioactive PGE_2 or LTB_4) competes with a non-radioactive antigen (an unknown concentration of PGE_2 or LTB_4 from the sample) for a fixed number of antibody binding sites. Thus, the higher concentration of **unlabelled eicosanoid** in the sample, the lower amount of **radioactive eicosanoid** will bind to the antibody and less radioactive emissions will be detected. The levels of radioactivity in counts per minute (cpm) were detected by scintillation counter (1450 Microbeta Trilux, Liquid Scintillation and Luminescence counter).

To measure the concentration of PGE_2 and LTB_4 in the samples, samples and standards were added into tubes and diluted with specific buffers at pH 7.4:

- **For PGE_2**
  -Buffer A1 (1.19 g/l of NaH_2PO_4 x $2H_2O$, 4.6 g/l of Na_2HPO_4, 0.1% of BSA and 0.1% of sodium azide) and buffer B1 (Buffer A1 with 9 g/l of NaCl).

- **For LTB_4**
  -Buffer A1 (1.19 g/l of NaH_2PO_4 x $2H_2O$, 4.6 g/l of Na_2HPO_4, 9 g/l of NaCl, 1 g/l of γ-globulin and 0.1% of sodium azide).

Then, the antibody anti-PGE_2 or anti-LTB_4 (Sigma-Aldrich®) and tritiated PGE_2 or LTB_4 were also added into the tubes which were incubated for 18 h at 4˚C. After incubation, activated carbon-dextran suspension was added to the tubes and incubated for 10 min at 4˚C. Later, tubes were centrifuged at 1,000 x g for 15 min at 4˚C and

tritiated and non-tritiated PGE_2 or LTB_4 that did not bind to the antibody were precipitated. Finally, the supernatant where eicosanoids were bound with the antibody were transferred into vials with scintillation liquid Optiphase "Supermix" (Perkin Elmer, Waltham, MA, USA) and the concentration of the tritiated eicosanoids bound to the antibody were determined using the scintillation counter Microbeta Trilux (Wallac, Turku, Finland). The values obtained were interpolated in the standard curve of PGE_2 and LTB_4.

7. Determination of MPO activity

Most of the inflammatory effects produced by neutrophils are due to releasing of the content of their intracellular granules by a process called degranulation of MPO and proinflammatory mediators.

MPO activity was measured in 96-well plates (De Young *et al.,* 1989). Supernatant of the exudates from MAP were incubated with PBS (pH 7.4) and sodium phosphate buffer solution (pH 5.4). After adding hydrogen peroxide (0.052%) the wells were incubated at 37˚C for 5 min. Then, 3,3',5,5'-tetramethylbenzidine (TMB) substrate solution (eBioscience™) was added and colour developed in proportion to the activity of MPO. After incubation, the reaction was stopped by sulphuric acid 2N. MPO activity quantification was performed by measuring the absorbance at 450 nm by the spectrophotometer VICTOR 2 Wallac 1420 multilabel counter.

The work solutions of hydrogen peroxide and sodium phosphate buffer (pH 5.4) used for this experiment were the following:

- Work solution of hydrogen peroxide 0.052% was freshly prepared and stored on ice, by dilution of hydrogen peroxide solution 30% (p/v) (Sigma) with distilled water.

- Sodium phosphate buffer (pH 5.4): 0.0866 % Na_2HPO_4 and 1.153 % NaH_2PO_4.

8. Determination of nitrite by fluorometry

The technique used to measure the levels of nitrite in the supernatant of macrophages and in the supernatant of exudates in MAP assay consists of a reaction of nitrite ion with 2,3-diaminonaphthalene (DAN) producing 1-(H)-naphtotriazole that emits fluorescence at 450 nm (**Figure 23**). Fluorescence intensity is proportional to the amount of nitrite released by the cells.

Macrophages were seeded on 24-well plates at 3 x 10^5 cells/well. After stimulation (with LPS) and the treatment of the cells with EV, CM and EV-free CM for different time points, 10 µl of the supernatant was collected and added into plates to measure fluorescence with 90 µl of saline. Sodium nitrite diluted in saline was used for the preparation of the standard curve. Then, 10 µl of DAN solution (50 µg/ml) was added into each well for 7 min in the dark at room temperature. Reaction was stopped by adding 10 µl/well of NaOH (1.4 M) for 10 min in the dark at room temperature. Finally, fluorescence was measured at 365 nm of excitation wavelength and 450 nm of emission with the spectrophotometer VICTOR 2TM V 1420 multilabel counter.

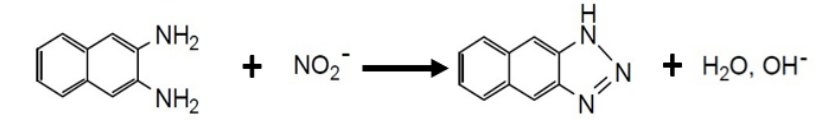

2,3-Diaminonaphtalene **Naphtotriazole**

Figure 23. Reaction of 2,3-Diaminonaphthalene with nitrite ion producing naphtotriazole.

9. Immunofluorescence

Cells present in air pouch exudates (MAP model) 4 h after zymosan administration were plated on an eight-well Lab-Tek chamber slide (Thermo Fisher Scientific) in an incubator at standard conditions. After adherence, cells were washed with PBS and fixed with the use of 4% (wt/vol) p-formaldehyde for 15 min. After washing

with PBS, 0.01% (vol/vol) Nonidet P-40 in PBS was added to each well for 5 min at room temperature to permeabilize the cells, followed by several washes with PBS. Cells were incubated overnight at 4˚C with monoclonal antibodies against P-p65 NF-κB (Ser 536) and total p65 NF-κB (Cell Signaling Technology). Goat anti-rabbit IgG-carboxyfluorescein (R&D Systems®) was used as a secondary antibody for 30 min at room temperature in the dark. Each section was examined under a fluorescence microscope (Leica DM IL LED). Cells were counted in six microscopic fields of each well and expressed as the ratio between cells positive for P-p65 NF-κB and those positive for total p65 NF-κB.

10. MIGRATION ASSAY

Migration assay was performed using transwell system with neutrophils and monocytes.

10.1. Neutrophils

In vitro migration assay of neutrophils was performed using a transwell system (6.5 mm-diameter polycarbonate membranes with 3 µm-diameter pores; Corning). In the upper compartment neutrophils were added, whereas in the lower compartment macrophages were seeded. Resident peritoneal macrophages were seeded at 3 x 10^5 cells/well in 500 µl of RPMI medium supplemented with 10% FBS and 1% penicillin/streptomycin on the lower compartment of transwells in a 24-well plate. Cells were maintained at 37˚C and 5% CO_2. Procedure of macrophages was developed as previously described in **section 1.3**.

Macrophages were incubated with 18 x 10^6 Ex/ml, 9 x10^4 Mv/ml, 500 µl CM and 500 µl EV-free CM in the presence or absence of 1 µg/ml LPS. Twenty hours later, 5 x 10^5 neutrophils were added to the upper compartment of the transwells (insert) and they were allowed to migrate to the lower compartment for 4 h. After this time, migrated cells and macrophages were harvested from the lower compartment,

and migrated neutrophils were determined using a flow cytometer (Becton Dickinson LSRFortessa™). Three migration assays were performed. The supernatants were collected to determine KC levels. DMEM HAM's F-12 with 10% EV-depleted FBS and 1% penicillin/streptomycin was used as a negative control and recombinant murine KC (PeproTech, Rocky Hill, USA) was used as a positive control (**Figure 24**).

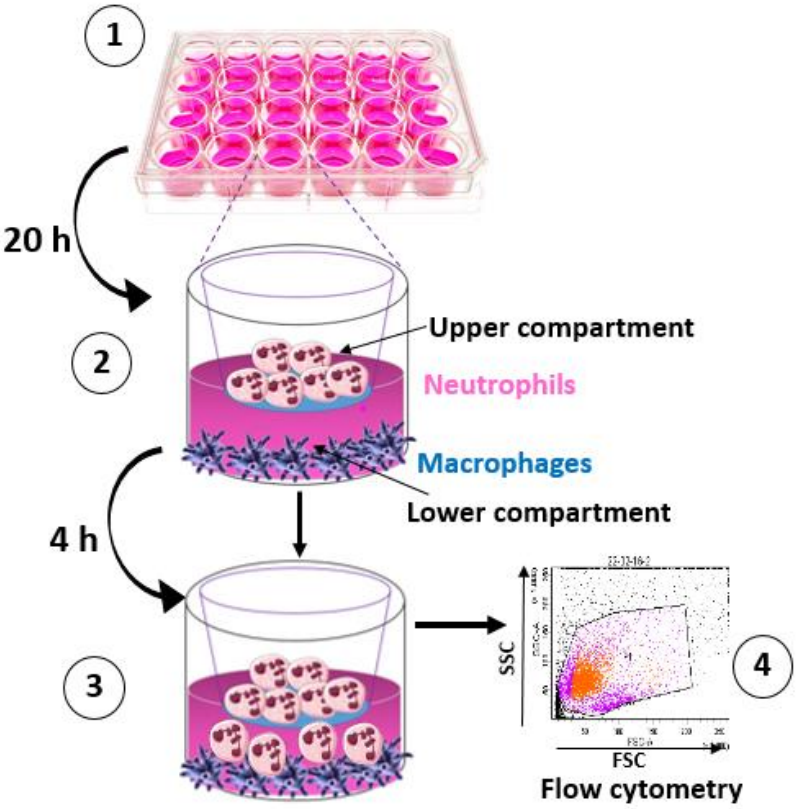

Figure 24. Neutrophils migration assay. Macrophages were incubated with EV, CM, EV-free CM in presence and absence of LPS (1 µg/ml) for 20 h (1). Then, neutrophils were added in the upper compartment (2) and were allowed to migrate to the lower compartment for 4 h (3). Finally, migrated cells and macrophages were harvested from the lower compartment, and migrated neutrophils were determined using a flow cytometer (4).

10.2. Monocytes

In vitro migration assay of monocytes was performed using a transwell system (6.5 mm-diameter polycarbonate membranes with 5 µm-diameter pores; Corning). In the upper compartment monocytes were added whereas in the lower compartment macrophages were seeded. Resident peritoneal macrophages were seeded at 3 x 10^5 cells/well in 500 µl of RPMI medium supplemented with 10% FBS and 1% penicillin/streptomycin on the lower compartment of transwells in a 24-well plate. Cells were maintained at 37˚C and 5% CO_2. Procedure of macrophages was developed as previously described in **section 1.3**. Macrophages were incubated with 18 x 10^6 Ex/ml, 9 x10^4 Mv/ml, 500 µl CM and 500 µl EV-free CM in the presence or absence of 1 µg/ml LPS. Twenty hours later, 5 x 10^5 monocytes were added to the upper compartment of the transwells (insert) and they were allowed to migrate to the lower compartment for 4 h. After this time, migrated cells and macrophages were harvested from the lower compartment, and migrated monocytes were determined using a flow cytometer (Becton Dickinson LSRFortessa™). Three migration assays were performed. The supernatants were collected to determine MCP-1 and MCP-5. DMEM HAM's F-12 with 10% EV-depleted FBS and 1% penicillin/streptomycin was used as a negative control and recombinant protein MCP-1 and MCP-5 (PeproTech, Rocky Hill, USA) were used as positive controls.

11. Phagocytosis assay by flow cytometry

Peritoneal exudate cells were seeded at 3 x 10^5 cells/well in 500 µl of RPMI with 10% FBS and 1% penicillin/streptomycin on a 24-well plate. Cells were maintained at 37˚C and 5% CO_2. Non-adherent cells were removed. Before performing the experiment, medium was replaced by DMEM HAM's F-12 supplemented with 10% EV-depleted FBS and 1% penicillin/streptomycin.

Cells were incubated with 18 x 10^6 Ex/ml, 9 x10^4 Mv/ml, 500 µl CM, and 500 µl EV-free CM in presence or absence of 1 µg/ml LPS for 20 h. Then, macrophages were incubated with 10 fluorescent polystyrene beads/cell (FluoSpheres® Molecular Probes, Invitrogen) and the phagocytosis process was allowed to proceed for 4 h. Phagocytosis was stopped by adding cold PBS into the wells or putting the plate on ice for 30 seconds. Macrophages were rinsed 3 times with PBS to wash off the extracellular beads and cells were collected, fixed with paraformaldehyde and phagocytic cells were determined by flow cytometry (Becton Dickinson LSRFortessa™). Fluorescent beads and macrophages without beads were used as controls. Phagocytic cells were determined as the median of fluorescence intensity (**Figure 25**).

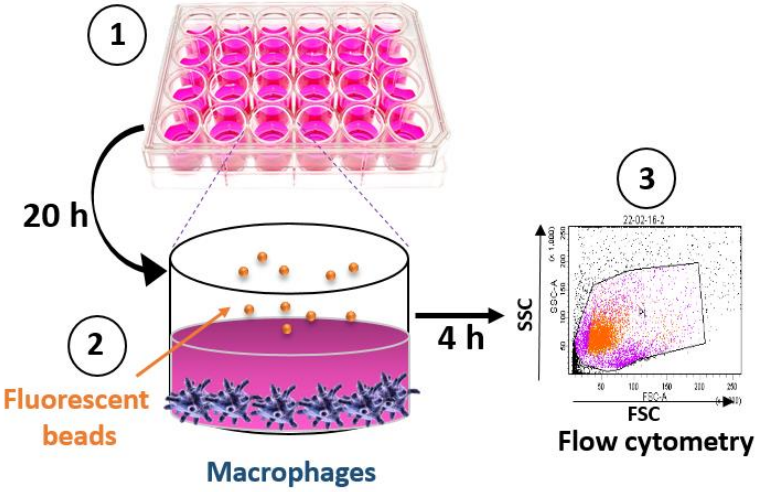

Figure 25. Representative scheme of the phagocytosis assay. Macrophages were incubated with EV, CM, EV-free CM in presence or absence of LPS (1µg/ml) for 20 h (1). Then fluorescent polystyrene beads were added (10 beads/cell) (2). After 4 h of phagocytosis, cells were collected, and the phagocytic activity was measured by flow cytometry (3).

12. Phagocytosis assay by confocal microscopy

The procedure was similar to that used for flow cytometry with the following differences: 1.2 x 10^5 cells were seeded onto wells from

Chamber slides (Labtek™, Thermo Scientific™). Cells were incubated with 18 x 10^6 Ex/ml, 9 x 10^4 Mv/ml, 400 µl CM and 400 µl EV-free CM in presence or absence of LPS (1 µg/ml) for 20 h. Cells were incubated with anti-CD11b-APC antibody overnight at 4˚C. Then, slides were mounted in ProLong® Gold Antifade Mountant with DAPI (Molecular Probes™, Invitrogen™) and examined under a confocal microscope (Olympus FV1000, Tokyo, Japan). To quench the fluorescence of beads remained outside of the cells, 0.04 % Trypan Blue solution was added for 30 min.

13. Apyrase activity blockade

Apyrase protein in the samples was blocked in the CM obtained from MSC and in the supernatant of macrophages by using an antibody anti-CANT-1 (Abcam®). Resident peritoneal macrophages were seeded onto 24-well plates (3 x 10^5 cells/well). Prior to the beginning of the experiment medium was changed to medium supplemented with 10% EV-depleted FBS and 1% penicillin/streptomycin. CM from MSC was incubated with antibody anti-CANT-1 at a concentration of 0.01 µg/µl for 2 h approximately at room temperature to block apyrase activity. Then, macrophages were incubated with CM in presence or absence of antibody anti-CANT-1 with or without 1 µg/ml LPS for 20 h. IgG was used as a control at the same concentration of anti-CANT-1. The levels of IL-1β, TNF-α, KC and nitrite were determined in the supernatant of macrophages. IL-1β, TNF-α, and KC were determined by ELISA and nitrite by fluorometry (**Section 5 and 8**, respectively).

14. Determination of ATP concentration

The ATP concentration was determined in the supernatant of macrophages. Mouse macrophages were seeded onto 96-well plates at a concentration of 450,000 cells/ml. After removing the non-adherent cells, 100 µl of CM, EV-free CM (CM EV-), medium DMEM HAM'S F-12 supplemented with 10% EV-depleted FBS and 1% penicillin/streptomycin were added into the wells for 4 h or 20 h in

presence or absence of 1 µg/ml LPS. Then, ATP concentration was measured in the supernatant of macrophages, according to manufacturer's instructions (PerkinElmer, MA, USA). The generation of the luminescent signal is proportional to the amount of ATP present.

15. Statistical analysis

Experimental data were analyzed using the GraphPad Prism version 5.00 for Windows (GraphPad Software). Data are expressed as the mean value ± SEM. The level of statistical significance was determined by using one-way analysis of variance (ANOVA) followed by Bonferroni's multiple comparison test. A value of $P < 0.05$ was considered to indicate statistical significance.

16. CULTURE OF HUMAN CELLS

Within the period of my predoctoral training, I completed two research stays with the purpose of developing other objectives initially proposed in the thesis which included the study of human mesenchymal stem cells. These stays were at the Maimonides Biomedical Research Institute of Cordoba (IMIBIC) and Reina Sofia University Hospital, within the collaboration in the Thematic Network Fragilidad y Envejecimiento (RETICEF ISCIII), and the laboratory of the Pr. E.C.M. Mariman, under the supervision of Dr Johan Renes at the Department of Human Biology NUTRIM School of Nutrition and Translational Research in Metabolism Faculty of Health, Medicine and Life Sciences in Maastricht (The Netherlands). During these stays, I learned different techniques with human mesenchymal stem cells and other human cells which contributed to broaden my experience and enhance my skills. However, I could not apply them in my thesis project due to the difficulty of obtaining human samples with the characteristics necessary to get a good cellular performance. In contrast, I was able to develop in Valencia consistent methods and obtained good preliminary results using mouse cells and animal

models. Therefore, I focused on *in vivo* and *in vitro* studies in mice. The following are some examples of methods with human cells that I developed in preliminary studies previous to the selection of the definitive techniques that gave the results included in this thesis.

16.1. Mesenchymal stem cells from bone marrow

Human MSC were isolated from the bone marrow from healthy donors as previously described (Kotobuki *et al.,* 2004; Casado-Díaz *et al*., 2008). After centrifugation, the cell fraction was seeded onto 75 cm^2 flasks in Minimum Essential Medium (MEM) with Alpha Modifications (α-MEM) (Lonza) supplemented with 10% of FBS, 2 mM of Ultraglutamine, 100 U of ampicillin, 0.1 mg of streptomycin/ml and 1 ng/ml of bFGF (Sigma-Aldrich®) (**Table 4**). Cultures were maintained at 37˚C in 5% CO_2. Medium was changed every 3-4 days until confluence. When cells were confluent they were trypsinized and reseeded with the same culture medium at 500 cells/cm^2 on 6-well and 24-well plates for the differentiation of MSC into osteoblasts. To differentiate MSC into chondrocytes, a pellet culture system was performed in polypropylene conical tubes.

Product	Company
Alpha MEM w/o L-glutamine	Lonza BioWhittaker®
DMEM with 4.5 g/L glucose w/o L-Glutamine	Lonza BioWhittaker®
Ultraglutamine 1, 200 mM in 0.85% NaCl Solution	Lonza BioWhittaker®
Fetal Bovine Serum	Gibco®

Table 4. Culture medium used for MSC before and after differentiation into osteoblasts and chondrocytes. Different types of medium were used for undifferentiated and differentiated MSC.

To differentiate MSC into **osteoblasts** MSC were first seeded onto 6-well and 24-well plates with α-MEM supplemented with 10% FBS,

2 mM UltraGlutamine, 100 U/ml penicillin/100 µg/ml streptomycin as previously described. When cells were 80-90% confluent, the medium was supplemented with 10 nM dexamethasone, 0.2 mM L-ascorbic acid-2 phosphate and 10 mM β-glycerophosphate to induce osteoblastic differentiation (**Table 5**). A final volume of 1.5 ml was added per well to a 6-well plate and 0.5 ml per well to a 24-well plate. The cells seeded on the 24-well plate were used to measure the phosphatase alkaline activity of the cells. The cells seeded on the 6-well plate were used to determine the osteoblast-related gene expression of MSC during the osteoblastic differentiation and to evaluate the calcium deposits by Alizarin red staining. A control of the differentiation was done at different time points: 7, 14 and 21 days. Alizarin red was used to determine the mineralization from the differentiated osteoblasts at the final time point of the osteoblastic differentiation (day 21). The supernatant of cells was removed, and cells were fixed with 4% formaldehyde for 15 min. After several washes in PBS, 1ml of 40 mM of Alizarin red at pH 4.1 was added into each well for 5 min. Then, cells were washed five times with 60% isopropanol (1 min each), dried and visualized under a light microscope (**Figure 26**)**.**

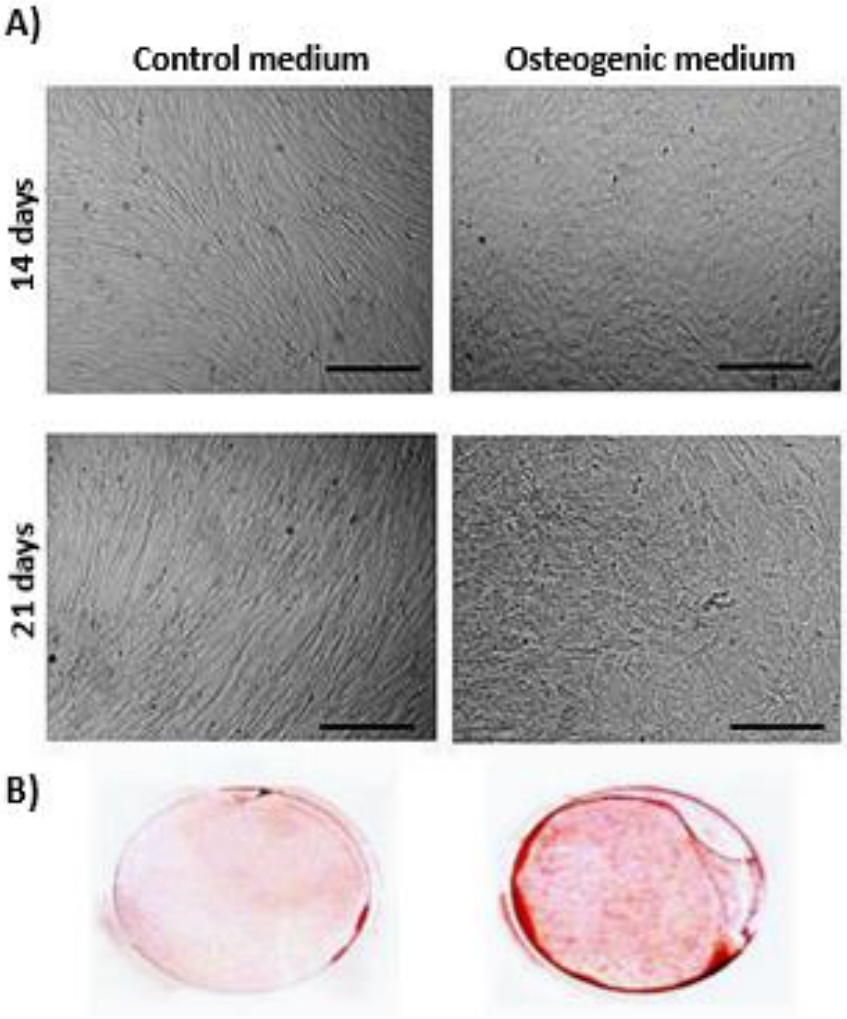

Figure 26. Osteogenic differentiation. Human MSC grown for 14 and 21 days in osteogenic medium and control medium (α-MEM supplemented with 10% FBS, 2 mM UltraGlutamine, 1% antibiotics) on a 6-well plate. Scale bar: 100 µm (A). Alizarin red staining of matrix extracellular mineralization in cultures of human MSC cultured for 21 days in control medium (left image) and in osteogenic medium (right image) (B).

Chondrogenic differentiation was induced by a 21-day culture in micropellet. This culture system allows cell–cell interactions analogous to those that occur in precartilage condensation during embryonic

development (Fell, 1925; Johnstone *et al*., 1998). The medium used to culture the differentiated chondrocytes was DMEM supplemented with glutamine and antibiotics, but without FBS. When cells were 80% to 90% confluent, the medium was supplemented with 100 nM dexamethasone, 0.2 mM L-ascorbic acid-2 phosphate, 0.4 mM L-proline, 1 mM pyruvate, 1x Insulin-Transferrin-Selenium (ITS) and 10 ng/ml Transforming Growth Factor (TGF)-β to induce chondrocyte differentiation (**Table 5**). A final volume of 0.5 ml was added per tube. Chondrocyte-related gene expression of MSC was determined during the chondrocytic differentiation. A control of the differentiation was done at different time points: 7, 14 and 21 days. To fixate undifferentiated and differentiated chondrocyte pellets, they were first collected and mounted in cassettes with biopsy blue pads. After being fixed with formaldehyde, they were dehydrated by immersion in a series of ethanol solutions of increasing concentration, followed by xylene and then paraffin in an automatized processor for paraffin inclusion for 16 h (Semi-enclosed Benchtop Tissue Processor Leica TP1020). Finally, samples were embedded in paraffin blocks where they were sectioned 5 µm using a microtome (Leica RM 2255) and placed in microscope slides (**Figure 27**).

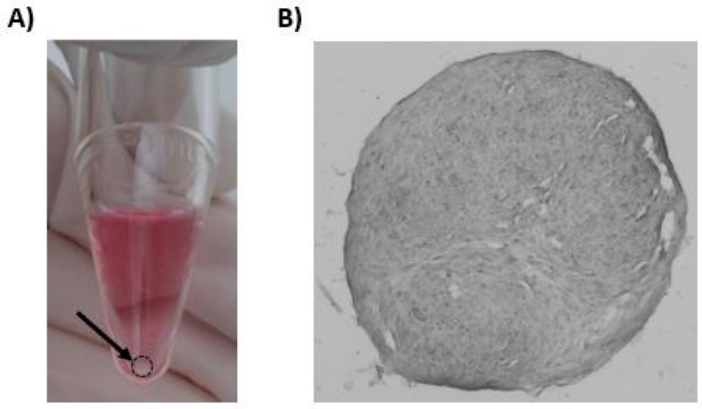

Figure 27. Chodrogenic differentiation. Human MSC pellet after 21 days of chondrogenic induction (arrow) (A). Histological analysis of chondrogenic pellet of human MSC after 21 days of condrogenic induction (x10 magnification) (B).

Product	Company
Sodium pyruvate	Sigma
ITS Liquid media supplement (100x)	Sigma
Ascorbic acid	Sigma
L-proline	Sigma
β-glycerol phosphate disodium salt hydrate	Sigma
TGF-β1	Tebu-bio
bFGF Human	Sigma
Dexamethasone	Sigma

Table 5. Differentiation factors for MSC into osteoblasts and chondrocytes. Different types of factors were used to differentiate MSC into osteoblasts and chondrocytes.

In our laboratory, to know if the adipose mesenchymal stem cells of the bone marrow from people with advanced ages have the same biological activity as young people, we performed preliminary tests with marrow adipose tissue (also known as yellow bone marrow). The marrow adipose tissue was obtained from the hollow interior of the diaphyseal portion of the femur from the knee by inducing an ischemia in the upper femur with a tourniquet. The samples were collected from the femur of approximately 70-year old female and male osteoarthritic (OA) patients. Samples were rinsed with medium and then centrifuged and seeded with Promocyte growth medium (kit from Promocell) onto 6-well plates. Cells were also observed after 24 h using a Leica DM IL LED (Leica Microsystems) microscope. Medium was changed every 2-3 days.

We performed the Oil Red staining with the purpose of knowing if the isolated cells had a preadipocyte phenotype. The tests were carried out with primary cultures of cells that had reached confluence five days after sowing (**Figure 28**).

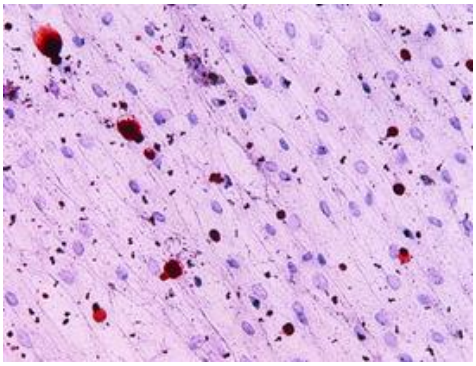

Figure 28. Representative image of Oil Red staining. Primary culture of confluent isolated cells from human marrow adipose tissue of a patient of 74 years old (x10 magnification).

We did not continue this line of research mainly due to the low yield of mesenchymal cells isolated from the bone marrow fat of elderly patients, and the difficulty in characterising them phenotypically.

16.2. Simpson-Golabi-Behmel syndrome (SGBS) preadipocyte strain

Due to the low number of cells present in the fat of the bone marrow of the OA patients, we wanted to start a cell line of human preadipocytes with the objective of knowing if they behaved in a similar way to the preadipocytes extracted from the bone marrow.

The human Simpson-Golabi-Behmel syndrome (SGBS) preadipocyte strain is derived from human subcutaneous adipose tissue and considered a representative human adipose tissue cell model due to their similar features to primary human preadipocytes regarding the morphology, biochemistry and function and often used to study the human adipocyte biology (Wabitsch *et al*., 2001; Fischer-Posovszky *et al.,* 2008). The differentiation yield into adipocytes is very high (up to 90%). This cell strain was used to differentiate the preadipocytes into adipocytes. SGBS cells were thawed and seeded on 75 cm^2 flasks to allow cells to proliferate.

The differentiation of SGBS preadipocytes into **adipocytes** was performed as follows. SGBS preadipocytes were seeded at a concentration of 8 x 10^5-9 x 10^5 cells on 150 mm Petri dishes and cultured until 80 to 90% confluence in 10% FBS-containing DMEM/F12 medium supplemented with 66 nM biotin, 33 nM D-pantothenic acid and 2% penicillin/streptomycin. Every 2 to 3 days the cells were washed with PBS and medium was changed. The number of preadipocytes per Petri dish was 2.68 x 10^6. When SGBS cells reached confluency, serum-free medium with adipogenic factors was added to initiate their differentiation into adipocytes for 14 days. First the Quick differentiation medium was added (0.01 mg/ml of transferrin, 20 nM of insulin, 100 nM cortisol, 0.2 nM triiodothyronine, 25 nM dexamethasone, 200 µM IBMX, 2 µM rosiglitazone) for 4 days (replacing medium every 2 days). Then, this medium was replaced by 3FC medium (0.01 mg/ml of transferrin, 20 nM of insulin, 100 nM cortisol, 0.2 nM triiodothyronine) to continue the adipocyte differentiation for 10 days more. Medium was replaced every 2 days. To check the differentiation of the cells into adipocytes, differentiated cells were observed and counted using a microscope.

Before being differentiated, SGBS cells present a spindle shape morphology. After adding the culture medium with adipogenic factors, most of the cells underwent adipose differentiation accumulating lipids and showing the typical morphological criteria of *in vitro*-differentiated adipose cells, such as round shape and a cytoplasm filled with lipid droplets (**Figure 29**). No morphological differences were observed between SGBS differentiated cells into adipocytes under starving and standard conditions (image not shown). Differentiated SGBS cells into adipocytes were counted in each plate by raster ocular (an average of 2.95 x 10^6 cells/plate). Photos were taken from each plate with the microscope.

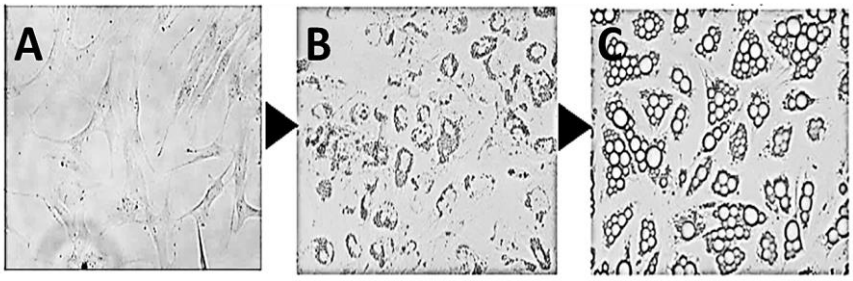

Figure 29. Representative images of undifferentiated SGBS cells (SGBS preadipocytes (A)) and adipocyte differentiated SGBS cells (SGBS adipocytes (C)). n=2 (x10 magnification)

We made a comparative study of the proteins that these cells secreted in the conditioned medium. To do this, the supernatants were collected from 48 h from undifferentiated SGBS preadipocytes, differentiated adipocytes under standard or starvation conditions, and the proteins were determined by LC-MS/MS. The results indicate that both adipocytes differentiated in standard or starving conditions had 126 proteins in common. However, differentiated adipocytes under standard conditions showed a greater amount of different proteins (249) compared to undifferentiated preadipocytes (32) and adipocytes differentiated in starvation conditions (48). (**Figure 30**).

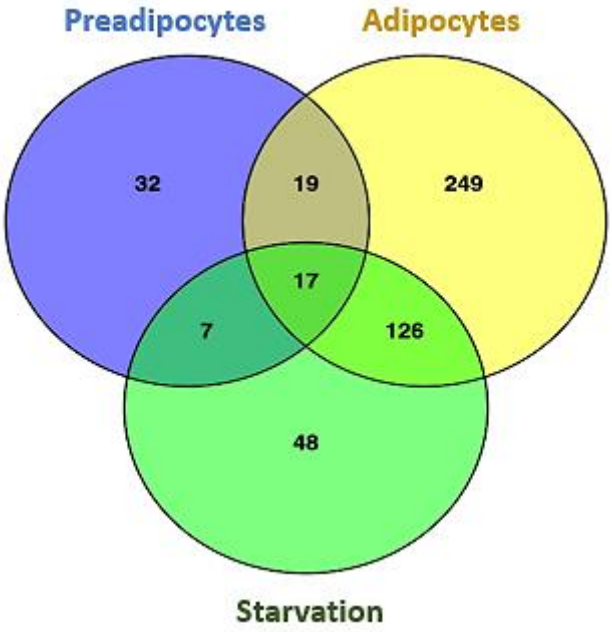

Figure 30. Proteomics of the SGBS cells (preadipocytes, SGBS differentiated into adipocytes under standard and starving conditions). The proteins were determined by LC-MS/MS. A Venn diagram was used to represent the data.

RESULTS

1. CHARACTERISATION OF DIFFERENT ADIPOSE TISSUE-DERIVED MSC FROM MOUSE

MSC were isolated from CD1 male mouse adipose tissue (inguinal and perigonadal fat pads). Both tissues were compared in terms of cell yield and the proliferative ability of cells, as shown in **Figure 31.**

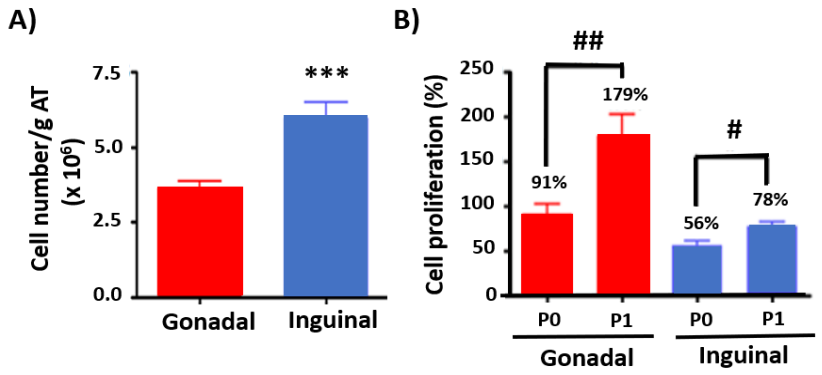

Figure 31. Cell yield and proliferation of mouse gonadal and inguinal adipose tissue. Cell yield expressed as cell number per gram of adipose tissue (AT) (gonadal or inguinal) (A). Cell proliferation at passage (P)0 and P1 (B)**.** Data are expressed as the mean ± SEM. Pooled data from 4 independent experiments. ***p<0.001 vs. gonadal cells. #p<0.05 and ##p<0.01. P=passage**.**

Although the yield of cells isolated from gonadal tissue was lower than cells obtained from inguinal tissue, gonadal cells had a greater capacity for proliferation (from 91% at Passage (P)0 to 179% at P1) than inguinal cells (from 56% at P0 to 78% at P1).

Mouse gonadal and inguinal MSC were characterised at P0, P1 and P3 by flow cytometry by using positive markers (CD29-PerCP-eFluor®710 and CD105-PE) and negative markers (CD45-FITC and CD11b-APC) (**Figure 32**). Cells from gonadal fat pads showed a lower expression of negative CD45 and CD11b markers and a higher expression of positive CD105 and CD29 markers, relative to cells from inguinal adipose tissue at P0, P1 and P3.

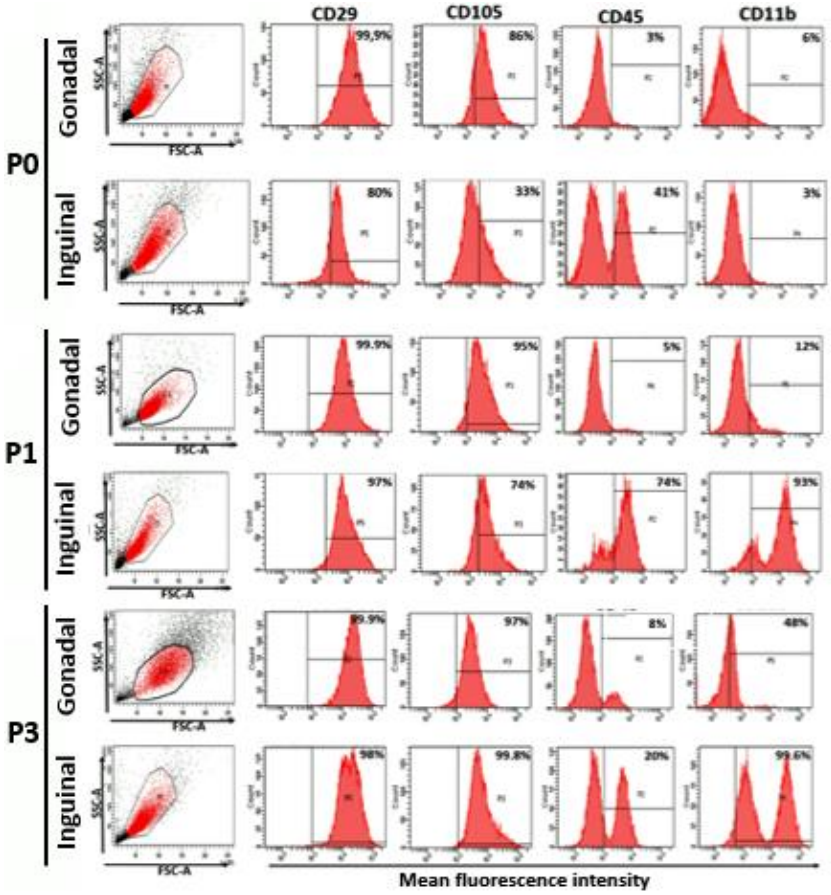

Figure 32. **Representative image of flow cytometric analysis of surface expression of phenotypic markers in gonadal and inguinal adipose tissue derived-MSC of CD1 male mice at P0, P1 and P3**. Analyzed markers are presented as red histograms. FSC/SSC graph shows the selected cell population. SSC: Side scatter. FSC: Forward scatter. FITC: Fluorescein isothiocyanate. PE: Phycoerythrin. APC: Allophycocyanin. PerCP: Peridinin chlorophyll.

The percentage of cell population expressing the marker CD29 increased from P0 (80%) to P3 (98%) on inguinal cells, whereas it remained constant on gonadal cells (99%). The CD105 marker showed a lower expression on inguinal cells at P0 (33%) and P1 (74%) than on gonadal cells (86% and 95% at P0 and P1, respectively). Nevertheless, this marker was similarly expressed at P3 on both cell types (gonadal 97% and inguinal 99%). On inguinal cells the negative marker CD45 showed a higher level of expression at P0, P1 and P3 compared with gonadal cells. The other negative marker, CD11b, was less represented on gonadal cells at P1 and P3 than on inguinal cells.

Since the expression of positive markers (CD105 and CD29) was higher and that of negative markers (CD11b and CD45) lower on cells from gonadal fat with respect to those from inguinal fat pads, we selected these gonadal MSC to study their effects on the early stage of the inflammation using the mouse air pouch model (MAP).

2. EFFECTS OF GONADAL MSC IN THE MOUSE AIR POUCH MODEL

2.1. Effects of MSC

The mouse air pouch model (MAP) is widely used to study the effects of new potential anti-inflammatory agents on the early stage of inflammation. Thus, we performed the zymosan-induced mouse air pouch model (MAP) (See **Material and methods section 2**) to determine the effects of the mouse adipose tissue-derived MSC on the innate immune response.

To achieve this purpose, we first studied which concentration of MSC was the most effective to downregulate the early inflammatory process induced by the inflammatory agent zymosan. In order to carry out this study, two different concentrations of MSC suspended in 500 µl of medium (1 x 10^6 and 2 x 10^6 MSC) were used in the MAP. Different experimental groups were used: control medium (M) (DMEM

HAM's F-12 medium containing 15% FBS and 1% penicillin/ streptomycin), control 1 x 10^6 MSC (C low), control 2 x 10^6 MSC (C high), zymosan control (Z), zymosan with 1 x 10^6 MSC (Z+C low) and zymosan with 2x 10^6 MSC (Z+C high). All treatments were administered by injection into the air pouch. Then, mice were sacrificed at 4 h after zymosan administration and several inflammatory parameters were measured.

We evaluated the effect of 1 x 10^6 MSC (C low) and 2 x 10^6 MSC (C high) suspended in 500 µl of medium on cell migration and myeloperoxidase (MPO) activity in the MAP model at 4 h (**Figure 33**).

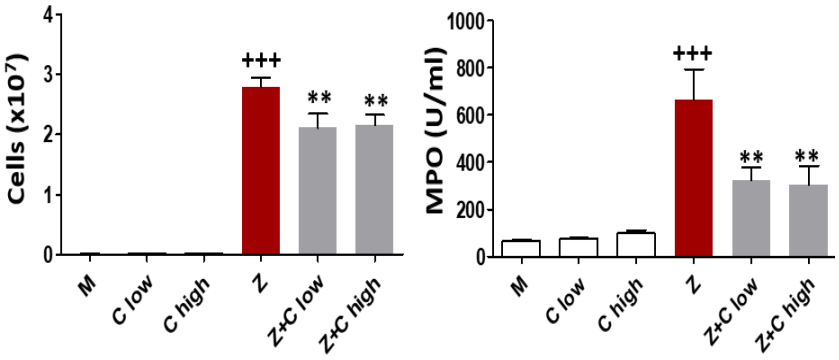

Figure 33. Effect of two different concentrations of MSC on cell migration and MPO activity in the MAP at 4 h. Cell number in MAP exudates were measured with the use of a Coulter counter. U indicates units. MSC are represented as "C". "C low" (1 x 10^6 MSC) and "C high" (2 x 10^6 MSC). Results show mean ± SEM (n=12, pooled results from two independent experiments). +++$p < 0.001$ with respect to medium (M); **$p < 0.01$ with respect to zymosan control (Z).

Zymosan significantly increased the migrated cells into the air pouch and the MPO activity. Both concentrations of MSC significantly decreased these two inflammatory parameters.

As most of the cells from the air pouch are activated neutrophils (Posadas *et al*., 2000), they may contribute significantly to the local production of chemotactic factors. Chemokines are quickly generated

and released into the inflammatory milieu. KC and LTB_4 production were determined in the MAP at 4 h. **Figure 34** shows that zymosan injection enhanced the production of both chemotactic factors.

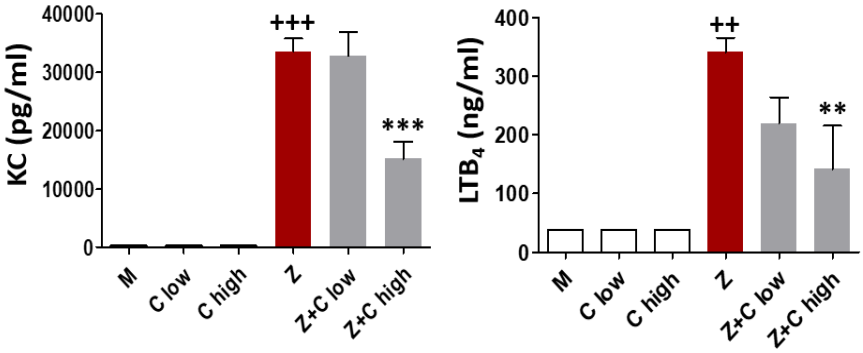

Figure 34. Effect of MSC on chemotactic factors present in MAP exudates at 4 h. KC was determined by means of ELISA and LTB_4 by RIA. Results show mean ± SEM (n=12, pooled results from two independent experiments). ++p <0.01, +++p < 0.001 with respect to medium (M); **p < 0.01, ***p < 0.001 with respect to zymosan control (Z).

The increased levels of KC and LTB_4 after zymosan injection were reversed with 2 x 10^6 MSC (Z+C high) administration into the MAP. However, 1 x 10^6 MSC did not contribute to a significant reduction of any of these chemokines (Z+C low).

IL-1β, TNF-α and IL-6 are cytokines that play an important role in the inflammatory processes. The production of IL-1β, TNF-α and IL-6 were determined in MAP exudates at 4 h (**Figure 35**). The levels of IL-1β, TNF-α and IL-6 increased significantly in the zymosan-injected mice. 2 x 10^6 MSC (Z+C high) significantly reduced the production of the three cytokines and to a higher extent than 1 x 10^6 MSC (Z+C low). The latter significantly decreased the levels of IL-1β and TNF-α after zymosan administration, but IL-6 levels were not significantly modified.

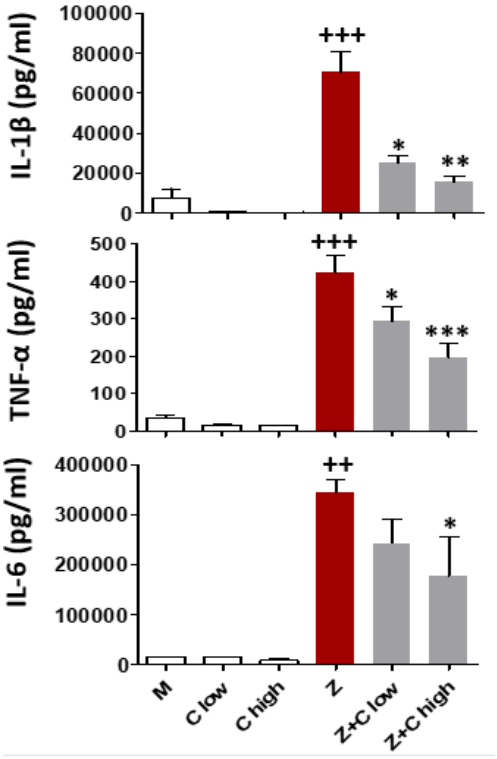

Figure 35. Effect of MSC on relevant pro-inflammatory cytokines IL-1β, TNF-α and IL-6 present in MAP exudates at 4 h. Cytokines were determined by means of ELISA. Results show mean ± SEM (n=12, pooled results from two independent experiments). ++p < 0.01, +++p < 0.001 with respect to medium (M); *p < 0.05, **p < 0.01, ***p<0.001 with respect to zymosan control (Z).

As the eicosanoid PGE_2 plays an important role in inflammatory responses, its levels were determined in the MAP exudates. As shown in **Figure 36**, PGE_2 was increased in exudates from zymosan-injected mice. Administration of 2 x 10^6 MSC significantly reduced the production of this eicosanoid, whereas 1 x 10^6 MSC did not alter its levels.

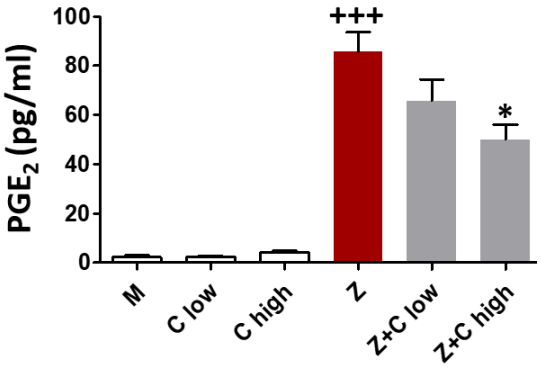

Figure 36. Effect of MSC on PGE_2 levels in MAP exudates at 4 h. PGE_2 levels were measured by means of RIA. Results show mean ± SEM (n=12, pooled results from two independent experiments). +++p < 0.001 with respect to medium (M); *p < 0.05 with respect to zymosan control (Z).

The results of this study indicated that 2 x 10^6 MSC was the appropriate dose to downregulate the innate inflammatory response in the zymosan-injected MAP at 4 h. Therefore, this concentration was selected for the next experiments in this *in vivo* model.

2.2. Effects of CM

Next, we wondered whether the paracrine factors of MSC (CM) could contribute to the anti-inflammatory effects elicited by MSC administration. Thus, we decided to study the effects of CM on the innate inflammatory response using the MAP at two different time points (4 h and 18 h after zymosan injection). MSC (2 x 10^6) were used as control as it showed higher anti-inflammatory effects than the low cell concentration (1 x 10^6 MSC). Different experimental groups were used: control medium (M) (DMEM HAM's F-12 medium containing 15% FBS and 1% penicillin/ streptomycin), control MSC (C), conditioned medium from MSC (CM), zymosan control (Z), zymosan with MSC (Z+C), zymosan with CM (Z+CM). All treatments were administered by injection into the air pouch.

We assessed whether the CM could modulate the migration of cells from the immune system involved in the inflammatory process (**Figure 37**).

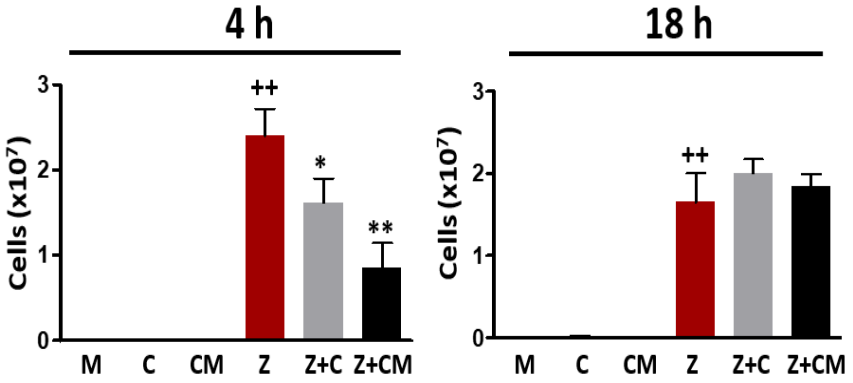

Figure 37. Effect of CM on cell migration in the MAP at 4 h and 18 h. Cell numbers in MAP exudates were measured with the use of a Coulter counter. MSC are represented as "C" and conditioned medium is represented as "CM". Results show mean ± SEM (n=12, pooled results from two independent experiments). ++p < 0.01 with respect to medium (M); *p < 0.05, **p < 0.01 with respect to zymosan control (Z).

Zymosan (Z) induced a higher cell activation and influx into the air pouch at 4 h after zymosan stimulation than at 18 h. It has been previously shown that the most predominant migrating cells found in this experimental model are neutrophils (Posadas *et al*., 2000). MSC (Z+C) and CM (Z+CM) administration resulted in a lower migration of cells into the air pouch exudates, with a higher reduction in the group treated with CM, at 4 h after addition of zymosan compared to zymosan-injected control mice (Z). After 18 h of zymosan addition, MSC and CM did not significantly alter the migration of cells into the air pouch exudates.

MPO is an enzyme present in the granules of neutrophils. This enzyme catalyzes the production of hypochlorous acid and other oxidants with potent microbicide activity able to damage and eliminate a wide spectrum of organisms (Prokopowicz *et al*., 2012).

Infiltration of neutrophils during the early phase of the inflammatory response can be measured by determining MPO activity. We determined the levels of MPO activity in the supernatant of MAP exudates (**Figure 38**).

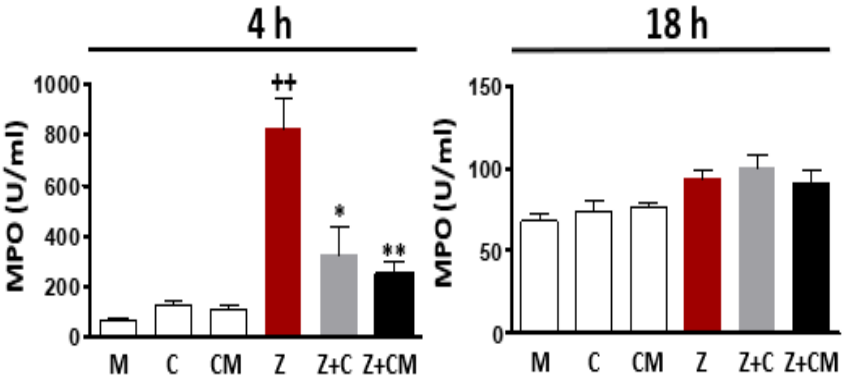

Figure 38. Effect of CM on MPO activity in MAP exudates at 4 h and 18 h. MPO activity was determined as units (U)/ml. MSC are represented as "C" and conditioned medium is represented as "CM". Results show mean ± SEM (n=12, pooled results from two independent experiments). ++p < 0.01 with respect to medium (M); *p < 0.05, **p < 0.01 with respect to zymosan control (Z).

At 4 h after zymosan injection into the air pouch, activated neutrophils secreted the content of their granules, strongly enhancing MPO activity. MSC and CM significantly decreased the activity of this enzyme compared to zymosan-injected mice. In contrast, at 18 h after zymosan injection, MPO activity in MAP exudates was small in the zymosan control and no significant changes were observed after treatment with either MSC or CM.

Cells migrated into the air pouch may contribute significantly to the local production of chemotactic factors. Therefore, we determined the levels of relevant chemotactic molecules KC, LTB_4 and MCP-1 in MAP exudates **(Figure 39).**

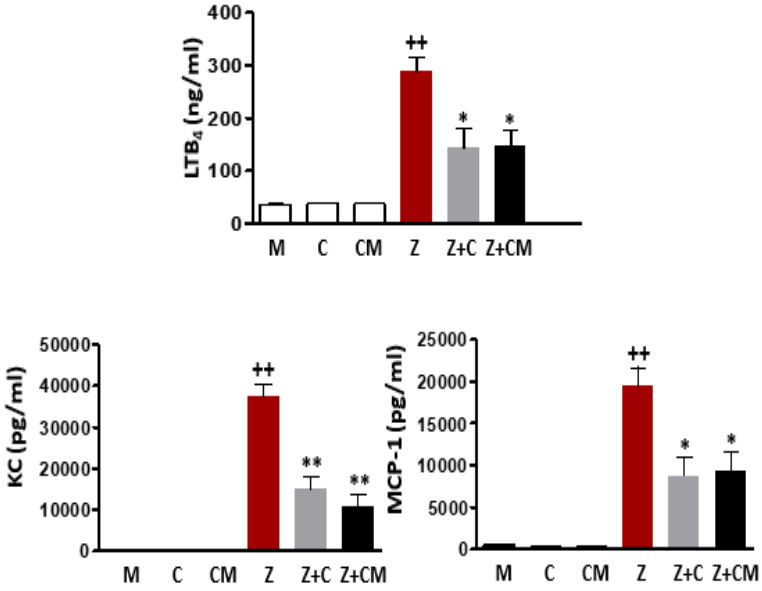

Figure 39. Effect of CM on chemotactic factors present in MAP exudates at 4 h. KC and MCP-1 were determined by means of ELISA and LTB_4 by RIA. MSC are represented as "C" and conditioned medium is represented as "CM". Results show mean ± SEM (n=12, pooled results from two independent experiments). ++$p < 0.01$ with respect to medium (M); *$p < 0.05$, **$p < 0.01$ with respect to zymosan control (Z).

We observed that zymosan administration significantly increased the levels of the eicosanoid LTB_4 and the chemokines KC and MCP-1 at 4 h, whereas MSC and CM strongly reduced the production of these chemotactic mediators. Nevertheless, after 18 h of zymosan administration, the levels of LTB_4, KC and MCP-1 were below the limit of quantification (data not shown). In addition, another chemokine, stromal cell-derived factor 1 α (SDF-1 α), also known as CXCL-12, was determined by ELISA in the supernatant of exudates at 4 h and 18 h, but the levels were below the limit of quantification (data not shown).

Not only chemotactic factors but also other inflammatory mediators such as cytokines and PGE_2 were released to the air pouch. In our *in vivo* model, zymosan induced the production of high levels of

the pro-inflammatory cytokines IL-1β, TNF-α and IL-6 in the air pouch exudates at 4 h, whereas at 18 h the levels of IL-1β and IL-6 strongly decreased. MSC and CM significantly reduced the levels of the three cytokines in the 4 h zymosan-injected MAP, with the highest effect on IL-1β. However, at 18 h after zymosan administration, MSC and CM were only effective on IL-6 (**Figure 40**).

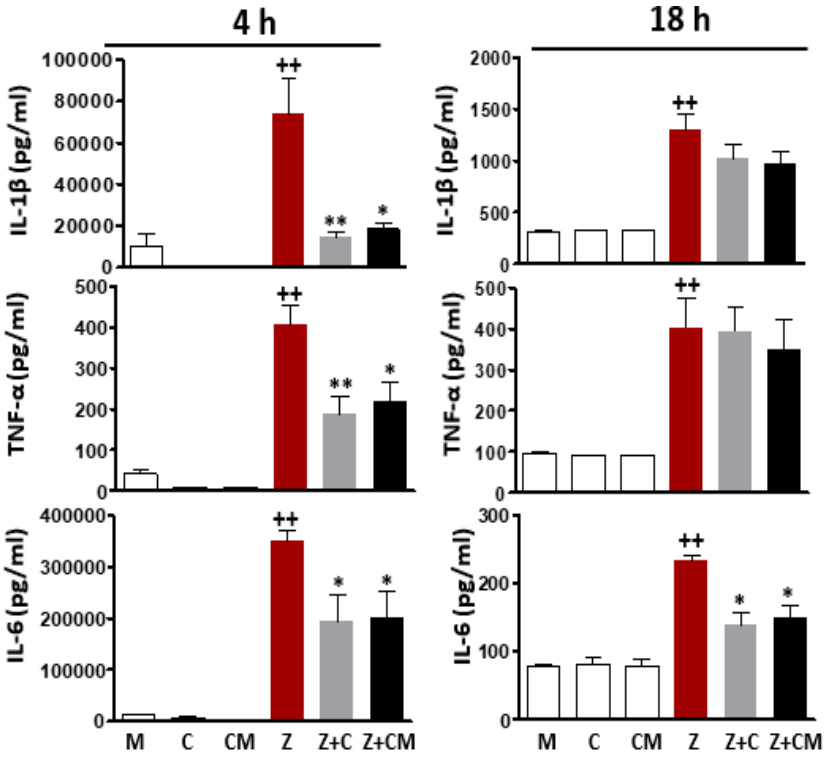

Figure 40. Effect of CM on relevant pro-inflammatory cytokines IL-1β, TNF-α and IL-6 present in MAP exudates. Cytokines were determined by means of ELISA. MSC are represented as "C" and conditioned medium is represented as "CM". Results show mean ± SEM (n=12, pooled results from two independent experiments). ++p < 0.01 with respect to medium (M); *p < 0.05, **p < 0.01 with respect to zymosan control (Z).

In addition, zymosan enhanced the production of IL-10 at 4 h and 18 h. Although IL-10 levels presented a tendency to decrease after MSC and CM addition, it did not reach statistical significance compared to zymosan-injected mice (**Figure 41**). TNF-α stimulated gene-6

(TSG-6) is a protein induced during inflammatory processes and tissue injury, which may be part of a negative feed-back loop (Roddy *et al.*, 2011). TSG-6 was significantly increased in air pouch exudates after 4 h and 18 h of zymosan injection compared to non-stimulated controls (**Figure 41**). MSC and CM significantly reduced the levels of this protein at both time points. Besides, the pro-inflammatory mediator PGE_2 significantly increased at 4 h and 18 h in exudates from zymosan-injected mice. MSC and CM treatment significantly reduced the levels of this eicosanoid at 4 h compared to zymosan control mice (**Figure 41**).

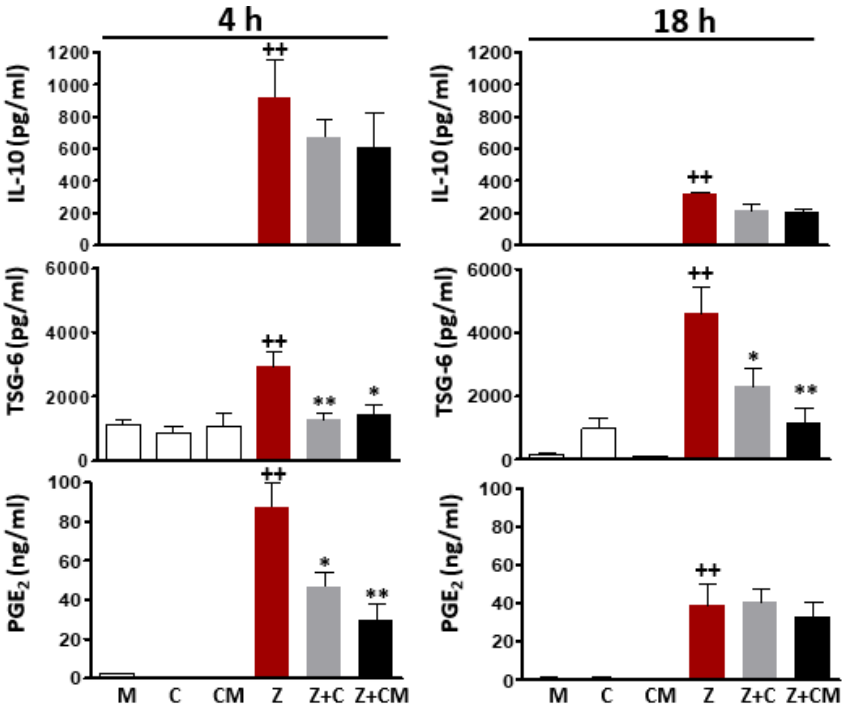

Figure 41. Effect of CM on IL-10, TSG-6 and PGE_2 levels in MAP exudates at 4 h and 18 h. Cytokines IL-10 and TSG-6 were measured by means of ELISA and PGE_2 levels by RIA. MSC are represented as "C" and conditioned medium is represented as "CM". Results show mean ± SEM (n=6 for the cytokines; n=12, pooled results from two independent experiments for PGE_2). ++$p < 0.01$ with respect to medium (M); *$p < 0.05$, **$p < 0.01$ with respect to zymosan control (Z).

Next, we evaluated the protein levels of COX-2 and mPGES-1 in the migrating cells by using immunoblotting. As previously described, PGE_2 production was significantly reduced by CM and MSC at 4 h after the administration of the inflammatory agent compared to zymosan-injected mice (**Figure 40**). COX-2 and mPGES-1 expression was determined in the cells migrated to the air pouch, since PGE_2 synthesis is produced by the coordinated action of both enzymes. Zymosan treatment significantly enhanced the expression of COX-2 and mPGES-1. The effects of zymosan on mPGES-1 expression were significantly decreased in the presence of CM and MSC, whereas the expression of COX-2 protein was not modified (**Figure 42**). So, the inhibitory effects of MSC and CM on the production of PGE_2 could be explained by the reduction in the expression of mPGES-1.

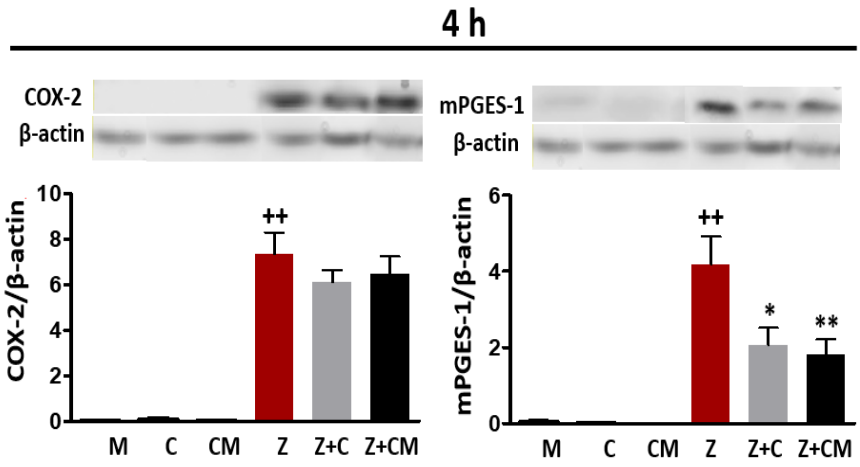

Figure 42. Effect of CM on COX-2 and mPGES-1 protein expression in cells migrating into the MAP at 4 h. COX-2 and mPGES-1 protein expression was determined by Western blotting. MSC are represented as "C" and conditioned medium is represented as "CM". Results show mean ± SEM (n=6). ++$p < 0.01$ with respect to medium (M); *$p < 0.05$, **$p < 0.01$ with respect to zymosan control (Z).

NF-κB is a known transcription factor that plays an important role in the transcription of inflammatory genes (Karin and Delhase, 2000). CM showed inhibitory effects higher than MSC on some inflammatory

parameters, suggesting that factors secreted by MSC play a relevant role in the observed anti-inflammatory activity. Therefore, we decided to study the contribution of CM to NF-κB activation *in vivo* by immunofluorescence.

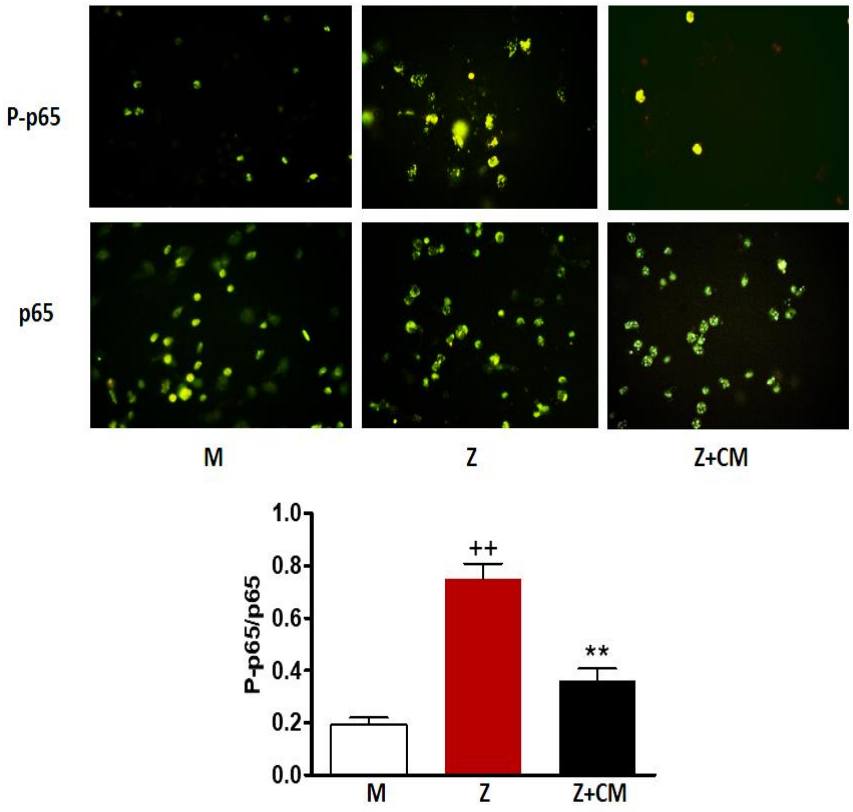

Figure 43. Effect of CM on p65 NF-κB phosphorylation on MAP at 4 h. Phosphorylation was analyzed by means of immunofluorescence and expressed as the ratio between cells positive for P-p65 NF-κB and those positive for total p65 NF-κB. Original magnification x 400. Results show mean ± SEM (n=6). ++$p < 0.01$ with respect to medium (M); **$p < 0.01$ with respect to zymosan control (Z).

As the highest inflammatory response of zymosan and anti-inflammatory effect of CM was at 4 h, we assessed the phosphorylation of p65 in the migrating cells at this time point. **Figure 43** shows that zymosan induced phosphorylation of p65 in the air

pouch exudate cells while CM treatment significantly diminished this process.

2.3. CM optimization studies

2.3.1. Effects of CM concentrated by lyophilization

As previously mentioned, CM showed higher anti-inflammatory effects than MSC in the MAP model. Thus, we decided to assess whether the concentration of the secreted paracrine factors from MSC by lyophilization of CM could increase this anti-inflammatory paracrine activity from MSC in the innate inflammatory response using the zymosan MAP model. To achieve this purpose, we lyophilized the CM from MSC and the powder obtained was resuspended in PBS. Two different concentrations were tested: a high concentration of 36 mg/ml (CM high) and a low concentration of 18 mg/ml (CM low). “CM” refers to non-lyophilized CM. “C” refers to a concentration of 2 x 10^6 MSC.

We assessed whether the lyophilized CM from MSC could modulate the migration of cells involved in the innate inflammatory response and the MPO activity. Zymosan significantly increased the cell migration and the MPO activity in comparison to control medium. After zymosan administration, only MSC and non-lyophilized CM significantly decreased the cell migration and MPO activity in comparison to zymosan control. Both concentrations of lyophilized CM (Z+CM low and Z+CM high) were ineffective on cell migration and MPO activity (**Figure 44**).

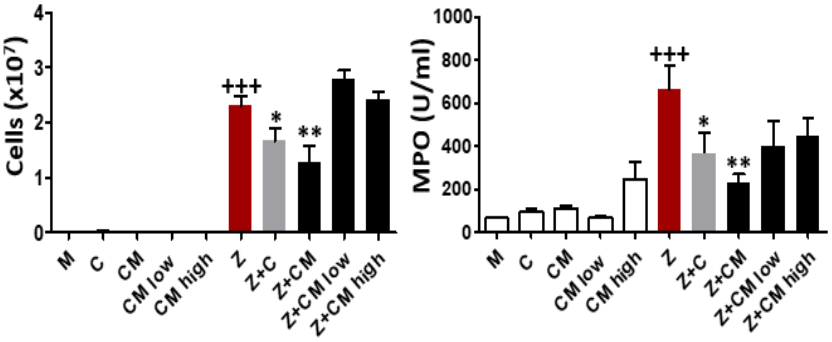

Figure 44. Effect of CM concentrated by lyophilization on cell migration and MPO activity in the MAP at 4 h. Cell number in MAP exudates were measured with the use of a Coulter counter. U indicates units. Results show mean ± SEM (n=12, pooled results from two independent experiments). +++p < 0.001 with respect to medium (M); *p<0.05, **p<0.01 with respect to zymosan control (Z).

As previously mentioned, other inflammatory mediators were released into the air pouch such as IL-1β, TNF-α, KC and PGE_2. Zymosan significantly increased the production of both cytokines IL-1β and TNF-α, the chemokine KC and the eicosanoid PGE_2 with respect to medium. After zymosan injection into the air pouch, the levels of IL-1β, TNF-α, KC and PGE_2 were significantly reduced in MSC (Z+C) and non-lyophilized CM (Z+CM) treated groups. However, the lyophilized CM (Z+CM low and Z+CM high) did not significantly decrease the levels of these mediators (**Figure 45**).

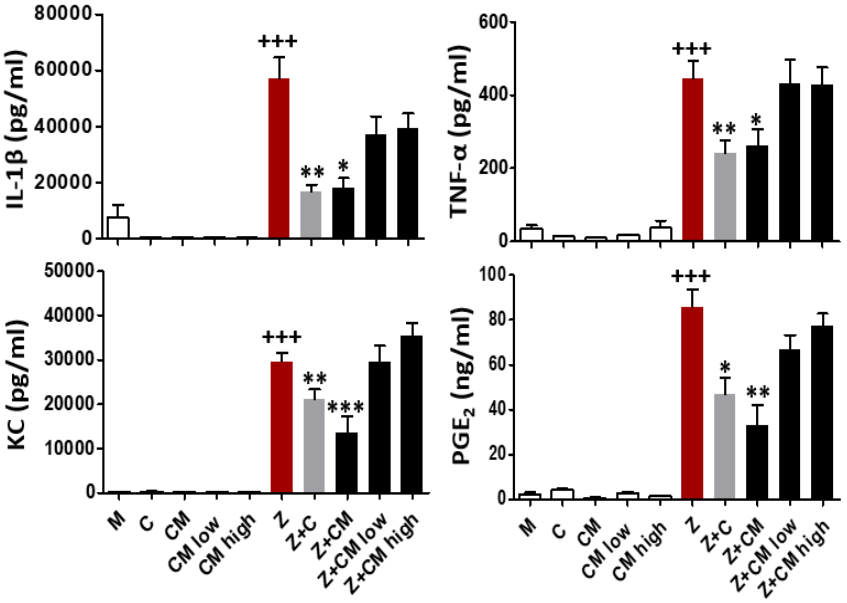

Figure 45. Effect of CM concentrated by lyophilization on relevant pro-inflammatory cytokines IL-1β, TNF-α, chemokine KC and PGE_2 present in MAP exudates at 4 h. Cytokines and chemokine KC were determined by means of ELISA. PGE_2 was measured by RIA. Results show mean ± SEM (n=12, pooled results from two independent experiments) +++ $p< 0.001$ with respect to medium (M); *$p < 0.05$, **$p < 0.01$, ***$p<0.001$ with respect to zymosan control (Z).

2.3.2. Effects of CM concentrated by filtration

We have shown that CM concentrated by lyophilization did not show any anti-inflammatory effects compared to non-lyophilized CM. We wondered whether the paracrine factors could have been affected by the lyophilization process losing their biological activity. Thus, we concentrated the CM by filtration using Centrifugal Filter Units (Millipore). CM was concentrated by filtration 2 and 4 times more in comparison to non-concentrated CM (CM). "C" refers to 2 x 10^6 MSC injected into the air pouch. "CM high" refers to 4x concentrated CM. "CM low" refers to 2x concentrated CM. This CM was obtained after dilution of the 4x concentrated CM with PBS to obtain a final 2x

concentrated CM. Non-concentrated CM was named "CM". This experiment was performed at 4 h after zymosan administration.

Zymosan significantly increased cell migration and MPO activity in the MAP. In both inflammatory parameters MSC (Z+C) and the non-concentrated CM (Z+CM) had a great anti-inflammatory effect after zymosan administration by reducing the activity of the enzyme and the cells migrated into the air pouch involved in the inflammatory immune response. However, the concentrated CM (Z+CM low and Z+CM high) did not significantly decrease the levels of these mediators (**Figure 46**).

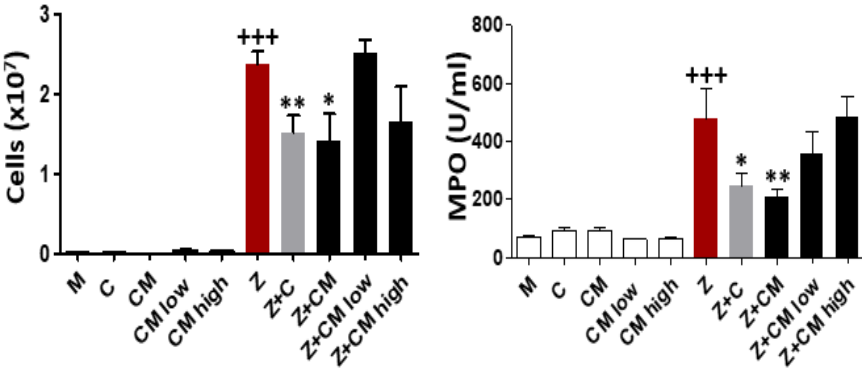

Figure 46. Effect of CM concentrated by filtration on cell migration and MPO activity in the MAP at 4 h. Cell number in MAP exudates were measured with the use of a Coulter counter. MPO activity was determined by fluorometry. U indicates units. Results show mean ± SEM (n=12, pooled results from two independent experiments). +++p < 0.001 with respect to medium (M); *p<0.05, **p<0.01 with respect to zymosan control (Z).

Zymosan induced the production of high levels of the cytokines IL-1β, TNF-α and chemokine KC. After zymosan injection, MSC (Z+C) and non-concentrated CM (Z+CM) significantly reduced the levels of the three cytokines, but CM to a higher extent. Comparing both CM concentrated by filtration, the high concentrated CM (Z+CM high) showed higher anti-inflammatory effects on the three cytokines than the low one (Z+CM low). The latter significantly decreased the production of IL-1β and KC, but it did not modify the effect of zymosan on TNF-α (**Figure 47**).

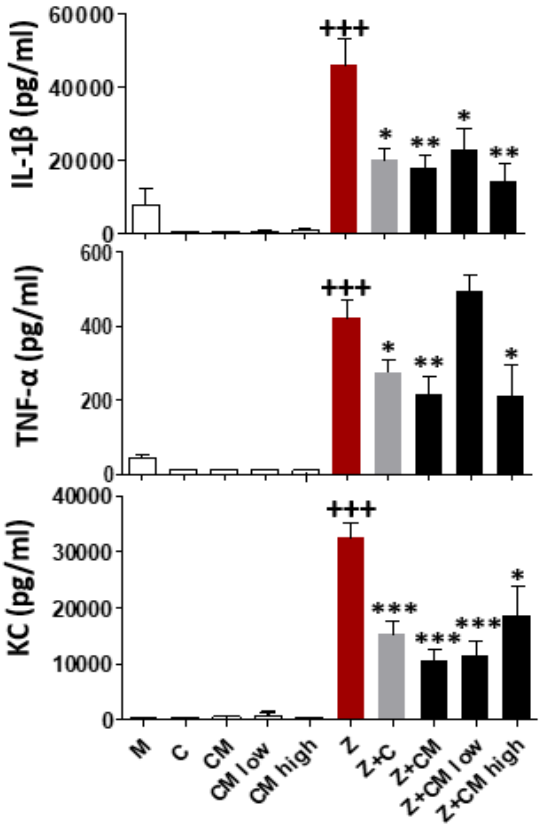

Figure 47. Effect of CM concentrated by filtration on relevant pro-inflammatory cytokines IL-1β, TNF-α and the chemokine KC present in MAP exudates at 4 h. Cytokines were determined by ELISA. Results show mean ± SEM, (n=12, pooled results from two independent experiments). +++ $p < 0.001$ with respect to medium (M); *$p < 0.05$, **$p < 0.01$, ***$p<0.001$ with respect to zymosan control (Z).

Zymosan significantly increased the levels of the eicosanoid PGE_2. Only non-concentrated CM and the CM high concentrated (Z+CM high) significantly reduced the levels of this eicosanoid (**Figure 48**).

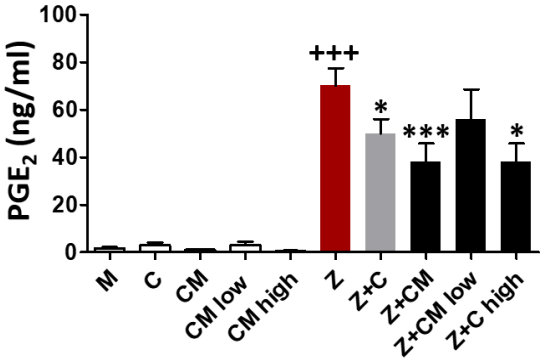

Figure 48. Effect of concentrated CM by filtration on PGE_2 present in MAP exudates at 4 h. PGE_2 levels were determined by RIA. Results show mean ± SEM, (n=12, pooled results from two independent experiments). +++ $p < 0.001$with respect to medium (M); *$p < 0.05$, ***$p < 0.001$ with respect to zymosan control (Z).

2.3.3. Effects of preconditioning MSC with cobalt protoporhyrin IX

HO-1 is a ubiquitously expressed inducible enzyme that catabolizes the heme group into carbon monoxide, biliverdin and Fe^{2+}. Its activation reduces oxidative stress in cells and inhibits inflammation, due to the removal of heme and the biological activity of HO-1 products (Grochot-Przeczek *et al*., 2012). In the MAP model, there is a time-dependent increase in HO-1 expression in the cells migrating into the air pouch exudate, as previously determined in our laboratory (Vicente *et al*., 2003). We wondered whether preconditioning MSC with the HO-1 inducer cobalt protoporphyrin IX (CoPP) could potentiate the anti-inflammatory activity of MSC in the early inflammatory response after 18 h of zymosan stimulation in the MAP model. To achieve this purpose, we induced the expression of HO-1 on MSC with CoPP at the concentration used in previous experiments in our laboratory (a final concentration of 10 µM) for 48 h. Before testing the effect of preconditioning MSC with CoPP on the MAP model, we verified the overexpression of HO-1 *in vitro* by seeding MSC on 6-well plates (75,000 cells/well) with CoPP (final

concentration 10 µM) for 48 h. Then, cells were lysed and HO-1 was determined by Western blotting. We observed an increased expression of HO-1 in MSC treated with CoPP (C_{CoPP}) in comparison with control MSC (C) (data not shown).

Next, we determined the effects of preconditioning MSC with CoPP on the zymosan-MAP model (**See Material and methods section 2**). We first assessed HO-1 protein expression in the cells migrating into the air pouch exudates from different groups (Z: Zymosan, Z+C: Zymosan and MSC, Z+C_{CoPP}: Zymosan and CoPP-preconditioned MSC, Z+CM: Zymosan and CM from MSC, Z+CM_{CoPP}: Zymosan and CM from CoPP-preconditioned MSC).

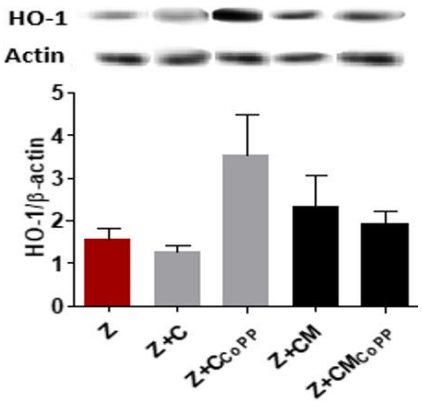

Figure 49. HO-1 expression in cells migrated into the MAP at 18 h. Migrated cells into the air pouch exudate were lysed, and then Western blotting was performed to determine the expression of HO-1. Results show mean ± SEM (n=6).

Figure 49 shows that CoPP pre-treatment of MSC enhanced HO-1 expression in cells present in MAP exudates from the Z+C_{CoPP} group 18 h after zymosan injection although there were no significant differences among groups.

We assessed whether the CoPP-preconditioned MSC (Z+C_{CoPP}) could modulate the migration of cells involved in the innate inflammatory process and MPO production. Migration of cells

significantly increased after the addition of the inflammatory agent zymosan compared to control medium and other control groups.

CoPP-preconditioned MSC and their CM (Z+C_{CoPP} and Z+CM_{CoPP}, respectively) did not alter the migration of the cells into the air pouch in comparison to zymosan group. In addition, no significant differences were observed with its corresponding non-CoPP treated group (Z+C or Z+CM, respectively). These results were in line with those obtained from the MPO activity. There were no significant differences among the CoPP-preconditioned MSC and their CM (Z+C_{CoPP} and Z+CM_{CoPP}) and their corresponding groups with non-treated MSC and CM (Z+C and Z+CM) (**Figure 50**).

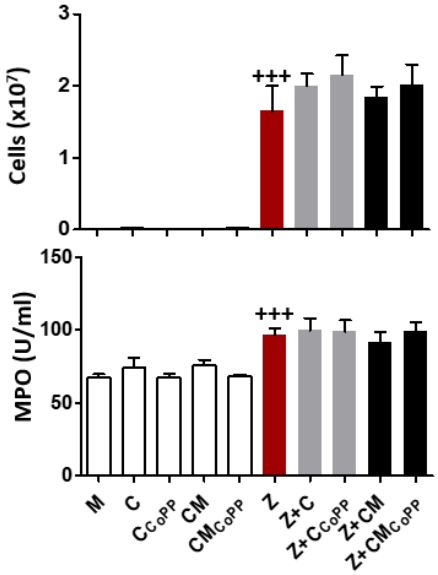

Figure 50. Effect of CoPP-preconditioned MSC and their CM on cell migration and MPO activity in the MAP at 18 h. Cell number in MAP exudates were measured with the use of a Coulter counter. MPO activity was determined by fluorometry. U indicates units. Results show mean ± SEM. (n=12, pooled results from two independent experiments). +++p < 0.001 with respect to medium (M).

As previously shown, other inflammatory mediators were released into the air pouch such as IL-1β, TNF-α and IL-6. After the

injection of zymosan into the air pouch, the levels of the cytokines IL-1β, TNF-α and IL-6 increased significantly in comparison to control medium (M). In line with our previous results (**Figure 51**), MSC and their CM (Z+C and Z+CM, respectively), significantly decreased the levels of IL-6 at 18 h in comparison with zymosan control, similar to CoPP-preconditioned MSC and their CM ($Z+C_{CoPP}$ and $Z+CM_{CoPP}$, respectively). After the injection of MSC preconditioned with CoPP and their CM ($Z+C_{CoPP}$ and $Z+CM_{CoPP}$, respectively) into the MAP, a significant reduction of IL-1β levels was observed compared with the zymosan control group (Z). However, TNF-α levels were significantly decreased by CoPP-preconditioned MSC ($Z+C_{CoPP}$) but not by $Z+CM_{CoPP}$ compared with zymosan control (Z). In addition, TNF-α was significantly reduced in the group treated with CoPP-preconditioned MSC ($Z+C_{CoPP}$) in comparison to its control MSC group (Z+C).

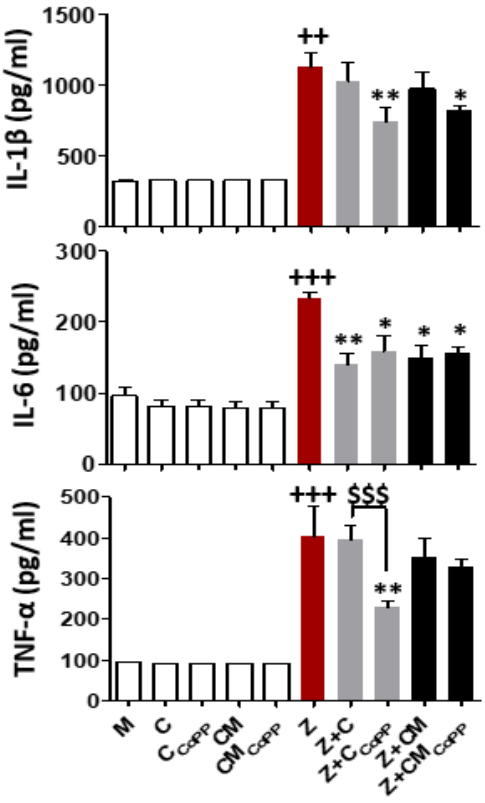

Figure 51. Effect of CoPP-preconditioned MSC and their CM on pro-inflammatory cytokines IL-1β, TNF-α and IL-6 in MAP exudates at 18 h. Cytokines were determined by means of ELISA. Results show mean ± SEM (n=12, pooled results from two independent experiments). ++p < 0.01, +++p < 0.001 with respect to medium (M); *p < 0.05, **p < 0.01 with respect to zymosan control (Z); $$$p < 0.001 with respect to its control group Z+C.

As PGE_2 is another relevant pro-inflammatory mediator present in the zymosan-injected MAP, we also decided to study whether the production of this eicosanoid in zymosan-treated groups was modified by CoPP-preconditioned MSC (**Figure 52**). In the group of mice treated with zymosan the production of PGE_2 increased significantly in comparison to control medium (M). Nevertheless, none of the treatments (Z+C_{CoPP}, Z+CM_{CoPP}, Z+C and Z+CM) significantly altered the levels of this eicosanoid.

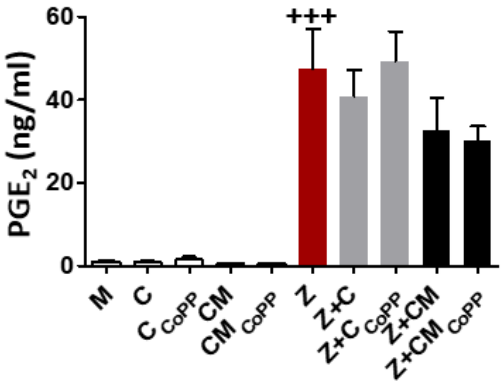

Figure 52. Effect of CoPP-preconditioned MSC and their CM on PGE_2 levels in MAP exudates at 18h. PGE_2 levels were determined by RIA at 18 h in the supernatant of the air pouch exudates. Results show mean ± SEM. (n=12, pooled results from two independent experiments). +++p < 0.001 with respect to medium (M).

The results of these series of experiments indicate that the induction of HO-1 in MSC only results in a very weak improvement in the anti-inflammatory activity of these cells in the zymosan-induced MAP model. Therefore, this strategy is not effective to enhance the anti-inflammatory properties of MSC and their CM in this experimental model.

3. STUDY OF CM COMPOSITION FROM ADIPOSE TISSUE-DERIVED MSC

Most of the results obtained in the MAP model demonstrated that MSC controlled the inflammatory response induced by zymosan primarily by paracrine effects. We wondered which components from the CM may be responsible for this anti-inflammatory activity in the innate inflammatory response. Thus, we decided to study the effects of soluble factors and the vesicular components such as extracellular vesicles (EV) from CM, specifically microvesicles (Mv) and exosomes (Ex) on the early stage of inflammation in several cells involved in the innate immune response such as mouse peritoneal macrophages, monocytes and neutrophils isolated from the bone marrow.

3.1. Proteomic study

In order to gain more insight into the secreted proteins responsible for the anti-inflammatory effect of MSC, a determination of proteins present in CM was performed in the Central Service for Experimental Research (SCSIE, University of Valencia), by liquid chromatography combined with tandem mass spectrometry (LC-MS/MS).

As CM and control medium (DMEM HAM's F-12 supplemented with 15% EV-depleted FBS and 1% penicillin/streptomycin) contained FBS, prior to LC-MS/MS, they were albumin-depleted by a cibacron blue affinity column (Zeulab). After performing LC-MS/MS in the SCSIE, several proteins were identified. The most abundant proteins (with the largest-fold change) were apyrase, phosphate-binding protein PstS and phosphate-import protein PhnD, being apyrase the most abundant one. PstS is the substrate-binding component of the ATP-binding cassette (ABC)-type transporter complex pstSACB, involved in phosphate import. PhnD is a phosphonate binding protein that is part of the phosphonate uptake system (**Figure 53**).

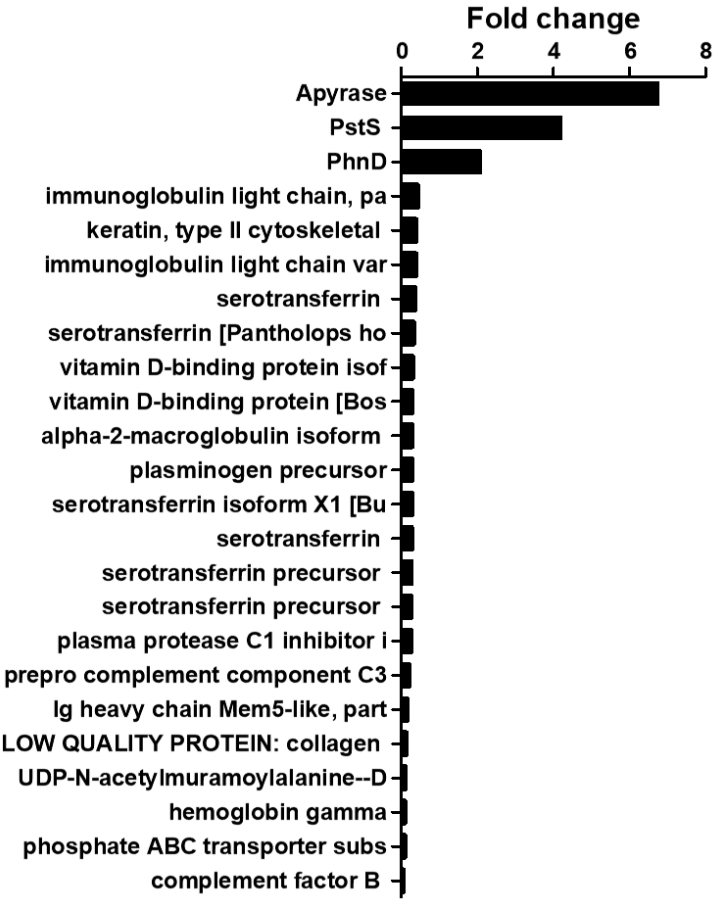

Figure 53. Determination of proteins in CM from mouse perigonadal adipose tissue-derived MSC vs control medium by LC-MS/MS. Results are expressed as fold change (CM from MSC vs. control medium).

3.2. Chemokine array

MSC have been shown to secrete not only vesicular components but also soluble factors into the extracellular compartment (Lavoie and Rosu-Myles, 2013).

Chemokines play an important role in migration of neutrophils and monocytes in the innate immune response (Keane and Strieter, 2000). It has been described that MSC secrete several soluble factors

that are implicated in migration (Chen *et al.*, 2008). Among these factors we can find chemokines**.**

To assess the presence of different chemoattractant cytokines in CM from MSC, we used a chemokine array. As a control we used DMEM HAM's F-12 supplemented with 10% EV-depleted FBS and 1% penicillin/streptomycin.

	A	B	C	D	E	F	G	H
1	POS	POS	NEG	NEG	6Ckine (CCL21)	BLC (CXCL13)	CTACK (CCL27)	CXCL16
2								
3	Eotaxin-1 (CCL11)	Eotaxin-2 (CCL24)	Fractalkine (CX3CL1)	I-TAC (CXCL11)	KC (CXCL1)	LIX	MCP-1 (CCL2)	MCP-5
4								
5	MDC (CCL22)	MIG (CXCL9)	MIP-1 alpha (CCL3)	MIP-1 gamma	MIP-2	MIP-3 beta (CCL19)	MIP-3 alpha (CCL20)	PF-4 (CXCL4)
6								
7	RANTES (CCL5)	SDF-1 (CXCL12)	TARC (CCL17)	I-309 (TCA-3/CCL1)	TECK (CCL25)	BLANK	BLANK	POS
8								

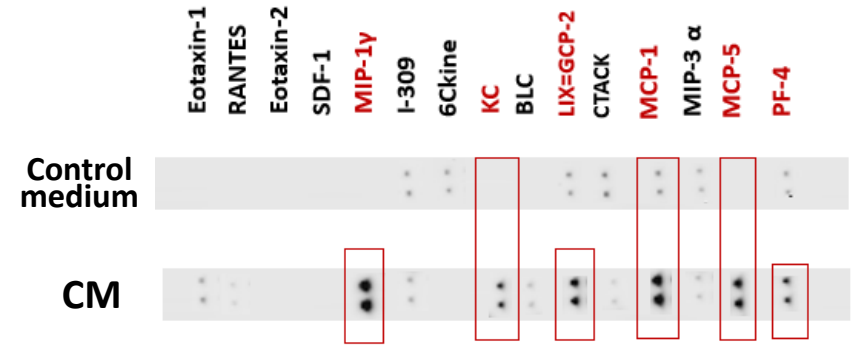

Figure 54. Determination of chemokines from control medium and CM from MSC. Chemokines determination was performed by using an array of chemokines. Each antibody is spotted in duplicate vertically. Representative images of two independent experiments.

Some of these chemokines were only present in the CM from MSC compared to control medium, such as MIP-1γ, MCP-5 and KC. A higher expression of MCP-1, LIX, MCP-5, KC, MIP-1γ, and PF-4 was detected compared to control medium. LIX is a member of the murine glutamate-leucine-argine (ELR^+) CCXC chemokines that is similar to two human chemokines epithelial cell-derived neutrophil activating peptide-78 (ENA-78) and granulocyte chemotactic protein-2 (GCP-2). LIX induces neutrophil chemotaxis (Smith *et al*., 2002). The highest expression was observed for MCP-1, MIP-1γ and MCP-5 (**Figure 54**).

3.3. EV characterisation

The extracellular vesicles (EV), microvesicles (Mv) and exosomes (Ex), are small membrane vesicles derived from the plasma membrane or multivesicular bodies, respectively, which can transport proteins, RNA, lipids... These EV are secreted to the extracellular medium, and have a very important role in intercellular communication (Raposo and Stoorvogel, 2013).

We first isolated the two types of EV (Ex and Mv) from CM using differential centrifugation combined with size filtration and we characterised them. To assess the morphology of Mv and Ex, we used TEM. To determine the concentration and size distribution we used the tunable resistive pulse sensing technology with qNano instrument from IZON. Mv and Ex differed in size and concentration. Ex showed a smaller size (90 nm) than Mv (271 nm) and a higher concentration (6×10^{11}Ex/ml vs. 1×10^{10}Mv/ml) (**Figure 55**).

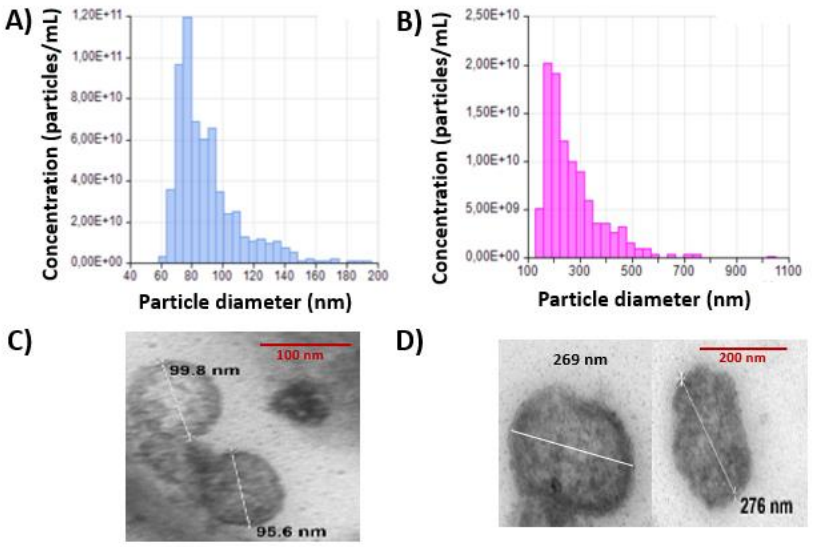

Figure 55. Characterisation of Ex and Mv isolated from mouse adipose tissue-derived MSC. Concentration and size distribution of Ex (A) and Mv (B) were measured using tunable resistive pulse sensing analysis by qNano instrument from IZON. Representative transmission electron microscopy images of Ex (C) and Mv (D).

4. EFFECT OF CM AND EV ON MACROPHAGES

Extracellular vesicles and soluble factors from MSC have been described to be involved in the regulation of immune responses (Fierabracci *et al.,* 2016). We wondered whether these EV or soluble factors present in CM from MSC (EV-free CM) could modulate the inflammatory process in the innate immune system.

4.1. Dose-response study of EV on inflammatory mediators

To evaluate the anti-inflammatory effects of EV in the innate inflammatory response, different concentrations of EV isolated from CM of MSC at P1 were tested on cultured mouse peritoneal macrophages after their stimulation with LPS for 20 h. Three different

concentrations of Ex from 0.9 x 10^6 to 36 x 10^6 Ex/ml and four different concentrations of Mv from 0.09 x 10^6 to 18 x 10^6 Mv/ml were used. Also, the effect of the combination of both types of EV was studied (18 x 10^6 Ex + 0.09 x 10^6 Mv). B group (untreated and unstimulated macrophages), LPS group (macrophages treated with LPS) and CM group (macrophages treated with CM and LPS) were used as control groups. Prior to this experiment, EV and CM from P0, P1 and P2 MSC were tested on macrophages. In fact, EV and CM at P1 showed more anti-inflammatory effects than EV and CM from MSC at P0 and P2 (data not shown) and therefore CM and EV from MSC at P1 were selected for this study.

LPS produced a great increase of IL-1β and TNF-α levels in the supernatant of macrophages which were significantly reduced by CM treatment. Whereas Ex significantly decreased the levels of IL-1β and TNF-α at the higher concentrations (18 x 10^6 and 36 x 10^6/ml), Mv only reduced the production of TNF-α at the concentration of 9 x 10^6/ml (**Figure 56**). In contrast, the combination of both EV and MV did not show any anti-inflammatory effect in the presence of LPS.

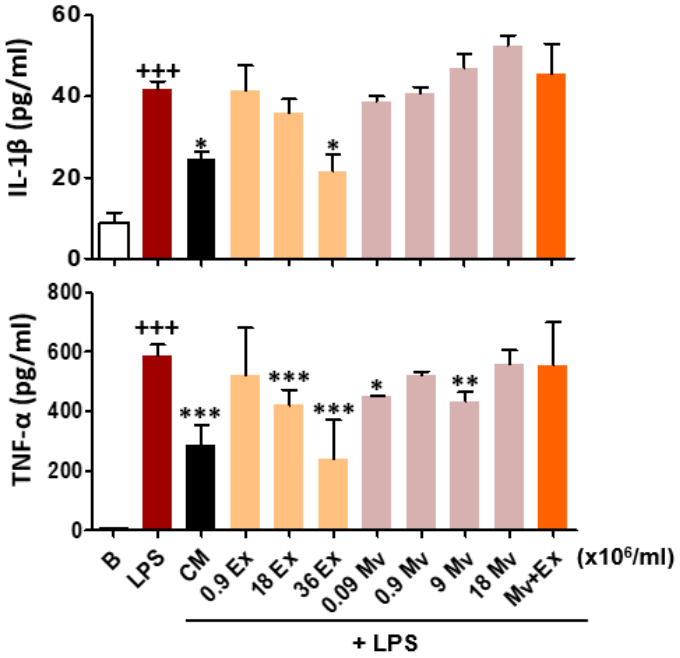

Figure 56. Effects of EV on the production of cytokines IL-1β and TNF-α in macrophages. Macrophages were treated with CM or different concentrations of EV in presence or absence of LPS for 20 h. CM was used as a control. IL-1β and TNF-α levels were determined by ELISA. Results show mean ± SEM. Pooled data from 4 independent experiments. +++$p < 0.001$ with respect to B group (B); *$p < 0.05$, **$p < 0.01$, ***$p < 0.001$ with respect to LPS control (LPS).

LPS stimulation of macrophages also increased the production of nitrite and the eicosanoid PGE_2 compared to untreated and unstimulated macrophages (B group). CM significantly reduced the levels of nitrite and PGE_2 in comparison to the LPS group. Only the concentration of 18 x 10^6 Ex/ml decreased the levels of both inflammatory mediators. Regarding the Mv, the lowest concentration (0.09 x 10^6 Mv/ml) was able to reduce the production of nitrite and PGE_2 in LPS-stimulated macrophages (**Figure 57**).

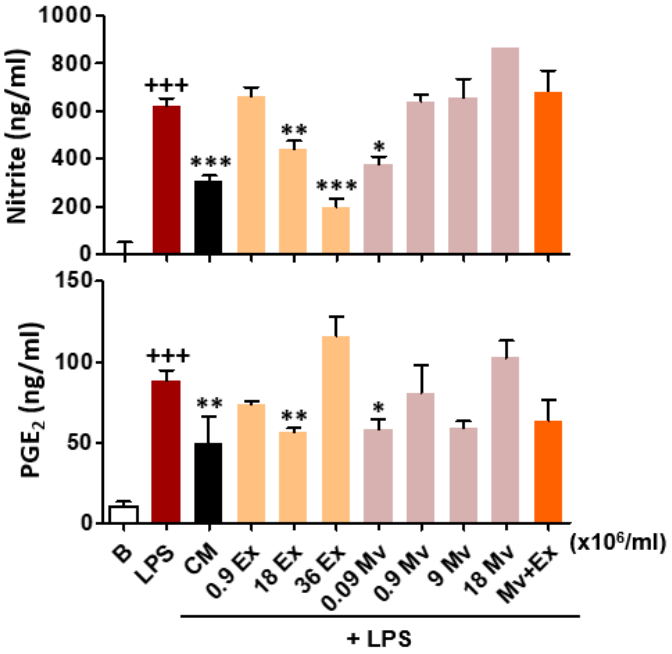

Figure 57. Effects of EV on nitrite and the eicosanoid PGE_2 production in macrophages. Macrophages were treated with CM or different concentrations of EV in presence or absence of LPS for 20 h. CM was used as a control. Nitrite and PGE_2 levels were determined by fluorometry and radioimmunoassay, respectively. Results show mean ± SEM. Pooled data from 4 independent experiments. +++$p < 0.001$ with respect to B group (B); *$p < 0.05$, **$p < 0.01$, ***$p < 0.001$ with respect to LPS control (LPS).

These results indicate that the concentration of Ex able to significantly decrease the levels of all the inflammatory mediators was 18 x 10^6 Ex/ml. The concentration of Mv that showed a higher anti-inflammatory effect was 0.09 x 10^6 Mv/ml. Therefore, the following experiments regarding the study of the effects of EV on the innate inflammatory response were performed with a concentration of 18 x 10^6 of Ex/ml and a concentration of 0.09 x 10^6 of Mv/ml.

As CM showed an anti-inflammatory effect higher than EV, we wondered whether a soluble factor could be responsible for these anti-inflammatory paracrine effects of MSC. To study the effects of the soluble fraction, CM free from EV (EV-free CM) was used.

4.2. Macrophages viability

To exclude any possible cytotoxic effect of the different treatments at the selected concentrations, we assessed whether EV, EV-free CM from MSC (CM EV-) or LPS could affect the viability of macrophages, using the MTT assay. We found no significant differences among macrophages treated with EV (Ex and Mv separately) or EV-free CM in the presence or absence of LPS compared to unstimulated and untreated macrophages (B group) (**Figure 58**).

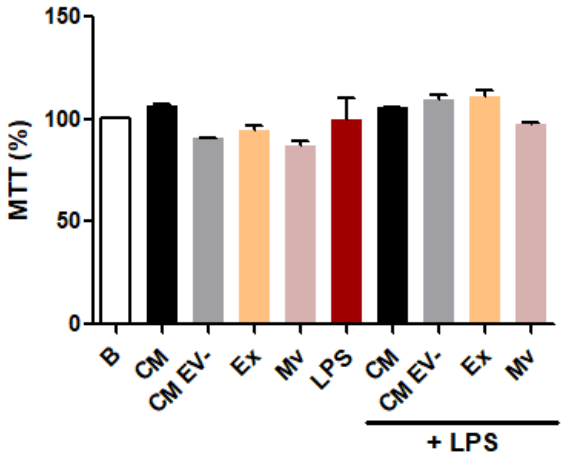

Figure 58. Effects of EV, CM, EV-free CM (CM EV-) and LPS on macrophage viability by MTT. Macrophages were treated with CM, EV-free CM, Ex or Mv in the presence or absence of LPS for 20h. Macrophage viability was determined by the MTT assay. Results are expressed as a percentage related to the untreated and unstimulated control cells (B group), mean ± S.E.M. Pooled data from 4 independent experiments.

4.3. Production of inflammatory mediators

In order to assess whether EV may alter the pro-inflammatory mediators produced by macrophages, we treated macrophages with Ex and Mv in the absence and presence of LPS (1 μg/ml) for 4 h and 20 h. CM and EV-free CM were used as controls. Then, the levels of IL-1β, TNF-α and nitrite were determined (**Figure 59**).

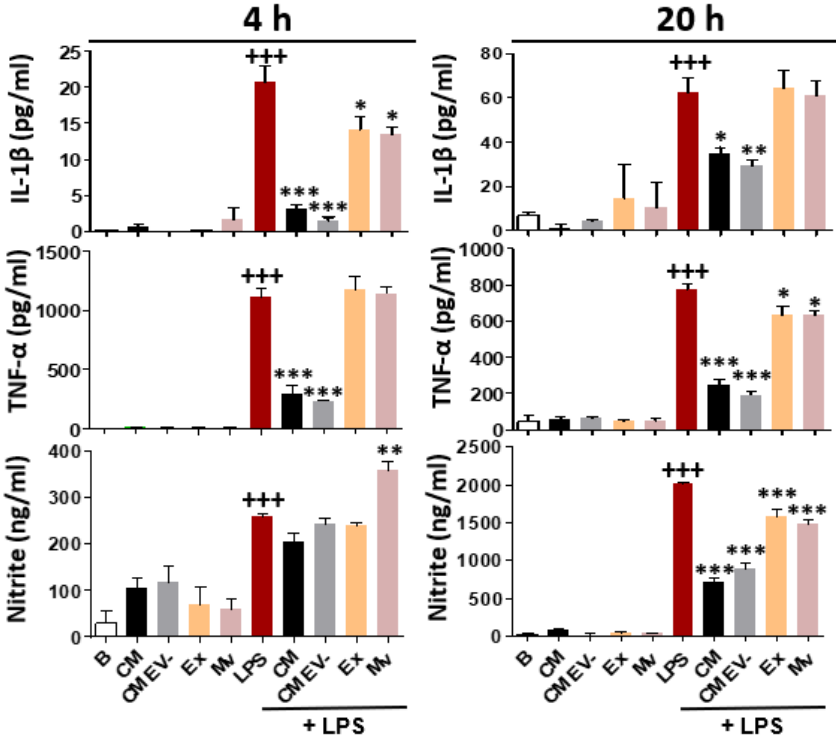

Figure 59. Determination of the effect of EV on the production of inflammatory mediators. Macrophages were treated with CM, Ex or Mv in the presence or absence of LPS for 4 h or 20 h. CM and CM EV- (EV-free CM) were used as controls. IL-1β, TNF-α, and nitrite levels were determined in the supernatant of macrophages. Results are expressed as the concentration of each inflammatory mediator. Results show mean ± SEM. Pooled data from 4 independent experiments. +++$p < 0.001$ vs B group; *$p < 0.05$, **$p < 0.01$ and ***$p < 0.001$ vs. LPS group.

As expected, the levels of all of these pro-inflammatory factors were up-regulated by LPS at the two different time points. CM and EV-free CM (CM EV-) significantly decreased IL-1β and TNF-α at 4 h, whereas at 20 h these two treatments also showed a significant reduction in the levels of nitrite compared to LPS-stimulated macrophages. (**Figure 59**). On the other hand, although Ex and Mv significantly decreased the levels of TNF-α and nitrite at 20 h, in

comparison to LPS-treated macrophages, no significant changes were observed on IL-1β levels. At 4 h Ex and Mv induced only the down-regulation of the levels of IL-1β in comparison to LPS-stimulated macrophages. Total CM and CM EV- showed a more efficient effect than EV at inhibiting the production of inflammatory mediators by LPS-stimulated macrophages.

4.4. Cell migration

As indicated previously, several chemokines were identified in CM by using a chemokine array. MCP-5, MCP-1 and KC are involved in neutrophils and monocytes migration. To evaluate their functionality, we performed neutrophil and monocyte migration assays using *transwells*.

In the first assay, we determined the migration of neutrophils with different treatments. For this purpose, macrophages were treated with CM, EV-free CM (CM EV-), Ex or Mv in the presence or absence of LPS for 20 h. Then, neutrophils isolated from bone marrow were added into the inserts for 4 h. Finally, neutrophils were collected and measured by flow cytometry. As shown in **Figure 60**, CM and EV-free CM (CM EV-) significantly enhanced neutrophil migration in the absence of LPS stimulation compared to the control group (B). In contrast, neutrophil migration stimulated by LPS was not affected by any of the treatments.

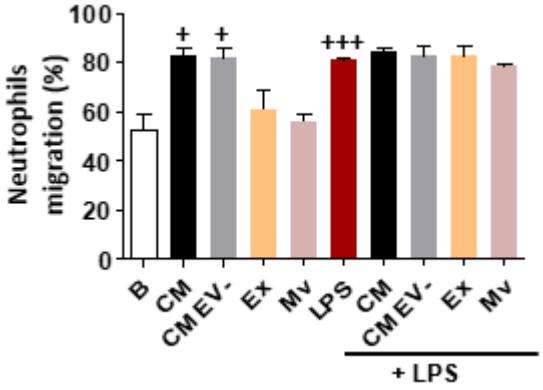

Figure 60. Determination of the effect of EV on neutrophil migration. CM and EV-free CM were used as controls. Results show mean values ± SEM. Pooled data from 3 independent experiments. +$p < 0.05$ and +++$p < 0.001$ vs untreated and unstimulated control cells (B group).

In the second assay, we determined the migration of monocytes. Macrophages were treated with CM, EV-free CM (CM EV-), Ex or Mv in the presence or absence of LPS for 20 h. Monocytes isolated from bone marrow were added into the inserts for 4 h. Then, monocytes were collected and measured by flow cytometry.

Figure 61 shows that none of the treatments affected monocyte migration in the absence of LPS. This stimulus significantly enhanced monocyte migration and treatment with CM or EV-free CM (CM EV-) further increased cell migration in LPS-stimulated macrophages compared to LPS control group (LPS).

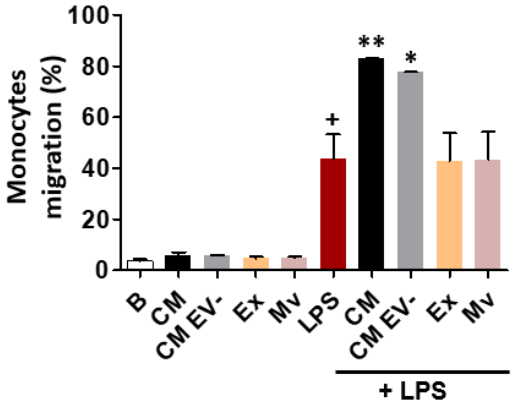

Figure 61. Determination of the effect of EV on monocyte migration. CM and EV-free CM were used as controls. Results show mean values ± SEM. Pooled data from 3 independent experiments. +$p < 0.05$ vs. B group; *$p < 0.05$ and **$p<0.01$ vs. stimulated control cells (LPS group).

Chemokine array detected the presence of several chemokines in the CM from MSC. Three of them (KC, MCP-1 and MCP-5) were markedly increased. KC is involved in neutrophil attraction to the focus of inflammation, whereas MCP-1 and MCP-5 are more involved in monocyte migration. Then, we wondered whether the production of the chemokines KC, MCP-1 and MCP-5 involved in the migration of neutrophils and monocytes could be affected by CM, CM EV- or EV in the presence and absence of LPS. Therefore, the levels of these three chemokines were evaluated in the supernatant of migration experiments by ELISA (**Figure 62**).

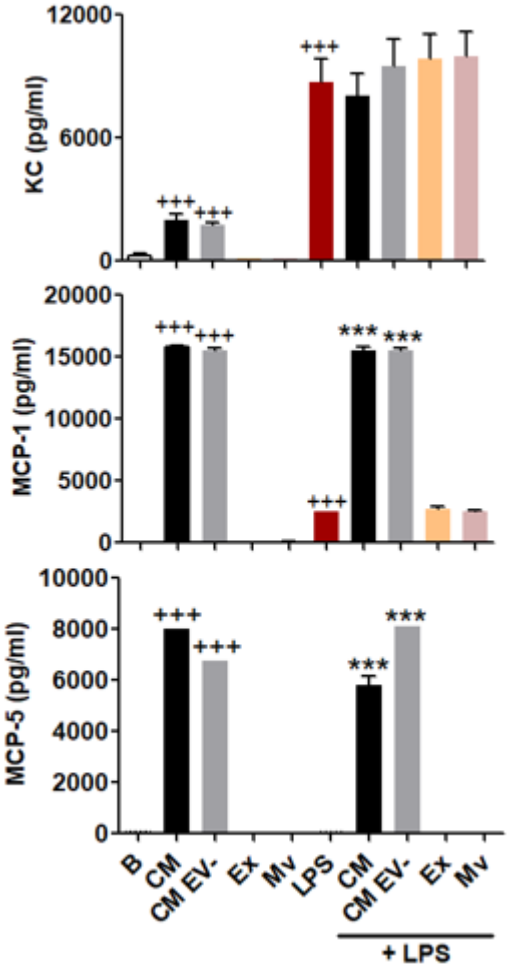

Figure 62. Determination of the effect of EV on the production of chemotactic factors. CM and EV-free CM were used as controls. The levels of KC (neutrophils), MCP-1 and MCP-5 (monocytes) were measured in the supernatant of the corresponding migration assays by ELISA. Results show mean ± SEM. Pooled data from 3 independent experiments. +++$p < 0.001$ vs. B group; ***$p < 0.001$ vs. LPS control group.

Whereas the levels of KC and MCP-1 in the supernatant of LPS-stimulated cells were significantly increased with respect to the B group (B), no changes were observed in MCP-5 levels compared to this control B group. MCP-1 and MCP-5 levels were also significantly

enhanced in CM and EV-free CM (CM EV-) in the absence and in the presence of LPS in comparison to B group and LPS control group, respectively. Regarding KC levels, no significant differences were shown by the treatments with respect to LPS-stimulated macrophages although in unstimulated cells, a higher level of KC was present in CM and CM EV- groups compared with the B group.

4.5. Phagocytic activity

Macrophages are important cells involved in the innate immune system. One of their main functions in an innate inflammatory response is the phagocytosis that consists of engulfing and removing pathogens, cell debris and foreign particles (Zent and Elliott, 2017). We wanted to study the effects of EV (Ex and Mv) on the phagocytic activity of macrophages using fluorescent beads. For this purpose, macrophages were treated with Ex or Mv in the presence or absence of LPS (1 µg/ml) for 20 h. After these 20 h, fluorescent beads were added into the wells for 4 h. The phagocytic activity was then measured by flow cytometry and confocal microscopy. CM and EV-free CM (CM EV-) were used as controls.

As shown in **Figures 63 and 64** (flow cytometry and confocal microscopy, respectively), CM significantly reduced the phagocytosis of fluorescent beads by macrophages either unstimulated or stimulated with LPS. CM EV- reduced phagocytosis only in LPS-stimulated macrophages but to a lesser extent. In contrast, Ex and Mv were ineffective in unstimulated cells but significantly increased the phagocytic activity of LPS-stimulated macrophages.

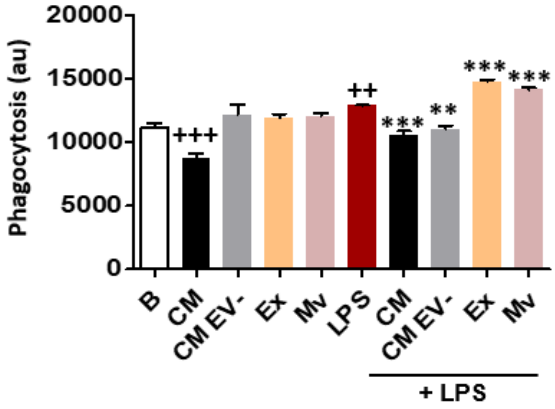

Figure 63. Determination of the effect of EV on the phagocytosis of macrophages by flow cytometry. The phagocytic activity was evaluated by flow cytometry, and the results are expressed as the mean fluorescence (in arbitrary units [au]) ± SEM of 3 independent experiments. +++$p < 0.001$, ++$p < 0.01$ vs. B group; **$p < 0.01$, ***$p < 0.001$ vs. LPS control group.

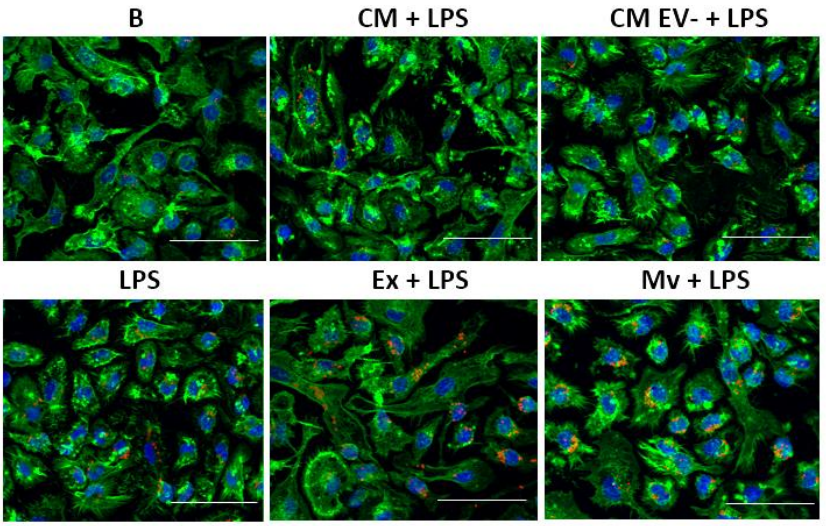

Figure 64. Representative image of the effect of EV on the phagocytosis of macrophages by confocal microscopy. Cells were washed and stained with CD11 b-APC antibody for the cytoplasm (green) and DAPI for the nuclei (blue). The fluorescent beads are in red. Representative images of 3 independent experiments. Scale bar: 50 µm.

4.6. Expression of TLR4

LPS/TLR4 signalling has been intensively studied in the past few years. The stimulation of Toll-like receptor 4 (TLR4) by LPS induces the internalization of the receptor followed by the release of critical proinflammatory cytokines that are necessary to activate potent immune responses (Lu *et al.*, 2008). We wondered whether EV (Ex and Mv) could alter TLR4 expression on the surface of macrophages. TLR4 surface expression on macrophages was determined by flow cytometry at two different time points (4 h and 20 h after LPS stimulation). CM and EV-free CM (CM EV-) were used as controls. **Figure 65** shows that LPS enhanced the expression of TLR4 at both time points compared to unstimulated and untreated macrophages (group B) although the results were significant at 20 h only.

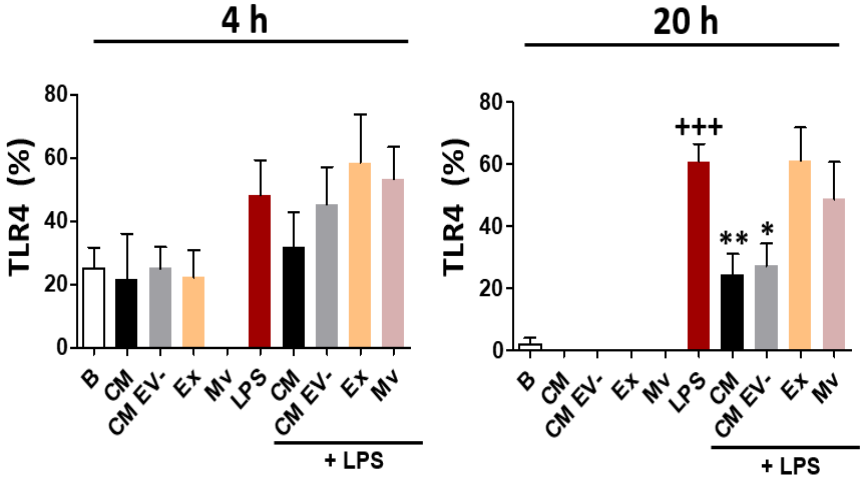

Figure 65. Determination of the effect of EV on the expression of TLR4 on the surface of macrophages. CM and EV-free CM were used as controls. The surface marker TLR4 was determined by flow cytometry. Results are shown as mean ± SEM. Pooled data from 3 experiments. +++$p < 0.001$ vs. B group; *$p < 0.05$, **$p < 0.01$ vs. LPS group.

We observed that CM, EV-free CM, Mv and Ex had no significant effect on TLR4 levels on the surface of macrophages after 4 h of LPS stimulus neither in the absence or presence of LPS nor at 20 h in the

absence of LPS. Whereas CM and EV-free CM (CM EV-) significantly decreased the TLR4 surface expression induced by LPS at 20 h, there were no significant changes in cells treated with Ex or Mv.

4.7. Expression of CD14

CD14 transfers LPS to TLR4, acting as an accessory protein (Ulevitch and Tobias, 1995). We investigated if the expression of CD14 may be affected by EV (Ex and Mv) in the presence or absence of LPS at two different time points (4 h and 20 h after LPS stimulus). CM and EV-free CM were used as controls. There were no significant changes on CD14 expression on the surface of macrophages neither in absence nor in presence of LPS after 4 h or 20 h of its addition (**Figure 66**).

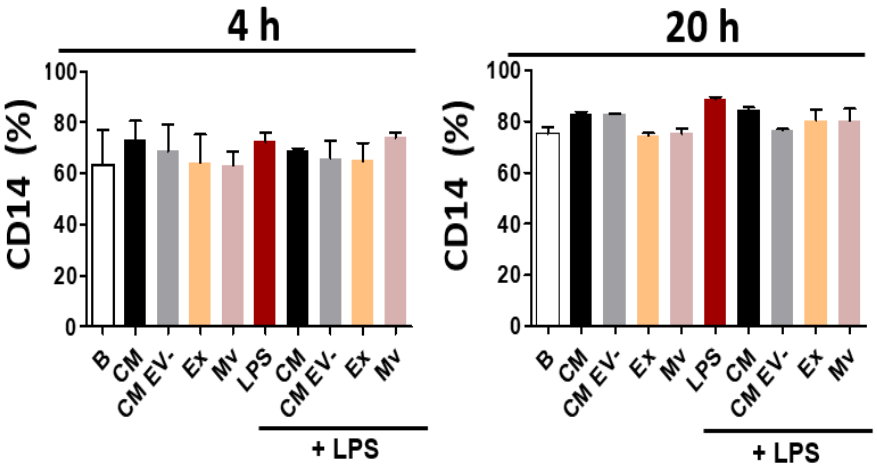

Figure 66. Determination of the effect of EV on the expression of CD14 on the surface of macrophages. CM and EV-free CM were used as controls. Macrophages were incubated in presence and absence of LPS for 4 and 20 h and then the surface expression of CD14 was determined by flow cytometry. Data are displayed as mean ± SEM. Pooled data from 3 independent experiments.

4.8 Apyrase blockade

Apyrase was shown as the protein with the highest level of expression in the CM from MSC (**Figure 53**). This protein is a highly

active ATP-diphosphohydrolase that catalyzes the sequential hydrolysis of ATP to ADP and ADP to AMP releasing inorganic phosphate. Under inflammatory conditions, immune cells secrete ATP that promotes inflammation. Apyrase hydrolises ATP and other nucleotides, contributing to an anti-inflammatory effect (Kukulski *et al*., 2007).

To examine a possible contribution of apyrase to the observed effects of CM in macrophages, this protein was blocked in CM by incubation with the antibody anti-CANT-1. Then, the levels of inflammatory mediators (IL-1β, TNF-α, KC and nitrite) were determined.

As shown in **Figure 67**, LPS strongly enhanced the production of TNF-α and KC in macrophages. In LPS-stimulated macrophages, CM and CM treated with anti-CANT-1 (CM + Ab) significantly reduced the production of both cytokines. No significant differences were observed between CM and apyrase-blocked CM (CM + Ab) in the presence of LPS.

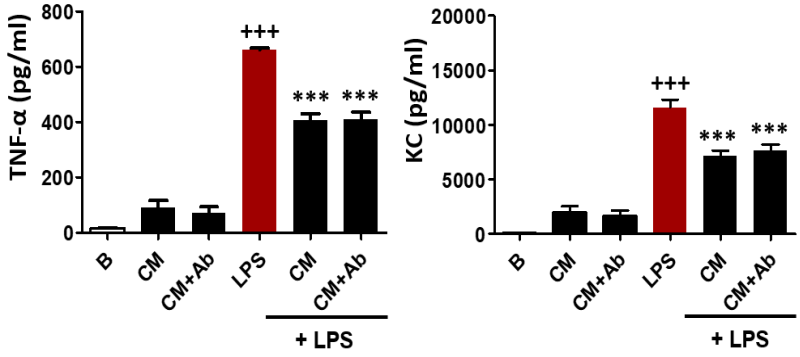

Figure 67. Determination of the effects of apyrase blockade on TNF-α and KC production at 20 h. TNF-α and KC were measured by ELISA. Results show mean ± SEM, pooled data from 3 independent experiments. +++$p < 0.001$ vs. B; ***$p < 0.001$ vs. LPS control group (LPS).

It has been described that ATP release induces an increase in IL-1β and NO (Mehta *et al*., 2001, Sperlagh *et al*., 1998). Since apyrase

catalyzes the hydrolysis of ATP, we studied the effect of CM after blocking apyrase. CM and CM EV- were incubated with anti-CANT-1 antibody to evaluate the effect on the production of IL-1β and nitrite. No significant differences were observed in the production of IL-1β and nitrite between CM and CM + CANT-1 groups in the absence of LPS stimulation (**Figure 68**). LPS-stimulated macrophages incubated with anti-CANT-1 antibody (LPS + Ab) or without anti-CANT-1 (LPS) showed an increased production of IL-1β and nitrite in comparison to unstimulated and untreated macrophages (B). As expected, CM and EV-free CM (CM EV-) without anti-CANT-1 significantly decreased the levels of IL-1β and nitrite in LPS-stimulated macrophages. Interestingly, incubation of CM with anti-CANT-1 partly counteracted the effect of CM on these inflammatory mediators. These results indicate that apyrase blockade results in a lower inhibitory effect of CM on LPS-stimulated nitrite and IL-1β production.

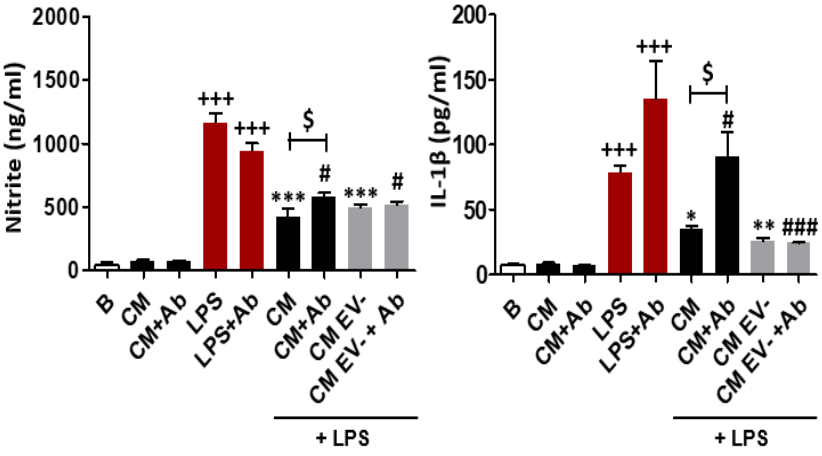

Figure 68. Determination of the effects of apyrase blockade on IL-1β and nitrite production at 20 h. IL-1β and nitrite levels were measured in the supernatant of macrophages by ELISA and fluorometry, respectively. Results show mean ± SEM, pooled data from 3 independent experiments. +++p < 0.001 vs. B; *p < 0.05, **p < 0.01, ***p < 0.001 vs. LPS control group (LPS); #p < 0.05, ###p < 0.001 vs. LPS-stimulated macrophages incubated with anti-CANT-1 (LPS + Ab); $p < 0.05 vs. CM incubated with anti-CANT-1 (CM + Ab).

4.9. ATP release

ATP released by the macrophages was evaluated in the cells with or without CM and CM EV- in the presence or absence of LPS at 4 h and 20 h after LPS administration (**Figure 69**).

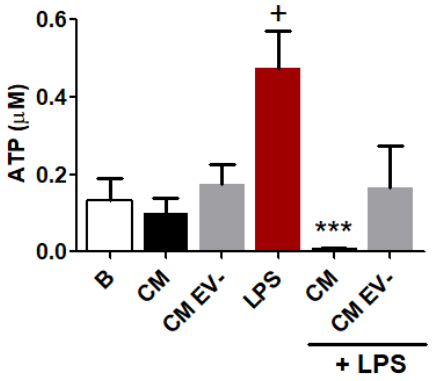

Figure 69. Determination of ATP concentration in supernatants of macrophages at 20 h. Results show mean ± SEM. Pooled data from 3 independent experiments. +p < 0.05 vs. B; ***p < 0.001 vs. LPS control group (LPS).

The concentrations of ATP released after 20 h of stimulation with LPS varied depending on the treatment. These results show that LPS stimulation enhanced the release of ATP into the medium which was significantly reduced in cells treated with CM while a tendency to a lower concentration was observed in the CM EV- group. ATP levels were not detected at 4 h (data not shown).

DISCUSSION

1. Effect of MSC and their CM on an *in vivo* inflammatory model (MAP model)

MSC have become a popular and promising therapeutic approach in many clinical conditions. They have been used in preclinical studies and clinical trials, showing their safety (Glenn and Whartenby, 2014) although many questions regarding their specificity, mechanisms, and therapeutic value remain to be answered (Duffy *et al*., 2011). Adipose tissue is an important source of MSC easier to obtain and with a high yield compared to MSC from other sources, such as bone marrow. In addition, adipose tissue-derived MSC have been found to exert a greater anti-inflammatory effect than the bone marrow in some *in vitro* models (Ivanova-Todorova *et al*., 2009).

We have determined the *in vivo* effects of adipose tissue-derived MSC from mice and their CM on the innate inflammatory response using the zymosan-injected MAP model. In our study MSC and CM significantly downregulated acute inflammatory parameters such as cell migration, degranulation and production of key inflammatory mediators.

The stimulating factor, zymosan, exerts an inflammatory effect inducing the activation and migration of neutrophils to the air pouch at an early time. These cells arrive at the site of inflammation in response to the presence of chemoattractants and in turn, they produce more inflammatory mediators such as cytokines, chemokines and lipid mediators contributing to the inflammatory response (Sadik *et al.*, 2011).

Activated neutrophils also release MPO, an enzyme which is the major component in the azurophilic granules of these cells and plays an important role in the production of reactive oxygen species. This enzyme catalyzes the production of potent oxidants such as hypochlorous acid from hydrogen peroxide and chloride anion, which can damage tissues during inflammatory processes (Prokopowicz *et*

al., 2012) and contribute to host defence against infections (Aratani *et al.*, 1999; Brennan *et al.*, 2001). Furthermore, MPO has been reported to recruit neutrophils by its positive surface charge, regulating the inflammatory response (Klinke *et al.*, 2011). Our results have shown that the number of leukocytes recruited into the air pouch was lower in animals treated with either MSC or CM compared to zymosan control, which was accompanied by a strong reduction in MPO levels. The reduction in cell migration would be the result of an inhibitory effect of MSC or CM on relevant chemoattractant mediators such as LTB_4, MCP-1 and KC.

Several immune cells produce LTB_4 in response to zymosan (Le Bel *et al.*, 2014). This eicosanoid is involved in the migration of neutrophils, attracting them to the site of inflammation. In pathological conditions, such as asthma and arthritis, LTB_4 contributes to the exacerbation of symptoms, as a result of the increased cell recruitment (Le Bel *et al.*, 2014; Brandt and Serezani, 2017). CM and MSC not only reduced the levels of LTB_4 but also of the CC chemokine MCP-1/CCL2 and the CXC chemokine KC/CXCL1, which participate and synergize in the migration response (Gouwy *et al.*, 2008). Neutrophils may amplify their own migration through the production of LTB_4 and chemokines such as KC, and also promote the following recruitment and activation of monocytes into inflammatory sites (Scapini *et al.*, 2000). Different mechanisms may be involved, as at an early time the quick release of granule proteins by activated neutrophils promote the production of monocyte-attracting chemokines such as MCP-1 by neighbouring endothelial cells and macrophages whereas at later time points, additional mechanisms, such as modulation of the chemokine network or the effect of apoptotic neutrophils, may be relevant for attracting monocytes to the inflamed tissue (Soehnlein *et al.*, 2009).

Pro-inflammatory cytokines are key factors for the initiation and maintenance of inflammatory processes. In MAP experiments, CM and MSC significantly reduced the levels of pro-inflammatory mediators IL-1β, IL-6 and TNF-α at the early stage of the inflammatory response.

Although these cytokines have not chemotactic properties, they activate transcription factors such as NF-κB in different cell types (Smale, 2012; Confalone *et al.*, 2010), which in turn results in the transcription of chemokines such as KC and MCP-1 (Matsushima *et al.*, 1989) which are upregulated in inflammatory conditions. Therefore, there are enhanced levels of MCP-1 in synovial fluid and macrophages of rheumatoid arthritis or osteoarthritis patients (Van Coillie *et al*., 1999) and they are also relevant in atherosclerosis pathophysiology (Lin *et al.*, 2014). CM and MSC reduced IL-6 levels *in vivo* at 4 and 18 h. This cytokine may also be induced by TNF-α and IL-1β (Confalone *et al.*, 2010) and is a main contributor to cytokine networks during inflammation. In addition, the IL-6-sIL-6Rα complex can activate endothelial cells to secrete IL-8 and MCP-1 to sustain cell migration and inflammation (Soehnlein et al., 2009). Therefore, this cytokine plays multiple roles in acute inflammation as well as in the evolution to chronicity. Furthermore, its overexpression is involved in diseases with an inflammatory component, such as rheumatoid arthritis (Fonseca *et al.*, 2009; Alonzi *et al.*, 1998).

IL-10 is a pleiotropic cytokine important for its anti-inflammatory and immunomoduatory role (Kyurkchiev *et al.*, 2014). Studies in IL-10 knock-out mice have demonstrated that IL-10 may regulate the chemokine-mediated cellular component of acute inflammation induced by zymosan as this cytokine may reduce the production of KC and MCP-1, and neutrophil influx (Ajuebor et al., 1999). In addition, CM from human adipose tissue-derived MSC have been reported to increase the number of CD4+FoxP3+ cells and the production of IL-10 in human T cell cultures (Ivanova-Todorova *et al.*, 2012). However, in our MAP model CM and MSC did not significantly modify the levels of IL-10, and previous studies have shown that T-cell subsets are not predominant within the cell population present in the air pouch (Posadas *et al.,* 2000). Our results thus suggest that IL-10 does not play a role in this model at the time points described.

TSG-6 is upregulated by a wide range of mediators such as the proinflammatory cytokines IL-1β, IL-6 and TNFα, growth factors and PGE_2. Consequently, TSG-6 have been reported to be highly expressed in sera and tissues from sepsis, inflammatory bowel disease, rheumatoid arthritis or osteoarthritis patients (Milner and Day, 2003). The inactivation and the over-expression of TSG-6 gene in transgenic mice increases and decreases inflammatory responses, respectively (Choi et al., 2011). TSG-6 has been described as a potent inhibitor of neutrophil migration through different processes regulating transendothelial migration (Cao *et al.*, 2004; Szanto et al., 2004). In fact, administration of human TSG-6 has been shown to inhibit neutrophil migration and the production of inflammatory mediators induced by stimuli such as carrageenan, zymosan or IL-1β in the MAP (Getting *et al.*, 2002; Wisniewski *et al*., 1996). Interestingly, secretion of TSG-6 could mediate the protective effects of human bone marrow MSC in a rodent model of myocardial infarction (Lee *et al.*, 2009), inflammatory damage to rat cornea (Roddy *et al.*, 2011) or peritonitis induced by zymosan in C57BL/6J mice (Choi *et al.*, 2011). In our study TSG-6 was upregulated in air pouch exudates during the early inflammatory response induced by zymosan. Administration of CM or MSC decreased the levels of this protein, likely related to the decreased production of inflammatory mediators. These data indicate that TSG-6 is not involved in the anti-inflammatory effects of either CM or MSC in the zymosan-injected MAP.

The expression of COX-2 and mPGES-1 in cells migrated to the MAP increased after zymosan administration, which resulted in enhanced PGE_2 levels in MAP exudates. Vasopermeability and vasodilation are some of the pro-inflammatory effects exerted by this eicosanoid, as well as the induction of the synthesis of matrix metalloproteinases by different cell types. PGE_2 also exhibits immunomodulatory properties, reducing type-1 immune responses in T cells and macrophages (Harris *et al*., 2002). We have shown *in vivo* a

significant reduction of PGE_2 by CM and MSC, which can be the consequence of the downregulation of mPGES-1 expression.

Zymosan is recognized by TLR2 in immune cells such as neutrophils leading to NF-κB activation (Muzio *et al*., 2000). This transcription factor is activated by pro-inflammatory cytokines and reactive oxygen species which results in the synthesis of cytokines, chemokines and enzymes involved in inflammation and tissue damage (Karin and Delhase *et al*., 2000). Our results show that zymosan induces the phosphorylation of p65 in migrating neutrophils, a key step in NF-κB activation which is downregulated by CM treatment. Our data thus suggest that this mechanism contributes to the control of the inflammatory response by CM. NF-κB plays a key role in the regulation of COX-2 and mPGES-1 expression (Bonizzi and Karin, 2004; Díaz-Muñoz *et al*., 2010). Nevertheless, no significant modification in COX-2 expression was observed after CM or MSC administration, which may be explained by the contribution of multiple transcription factors (NF-κB but also C/EBP, CRE and AP-1) to COX-2 induction by zymosan (Santos *et al*., 2011).

In another series of experiments, we assessed whether the anti-inflammatory activity of MSC in the MAP may be enhanced by HO-1 induction. HO-1 is expressed by MSC, but in a limited manner. Since HO-1 has shown beneficial effects in several clinical conditions (retinal ischemia/reperfusion injury, acute liver failure, etc.), various preclinical studies have been developed to overexpress this enzyme in MSC by treatment with CoPP, hemin, lentivirus transduction, etc. (Li *et al*., 2017, Zhang *et al*., 2017). In our laboratory, we used the MAP model to induce an *in vivo* acute inflammatory response with zymosan in order to investigate whether preconditioning MSC with CoPP (an HO-1 inducer) can promote the beneficial effects of these cells in the innate inflammatory response. According to previous studies in our laboratory (Vicente *et al*., 2003), zymosan increased the migration of cells into the air pouch exudate, whereas hemin (another HO-1 inducer) added into the air pouch significantly decreased it. In our

current study we observed a strong pro-inflammatory response with zymosan similar to that reported previously. In contrast, our results showed no alteration on the cells migrating into the air pouch after administration of MSC preconditioned with CoPP or their CM. Also, MPO activity was not modified by these treatments. In addition, Vicente *et al*. (2003) showed a decrease in the production of some cytokines such as IL-1β and TNF-α with hemin treatment. In our experiments, preconditioning MSC with CoPP decreased the production of these cytokines, and IL-6. In line with the results of Vicente *et al*. (2003), PGE_2 levels in exudates were not modified by CoPP preconditioning. These results suggest that preconditioning of MSC with CoPP may weakly improve the beneficial anti-inflammatory effects of MSC.

A wide range of evidence indicates that the immunomodulatory properties of MSC can depend on cell contact or the secretion of different factors which are present in their CM (Ivanova-Todorova *et al*., 2012). In the zymosan-injected MAP, the observed *in vivo* anti-inflammatory properties of MSC were reproduced by their CM which exerted a higher effect on some parameters thus suggesting that these properties are mainly mediated by the secretome of these cells. Nevertheless, in this experimental model, the anti-inflammatory activity was not dependent on the increased production of soluble factors such as PGE_2 or TSG-6 reported in other experimental models (Prockop, 2013). After having demonstrated the anti-inflammatory activity of MSC and their CM in the MAP model, we focused on the secretome of these cells in order to gain more insight into the components that may be responsible for the activity.

2. CM composition

We have studied some of the possible factors that may be responsible for the anti-inflammatory activity of CM by proteomic analyses, chemokine array and the isolation of the EV fraction of MSC secretome.

The proteomic analysis of the CM from MSC revealed an increased expression of several proteins, specifically PhnD, PstS and apyrase compared to the control medium. Interestingly, apyrase was found to be the most abundant protein. Apyrase catalyzes the hydrolysis of extracellular ATP which is involved in the promotion of inflammation inducing pro-inflammatory cytokines and other mediators (Kukulski *et al*., 2007).

In addition, we determined the main chemokines present in CM from MSC with an array. The analysis showed a high expression of chemokines MIP-1γ, KC, LIX, MCP-1, MCP-5 and PF-4 present in the CM of MSC in comparison to control medium. These chemokines play an important role to attract neutrophils or monocytes to the inflammatory focus (Sadik *et al*., 2011).

Furthermore, we isolated the EV fraction of CM. Therefore, Mv and Ex were isolated from CM by differential centrifugation combined with size filtration. Both types of EV were characterised by TRPS and TEM. EV participate in various physiological processes and have important roles in immune regulation. Besides, EV have been tested as potential therapeutic tools for the treatment of inflammatory and autoimmune diseases (Tofiño-Vian *et al*., 2018). In this context, we wanted to investigate the possible contribution of CM components to the anti-inflammatory activity of MSC. For this purpose, we used an *in vitro* model: mouse peritoneal macrophages stimulated with LPS.

3. Effects of CM and EV on mouse peritoneal macrophages

Macrophages are distributed in tissues throughout the body and contribute to both homeostasis and disease. Macrophages play an important role in inflammation and they are also the link between the innate and the adaptive response (Taylor *et al*., 2005; Varol *et al*., 2015). TLRs expressed in macrophages detect pathogens and sense danger signals generated by tissue damage, e.g. extracellular matrix components, DNA complexes, oxidized lipoproteins, heat shock

proteins, etc. As a result, TLRs activate signalling pathways inducing the expression of immune and pro-inflammatory genes and they have also been implicated in several immune-mediated and inflammatory diseases. In particular, activation of TLR4 following LPS stimulation activates the NF-κB signalling pathway leading to the synthesis of inflammatory mediators such as cytokines, chemokines, NO, etc. (Kaczorowski *et al*., 2008).

The regulation of macrophage activation by LPS is critical for controlling the initial phases of the immune response. We have shown that CM and its EV-free fraction significantly reduce the production of relevant inflammatory mediators such as IL-1β, TNF-α and NO in macrophages whereas the EV fraction exert a limited effect. The IL-1 family of cytokines is associated with acute and chronic inflammation, and plays an essential role in the innate response to infection but also in damaging processes and inflammatory diseases (Van de Veerdonk and Netea, 2013). A broad range of immune and inflammatory functions have been adscribed to TNF-α, a key mediator of septic shock also associated with autoimmune diseases (Beutler, 1999). Cytokines and microbial products induce nitric oxide synthase in macrophages leading to an enhanced synthesis of this mediator, considered as a key mediator of nonspecific immunity. Overproduction of NO has been implicated in sepsis, neurodegenerative disorders, inflammation, etc. (MacMicking *et al*., 1997). Therefore, the downregulation of these mediators could play an important role in the anti-inflammatory effects of CM and would be mediated by its soluble fraction but not by EV.

Other macrophage responses were also differently affected by CM fractions. The inflammatory mediators released by macrophages during the early stage of inflammation induce an increase in the migration of immune cells such as neutrophils and monocytes to the site of injury/inflammation. Neutrophils are the first cells to migrate within minutes to the focus of the inflammation (Le Blanc and Davies, 2015) to release bactericidal molecules, cytokines, chemokines,

reactive oxygen species and produce neutrophil extracellular traps, webs of chromatin derived from the neutrophil nucleus containing proteases (Weiss, 1989). They also interact with other cells such as macrophages, dendritic cells, natural killer cells, T cells and B cells, potentiating or downmodulating the innate and adaptive immunity (Yang *et al*., 2017). Our data from co-culture experiments indicate that CM and CM EV- are active on cell migration whereas Mv and Ex do not affect this function. We have also studied the possible contribution to leukocyte migration of some chemoattractive components present in CM. In unstimulated macrophages, CM and EV-depleted CM enhanced neutrophil migration which would depend on the presence of the neutrophil chemokine KC. In addition, another chemokine involved in neutrophil recruitment, LIX, was detected in CM by the chemokine array and may contribute to its effects on migration. In contrast, our results suggest that CM does not modulate the migratory capacity of neutrophils in the presence of LPS-stimulated macrophages as similar levels of KC are released in all experimental groups upon LPS stimulation.

Monocytes play an important role in tissue homeostasis and immunity. During an inflammatory process, these cells migrate from the bone marrow to the focus of inflammation and then give rise to macrophages. Some of the bioactive molecules secreted by MSC are chemokines, which are involved in the recruitment of different cells from the immune system. For instance, MCP-1/CCL2 and its receptor chemokine (C-C motif) receptor-2 (CCR2) play a leading role in the recruitment of monocytes (Leuschner *et al*., 2015). In our laboratory, we studied the chemokines secreted by MSC into their CM with a chemokine array, where we obtained a high expression of MCP-1 and MCP-5. As both chemokines are involved in the recruitment of monocytes, we investigated whether LPS-stimulated macrophages can influence monocyte migration in the presence of CM as well as EV using transwell migration chambers. We have shown that CM and EV-depleted CM increased monocyte migration in the presence of LPS stimulation but not in unstimulated macrophages, whereas EV did not

show any effect. Lee *et al*. (2010) reported that human adipose tissue-derived MSC treated with TNF-α increased the migration of monocytes due to the participation of IL-6, IL-8 and MCP-1. In our experiments, similar levels of MCP-1 and MCP-5 were measured in the supernatant of unstimulated macrophages and LPS-stimulated macrophages when cells were treated with CM or EV-depleted CM although an enhancement in migration was only observed in the presence of LPS, suggesting that other mechanisms may be involved in the observed effect on monocyte migration. Although MCP-1 and MCP-5 levels did not elicit monocyte migration in unstimulated cells, the increased migration of CM and CM EV- treated cells in the presence of LPS may be related to these chemokines, as LPS can potentiate their effects on migration (Liu *et al*., 2013). Therefore, the presence in CM of molecules chemoattractive to monocytes may augment the repair response as tissue macrophages have been shown to play a main role in tissue repair whereas MCP-1 deficiency decreases macrophage infiltration and delayed replacement of injured cells (Dewald *et al*., 2005).

Phagocytosis is an essential function of macrophages which takes part in the uptake of pathogens during the inflammation process. Additionally, phagocytosis of apoptotic bodies and debris is necessary for tissue resolution and termination of inflammation (Greenberg and Grinstein, 2002). Macrophages are activated during inflammation, increasing their phagocytic activity to remove the strange particles or bacteria that can damage our organism. Many studies have demonstrated that MSC can regulate the activation and function of macrophages through the secretion of soluble factors or by cell-to-cell contact. However, little is known about the influence of EV from MSC on the phagocytic activity of macrophages. In contrast to the inhibitory effect of CM, our results have shown that Ex and MV increased the phagocytic activity of inert particles by LPS-stimulated macrophages. These data are in line with the work of Monsel *et al.* (2015) which reported an increased monocyte phagocytosis in a severe pneumoniae mouse model by Mv from MSC while decreasing

inflammatory cytokine secretion and increasing intracellular ATP levels in injured alveolar epithelial type 2 cells. EV-mediated mitochondrial transfer has been suggested as responsible for the enhanced phagocytic phenotype in alveolar macrophages (Morrison *et al*., 2017).

As the proteomic analysis indicated that apyrase is the most abundant protein in CM, we evaluated whether blocking apyrase in CM could influence the production of pro-inflammatory mediators in LPS-stimulated macrophages. Apyrase is a soluble e-NTPDase which efficiently hydrolyses ATP and other nucleotides (Kukulski *et al*., 2007). The release of ATP in response to LPS, formation of adenosine and upregulation of A2bR on macrophages have been related to the induction of a regulatory phenotype in these cells to limit the inflammatory response (Cohen *et al.*, 2013). The NLRP3 inflammasome is involved in IL-1β and IL-18 processing in response to pathogen-and danger-associated molecular patterns. The synthesis of pro-IL-1β and NLRP3 is transcriptionally induced via activation of TLRs, followed by a second stimulus leading to inflammasome oligomerization, caspase-1 auto-activation and cleavage of pro-IL-1β to release active IL-1β (Gombault *et al*., 2012). In addition, different neutrophil- and macrophage-derived proteases have been reported to process pro-IL-1β in an inflammasome-independent manner (Netea *et al*., 2015). Cellular stimulation triggers ATP release which is degraded by ectonucleotidases to ADP, AMP and adenosine. ATP and its metabolites activate different purinergic receptors on cells to modulate cellular functions in immunity (Gombault *et al*., 2012).

LPS induces ATP production, which stimulates NO (Sperlagh *et al.*, 1998) and IL-1β release in mouse macrophages (Perregaux and Gabel, 1998). In our experiments, apyrase blockade partly counteracted the inhibitory effects of CM on the expression of these pro-inflammatory mediators suggesting the contribution of this enzyme to some of CM anti-inflammatory effects. Furthermore, we confirmed the inhibitory effect of CM on ATP release by LPS-stimulated macrophages. In contrast, TNF-α and KC levels were not modified after apyrase blockade suggesting that these mediators are not regulated by ATP in this experimental model. Although ATP is involved in monocyte

migration (Kronlage *et al*., 2010), it is known that apyrase does not affect monocyte migration to MCP-1 (Elliott *et al*., 2009) which is in line with the results from migration experiments obtained in the current study.

Abnormal activation of TLR4, contributes to cardiovascular dysfunction, kidney disease, and central nervous system dysregulation (Nunes *et al*., 2018). In many inflammatory conditions there is an increased TLR expression leading to aberrant TLR activation. Therefore, there are a number of negative regulatory mechanisms to prevent autoimmune damage, such as extracellular decoy receptors, intracellular inhibitors, membrane-bound suppressors, degradation of TLRs, and TLR-induced apoptosis (Liew *et al*., 2005). Some inhibitors of TLR4 signalling have been shown to be effective in sepsis and neuropathic pain and potential indications can be asthma and rheumatoid arthritis. Therefore, in preclinical models, TLR4 deficiency prevented the production of pro-inflammatory cytokines and the development of arthritis (Elshabrawy *et al*., 2017). To explore the mechanisms responsible for the anti-inflammatory effects of CM, TLR4 and CD14 protein expression was analysed by flow cytometry. These experiments indicated that CM was able to downregulate TLR4 expression stimulated by LPS. Our results suggest that the anti-inflammatory activity of CM may be related, at least in part, to the reduction of the TLR4 signalling pathway.

Macrophages mediate the inflammatory response, but they also contribute later to tissue remodeling and restoration of function. Recent evidence has revealed the plasticity of these cells in different environments and the possible contribution of MSC to this property. Thus, MSC may promote the development of anti-inflammatory monocytes and macrophages. Factors present in MSC secretome and/or cell-to-cell contact can lead to the generation of different types of immunoregulatory macrophages, exhibiting different functional properties in innate or adaptive immunity (Chiossone *et al*., 2016). Our data indicate that MSC secretome has the ability to modify the functional properties of mouse peritoneal macrophages inducing the

secretion of less inflammatory mediators, a higher migration of leukocytes by the soluble fraction, and opposite effects on phagocytic activity according to the fraction considered. The downregulation of TLR4 expression and the presence of apyrase may contribute to some of the effects of CM. These results suggest that the anti-inflammatory effects of MSC on the innate immune response are mainly mediated by the soluble fraction of their secretome. More studies are necessary for a complete characterisation of the secretory profile of mouse perigonadal adipose tissue-derived MSC. Furthermore, a broader understanding of the regulatory properties of MSC secretome on inflammatory and immune responses may lead to the development of new targets and therapeutic approaches in inflammatory diseases.

Conclusions

1. Mouse adipose tissue-derived mesenchymal stem cells (MSC) control the innate inflammatory response induced by zymosan in the mouse air pouch model. This effect is mainly mediated by the secretome (CM) of these cells and related to the downregulation of cell migration, degranulation and production of key inflammatory mediators.

2. This reduction in cell migration would be the result of the inhibitory effect of MSC or CM on relevant chemoattractant mediators such as LTB_4, MCP-1 and KC. Besides, MSC and CM significantly reduced the levels of pro-inflammatory mediators IL-1β, IL-6 and TNFα at the early stage of the inflammatory response, which can be the consequence of the inhibition of NF-κB activation.

3. The CM from MSC contains soluble factors and extracellular vesicles (EV) (exosomes and microvesicles). Proteomic analysis has shown that apyrase is a highly abundant protein in CM which may contribute to its anti-inflammatory effects regulating the production of IL-1β and NO in primary mouse peritoneal macrophages. CM also contains chemokines (KC, MCP-1 and MCP-5) involved in the migration ability of neutrophils and monocytes.

4. In mouse peritoneal macrophages stimulated with LPS, CM regulates phagocytosis, cell migration and production of inflammatory mediators. The soluble fraction of CM plays a more important role than EV in mediating such effects.

5. The anti-inflammatory activity of CM in this *in vitro* model may be related, at least in part, to the downregulation of TLR4 expression and therefore to the reduction of the TLR4 signalling pathway.

Conclusions

1. Les cèl·lules mare mesenquimals del teixit adipós (MSC) controlen la resposta inflamatòria innata induïda per zimosan en un model de bolsa d'air en ratolí. Aquest efecte està principalment mediat pel secretoma (CM) d'aquestes cèl·lules i es relaciona amb la disminució de la migració cel·lular, la degranulació i la producció de mediadors inflamatoris clau.

2. Aquesta reducció en la migració cel·lular seria el resultat de l'efecte inhibidor de MSC o CM en els mediadors quimioatraients rellevants com LTB_4, MCP-1 i KC. A més, MSC i CM van reduir significativament els nivells de mediadors proinflamatoris IL-1β, IL-6 i TNF-α en la fase inicial de la resposta inflamatòria, que pot ser la conseqüència de la inhibició de l'activació NF-κB.

3. El CM de MSC conté factors solubles i vesícules extracel·lulars (EV) (exosomes i microvesícules). L'anàlisi de la proteòmica ha demostrat que l'apirasa és una proteïna altament abundant en CM que pot contribuir als seus efectes antiinflamatoris que regulen la producció d'IL-1β i NO en els macròfags peritoneals primaris del ratolí. CM també conté quimiocines (KC, MCP-1 i MCP-5) que participen en la capacitat de migració de neutròfils i monòcits.

4. En els macròfags peritoneals del ratolí estimulats amb LPS, CM regula la fagocitosi, la migració cel·lular i la producció de mediadors inflamatoris. La fracció soluble de CM té un paper més important que EV en la mediació d'aquests efectes.

5. L'activitat antiinflamatòria de CM en aquest model *in vitro* pot estar relacionada, almenys en part, amb la disminució de l'expressió TLR4 i, per tant, a la reducció de la via de senyalització TLR4.

Conclusiones

1. Las células madre mesenquimales derivadas de tejido adiposo de ratón (MSC) controlan la respuesta inflamatoria innata inducida por zimosán en el modelo de bolsa de aire en ratón. Este efecto está mediado principalmente por el secretoma (CM) de estas células y está relacionado con la disminución de la migración celular, la desgranulación y la producción de importantes mediadores inflamatorios.

2. Esta reducción en la migración celular sería el resultado del efecto inhibidor de las MSC o del CM en los mediadores quimioatrayentes relevantes tales como LTB_4, MCP-1 y KC. Además, las MSC y el CM redujeron significativamente los niveles de mediadores proinflamatorios IL-1β, IL-6 y TNF-α en la etapa temprana de la respuesta inflamatoria, lo que puede ser debido a la inhibición de la activación de NF-κB.

3. El CM de las MSC contiene factores solubles y vesículas extracelulares (EV) (exosomas y microvesículas). El análisis proteómico ha demostrado que la apirasa es una proteína muy abundante en el CM que puede contribuir a sus efectos antiinflamatorios que regulan la producción de IL-1β y NO en macrófagos peritoneales primarios de ratón. El CM también contiene quimiocinas (KC, MCP-1 y MCP-5) implicadas en la capacidad de migración de neutrófilos y monocitos.

4. En los macrófagos peritoneales de ratón estimulados con LPS, CM regula la fagocitosis, la migración celular y la producción de mediadores inflamatorios. La fracción soluble de CM juega un papel más importante que las EV en la mediación de tales efectos.

5. La actividad antiinflamatoria del CM en este modelo *in vitro* puede estar relacionada, al menos en parte, con la regulación a la baja de la expresión de TLR4 y, por lo tanto, con la reducción de la ruta de señalización de TLR4.

References

Addison CL, Arenberg DA, Morris SB, Xue YY, Burdick MD, Mulligan MS, Iannettoni MD, Strieter RM. (2000). The CXC chemokine, monokine induced by interferon-gamma, inhibits non-small cell lung carcinoma tumor growth and metastasis. *Hum Gene Ther.* 11(2):247-61.

Ajuebor MN, Das AM, Virag L, Flower RJ, Szabo C, Perretti M. (1999). Role of resident peritoneal macrophages and mast cells in chemokine production and neutrophil migration in acute inflammation: evidence for an inhibitory loop involving endogenous IL-10. *J Immunol*. 162(3):1685-91.

Akira S, Uematsu S, Takeuchi O. (2006). Pathogen recognition and innate immunity. *Cell*. 124(4):783-801.

Alonzi T, Fattori E, Lazzaro D, Costa P, Probert L, Kollias G, De Benedetti F, Poli V, Ciliberto G. (1998). Interleukin 6 is required for the development of collagen-induced arthritis. *J Exp Med*. 187:461-8.

Arango Duque G, Descoteaux A. (2014). Macrophage cytokines: involvement in immunity and infectious diseases. *Front Immunol*. 5:491.

Aratani Y, Koyama H, Nyui S, Suzuki K, Kura F, Maeda N. (1999). Severe impairment in early host defense against Candida albicans in mice deficient in myeloperoxidase. *Infect Immun*. 67(4):1828-36.

Awasthi S. (2014). Toll-like receptor-4 modulation for cancer immunotherapy. *Front Immunol*. 5:328.

Bachelerie F, Ben-Baruch A, Burkhardt AM, Combadiere C, Farber JM, Graham GJ, Horuk R, Sparre-Ulrich AH, Locati M, Luster AD, Mantovani A, Matsushima K, Murphy PM, Nibbs R, Nomiyama H, Power CA, Proudfoot AE, Rosenkilde MM, Rot A, Sozzani S, Thelen M, Yoshie O, Zlotnik A. (2014a). International Union of basic and clinical pharmacology: corrected. I.XXXIX. Update on the extended family of chemokine receptors. *Pharmacol Rev*. 66(1):1-79.

Bachelerie F, Graham CJ, Locati M, Mantovani A, Murphy PM, Nibbs R, Rot A, Sozzani S, Thelen M. (2014b). New nomenclature for atypical chemokine receptors. *Nat Imunol*. 15(3):2017-8.

Ben-Sasson SZ, Hu-Li J, Quiel J, Cauchetaux S, Ratner M, Shapira I, Dinarello CA, Paul WE. (2009). IL-1 acts directly on CD4 T cells to enhance their antigen-driven expansion and differentiation. *Proc Natl Acad Sci U S A*. 106(17):7119–24.

Beutler BA. (1999). The role of tumor necrosis factor in health and disease. *J Rheumatol*. 26 Suppl 57:16-21.

Bianchi ME. (2007). DAMPs, PAMPs and alarmins: all we need to know about danger. *J Leukoc Biol*. 81(1):1-5.

Birben E, Sahiner UM, Sackesen C, Erzurum S, Kalayci O. (2012). Oxidative stress and antioxidant defence. *World Allergy Organ J*. 5(1):9-19.

Biswas SK, Mantovani A. (2010). Macrophage plasticity and interaction with lymphocyte subsets: cancer as a paradigm. *Nat Immunol*. 11(10):889-96.

Blázquez R, Sanchez-Margallo FM, de la Rosa O, Dalemans W, Alvarez V, Tarazona R, Casado JG. (2014). Immunomodulatory Potential of Human Adipose Mesenchymal Stem Cells Derived Exosomes on in vitro Stimulated T Cells. *Front Immunol*. 5:556.

Bonizzi G, Karin M. (2004). The two NF-kappaB activation pathways and their role in innate and adaptive immunity. *Trends Immunol*. 25(6):280-8.

Boyaka PN, McGhee JR. (2001). Cytokines as adjuvants for the induction of mucosal immunity. *Adv Drug Deliv Rev*. 51(1-3):71-9.

Brandt SL, Serezani CH. (2017). Too much of a good thing: How modulating LTB_4 actions restore host defence in homeostasis or disease. *Semin Immunol*. 33:37-43.

Brennan ML, Anderson MM, Shih DM, Qu XD, Wang X, Mehta AC, Lim LL, Shi W, Hazen SL, Jacob JS, Crowley JR, Heinecke JW, Lusis AJ. (2001). Increased atherosclerosis in myeloperoxidase-deficient mice. *J Clin Invest*. 107(4):419-30.

Brough D, Rothwell NJ. (2007). Caspase-1-dependent processing of pro-interleukin-1beta is cytosolic and precedes cell death. *J Cell Sci*. 120(Pt 5):772-81.

Campagnoli C, Roberts IA, Kumar S, Bennet PR, Bellantuono I, Fisk NM. (2001). Identification of mesenchymal stem/progenitor cells in human first-trimester fetal blood, liver, and bone marrow. *Blood*. 98(8):2396-402.

Cao TV, La M, Getting SJ, Day AJ, Perretti M. (2004). Inhibitory effects of TSG-6 Link module on leukocyte-endothelial cell interactions in vitro and in vivo. Microcirculation. 11(7):615-24.

Caplan AI. (1991). Mesenchymal stem cells. *J Orthop Res*. 9(5):641-50.

Carmi Y, Voronov E, Dotan S, Lahat N, Rahat MA, Fogel M, Huszar M, White MR, Dinarello CA, Apte RN. (2009). The role of macrophage-derived IL-1 in induction and maintenance of angiogenesis. *J Immunol*. 183(7):4705-14.

Carswell EA, Old LJ, Kassel RL, Green S, Fiore N, Williamson B. (1975). An endotoxin-induced serum factor that causes necrosis of tumors. *Proc Natl Acad Sci U S A*. 72(9):3666-70.

Casado-Díaz A, Santiago-Mora R, Jiménez R, Caballero-Villarraso J, Herrera C, Torres A, Dorado G, Quesada-Gómez JM. (2008) Cryopreserved human bone marrow mononuclear cells as a source of

mesenchymal stromal cells: application in osteoporosis research. *Cytotherapy*. 10(5):460-8.

Cawthorn WP, Scheller EL, MacDougald OA. (2012). Adipose tissue stem cells meet preadipocyte commitment: going back to the future. *J Lipid Res*. 53(2):227-46.

Chadban SJ, Tesch GH, Foti R, Lan HY, Atkins RC, Nikolic-Paterson DJ. (1998). Interleukin-10 differentially modulates MHC class II expression by mesangial cells and macrophages *in vitro* and *in vivo*. *Immunology*. 94(1):72-8.

Chen L, Tredget EE, Wu PY, Wu Y. (2008). Paracrine factors of mesenchymal stem cells recruit macrophages and endothelial lineage cells and enhance wound healing. *PLoS One*. 3:e1886

Chiossone L, Conte R, Spaggiari GM, Serra M, Romei C, Bellora F, Becchetti F, Andaloro A, Moretta L, Bottino C. (2016). Mesenchymal stromal cells induce peculiar alternatively activated macrophages capable of dampening both innate and adaptive immune responses. *Stem Cells*. 34:1909-21.

Choi H, Lee RH, Bazhanov N, Oh JY, Prockop DJ. (2011). Antiinflammatory protein TSG-6 secreted by activated MSCs attenuates zymosan-induced mouse peritonitis by decreasing TLR2/NF-kappaB signaling in resident macrophages. *Blood*. 118(2):330-8.

Cohen HB, Briggs KT, Marino JP, Ravid K, Robson SC, Mosser DM. (2013). TLR stimulation initiates a CD39-based autoregulatory mechanism that limits macrophage inflammatory responses. *Blood*. 122:1935-45.

Cole KE, Strick CA, Paradis TJ, Ogborne KT, Loetscher M, Gladue RP, Lin W, Boyd JG, Moser B, Wood DE, Sahagan BG, Neote K. (1998). Interferon-inducible T cell alpha chemoattractant (I-TAC): a novel non-

ELR CXC chemokine with potent activity on activated T cells through selective high affinity binding to CXCR3. *J Exp Med*. 187(12):2009-21.

Colombo M, Raposo G, Théry C. (2014). Biogenesis, secretion, and intercelullar interactions of exosomes and other extracelullar vesicles. *Annu Rev Cell Dev Biol.* 30:255-89.

Confalone E, D'Alessio G, Furia A. (2010). IL-6 Induction by TNF-α and IL-1β in an Osteoblast-Like Cell Line. *Int J Biomed Sci*. 6(2):135-40.

Coumans FAW, Brisson AR, Buzas EI, Dignat-George F, Drees EEE, El-Andaloussi S, Emanueli C, Gasecka A, Hendrix A, Hill AF, Lacroix R, Lee Y, van Leeuwen TG, Mackman N, Mäger I, Nolan JP, van der Pol E, Pegtel DM, Sahoo S, Siljander PRM, Sturk G, de Wever O, Nieuwland R. (2017). Methodological Guidelines to Study Extracellular Vesicles. *Circ Res*. 120(10):1632-1648.

Crofford LJ. (1997). COX-1 and COX-2 tissue expression: implications and predictions. *J Rheumatol Suppl*. 49:15-9.

Cunha FQ, Moncada S, Liew FY. (1992). Interleukin-10 (IL-10) inhibits the induction of nitric oxide synthase by interferon-gamma in murine macrophages. *Biochem Biophys Res Commun*. 182(3):1155-9.

De Bari C, Dell'Accio F, Tylzanowski P, Luyten FP. (2001). Multipotent mesenchymal stem cells from adult human synovial membrane. *Arthritis Rheum*. 44(8):1928-42.

Defrance T, Vanbervliet B, Briere F, Durand I, Rousset F, Banchereau J. (1992). Interleukin 10 and transforming growth factor beta cooperate to induce anti-CD40-activated naive human B cells to secrete immunoglobulin A. *J Exp Med*. 175(3):671–82.

DelaRosa O, Lombardo E, Beraza A, Mancheño-Corvo P, Ramirez C, Menta R, Rico L, Camarillo E, García L, Abad JL, Trigueros C, Delgado M, Büscher D. (2009). Requirement of IFN-gamma-mediated

indoleamine 2,3-dioxygenase expression in the modulation of lymphocyte proliferation by human adipose-derived stem cells. *Tissue Eng Part A*. 15(10):2795-806.

Dewald O, Zymek P, Winkelmann K, Koerting A, Ren G, Abou-Khamis T, Michael LH, Rollins BJ, Entman ML, Frangogiannis NG (2005). CCL2/Monocyte Chemoattractant Protein-1 regulates inflammatory responses critical to healing myocardial infarcts. *Circ Res*. 96:881-9.

De Young LM, Kheifets JB, Ballaron SJ, Young JM. (1989). Edema and cell infiltration in the phorbol ester-treated mouse ear are temporally separate and can be differentially modulated by pharmacologic agents. *Agents Actions*. 26(3-4):335-41.

Díaz-Muñoz MD, Osma-Garcia IC, Cacheiro-Llaguno C, Fresno M, Iñiguez MA. (2010). Coordinated up-regulation of cyclooxygenase-2 and microsomal prostaglandin E synthase 1 transcription by nuclear factor kappa B and early growth response-1 in macrophages. *Cell Signal*. 22(10):1427-36.

Dominici M, Le Blanc K, Mueller I, Slaper-Cortenbach I, Marini F, Krause D, Deans R, Keating A, Prockop DJ, Horwitz E. (2006). Minimal criteria for defining multipotent mesenchymal stromal cells. The International Society for Cellular Therapy position statement. *Cytotherapy*. 8(4):315-7.

Donlon TA, Krensky AM, Wallace MR, Collins FS, Lovett M, Clayberger C. (1990). Localization of a human T-cell-specific gene, RANTES (D17S136E), to chromosome 17q11.2-q12. *Genomics*. 6(3):548-53.

Doughty MJ, Bergmanson JP, Blocker Y. (1997). Shrinkage and distortion of the rabbit corneal endothelial cell mosaic caused by a high osmolality glutaraldehyde-formaldehyde fixative compared to glutaraldehyde. *Tissue Cell*. 29(5):533-47.

Duffy MM, Pindjakova J, Hanley SA, McCarthy C, Weidhofer GA, Sweeney EM, English K, Shaw G, Murphy JM, Barry FP, Mahon BP, Belton O, Ceredig R, Griffin MD. (2011). Mesenchymal stem cell inhibition of T-helper 17 cell- differentiation is triggered by cell-cell contact and mediated by prostaglandin E2 via the EP4 receptor. *Eur J Immunol*. 41:2840-51.

Duggal S, Brinchmann JE. (2011). Importance of serum source for the in vitro replicative senescence of human bone marrow derived mesenchymal stem cells. *J Cell Physiol*. 226(11):2908-15.

Dupont N, Jiang S, Pilli M, Ornatowski W, Bhattacharya D, Deretic V. (2011). Autophagy-based unconventional secretory pathway for extracellular delivery of IL-1β. *EMBO J*. 30(23):4701-11.

Elliott MR, Chekeni FB, Trampont PC, Lazarowski ER, Kadl A, Walk SF, Park D, Woodson RI, Ostankovich M, Sharma P, Lysiak JJ, Harden TK, Leitinger N, Ravichandran KS. (2009). Nucleotides released by apoptotic cells act as a find-me signal for phagocytic clearance. *Nature*. 461:282-6.

Elliott DE, Siddique SS. (2014). Weinstock JV. Innate immunity in disease. *Clin Gastroenterol Hepatol*. 12(5):749-55.

Elshabrawy HA, Essani AE, Szekanecz Z, Fox DA, Shahrara S. (2017). TLRs, future potential therapeutic targets for RA. *Autoimmun Rev*. 16:103-13.

Erices A, Conget P, Minguell JJ. (2000). Mesenchymal progenitor cells in human umbilical cord blood. *Br J Haematol*. 109(1):235-42.

Fell HB. (1925). The histogenesis of cartilage and bone in the long bones of the embryonic fowl. *J Morphol Physiol.* 40:417-59.

Fierabracci A, Del Fattore A, Muraca M. (2016). The Immunoregulatory activity of mesenchymal stem cells: 'State of Art' and 'Future Avenues'. *Curr Med Chem*. 23(27):3014-24.

Fiorentino DF, Zlotnik A, Mosmann TR, Howard M, O'Garra A. (1991). IL-10 inhibits cytokine production by activated macrophages. *J Immunol*. 147(11):3815-22.

Fischer-Posovszky P, Newell FS, Wabitsch M, Tornqvist HE. (2008). Human SGBS cells - a unique tool for studies of human fat cell biology. *Obes Facts*. 1(4):184-9.

Fonseca JE, Santos MJ, Canhão H, Choy E. (2009). Interleukin-6 as a key player in systemic inflammation and joint destruction. *Autoimmun Rev*. 8(7):538-42.

Ford-Hutchinson AW, Bray MA, Doig MV, Shipley ME, Smith MJ. (1980) Leukotriene B, a potent chemokinetic and aggregating substance released from polymorphonuclear leukocytes. *Nature*. 286:264-5.

Frese L, Dijkman PE, Hoerstrup SP. Adipose tissue-derived stem cells in regenerative medicine. (2016). *Transfus Med Hemother*. 43(4):268-74.

Friedenstein AJ. (1990). Osteogenic stem cells in bone marrow. In: Heersche JNM, Kanis JA, editors. Bone and Mineral Research. *Amsterdam: Elsevier*. 243–272.

Funk CD. (2001). Prostaglandins and leukotrienes: advances in eicosanoid biology. *Science*. 294(5548), 1871-5.

García-Olmo D, García-Arranz M, Herreros D, Pascual I, Peiro C, Rodríguez-Montes JA. (2005). A phase I clinical trial of the treatment

of Crohn's fistula by adipose mesenchymal stem cell transplantation. *Dis Colon Rectum*. 48(7):1416-23**.**

García-Olmo D, Herreros D, Pascual M, Pascual I, De-La-Quintana P, Trebol J, Garcia-Arranz M. (2009) Treatment of enterocutaneous fistula in Crohn's Disease with adipose-derived stem cells: a comparison of protocols with and without cell expansion. *Int J Colorectal Dis*. 24(1):27-30.

Gatti S, Beck J, Fantuzzi G, Bartfai T, Dinarello CA. (2002). Effect of interleukin-18 on mouse core body temperature. *Am J Physiol Regul Integr Comp Physiol*. 282(3):R702-9.

Gaudreault E, Paquet-Bouchard C, Fiola S, Le Bel M, Lacerte P, Shio MT, Olivier M, Gosselin J. (2012). TAK1 contributes to the enhanced responsiveness of LTB (4)-treated neutrophils to Toll-like receptor ligands. *Int Immunol*. 24(11):693-704.

Getting SJ, Mahoney DJ, Cao T, Rugg MS, Fries E, Milner CM, Perretti M, Day AJ. (2002). The link module from human TSG-6 inhibits neutrophil migration in a hyaluronan- and interalpha -inhibitor-independent manner. *J Biol Chem*. 277(52):51068-76.

Gijsbers K, Van Assche G, Joossens S, Struyf S, Proost P, Rutgeerts P, Geboes K, Van Damme J. (2004). CXCR1-binding chemokines in inflammatory bowel diseases: down-regulated IL-8/CXCL8 production by leukocytes in Crohn's disease and selective GCP-2/CXCL6 expression in inflamed intestinal tissue. *Eur J Immunol*. 34(7):1992-2000.

Glenn JD, Whartenby KA. (2014). Mesenchymal stem cells: Emerging mechanisms of immunomodulation and therapy. *World J Stem Cells*. 6(5):526-39.

Gnecchi M, Danieli P, Malpasso G, Ciuffreda MC. (2016). Paracrine mechanisms of mesenchymal stem cells in tissue repair. *Methods in Molecular Biology*.1416:123-46.

Gnecchi M, He H, Noiseux N, Liang OD, Zhang L, Morello F, Mu H, Melo LG, Pratt RE, Ingwall JS, Dzau VJ. (2006). Evidence supporting paracrine hypothesis for Akt-modified mesenchymal stem cell-mediated cardiac protection and functional improvement. *FASEB J*. 20(6):661-9.

Gnecchi M, Zhang Z, Ni A, Dzau VJ. (2008). Paracrine mechanisms in adult stem cell signaling and therapy. *Circ Res*. 103(11):1204-19.

Gombault A, Baron L, Couillin I. (2012). ATP release and purinergic signaling in NLRP3 inflammasome activation. *Front Immunol*. 3:414.

González-Rey E, Anderson P, González MA, Rico L, Büscher D, Delgado M. (2009). Human adult stem cells derived from adipose tissue protect against experimental colitis and sepsis. *Gut*. 58(7):929-39.

Gouwy M, Struyf S, Catusse J, Proost P, Van Damme J. (2004). Synergy between proinflammatory ligands of G protein-coupled receptors in neutrophil activation and migration. *J Leukoc Biol*. 76(1):185-94.

Gouwy M, Struyf S, Noppen S, Schutyser E, Springael JY, Parmentier M, Proost P, Van Damme J. (2008). Synergy between coproduced CC and CXC chemokines in monocyte chemotaxis through receptor-mediated events. *Mol Pharmacol*. 74(2):485-95.

Graf T. (2002). Differentiation plasticity of hematopoietic cells. *Blood*. 99(9):3089-101.

Greenberg S, Grinstein S. (2002). Phagocytosis and innate immunity. *Curr Opin Immunol*. 14(1):136-45.

Griffin GK, Newton G, Tarrio ML, Bu D-X, Maganto-Garcia E, Azcutia V, Alcaide P, Grabie N, Luscinskas FW, Croce KJ, Lichtman AH. (2012).

IL-17 and TNF-α sustain neutrophil recruitment during inflammation through synergistic effects on endothelial activation. *J Immunol*. 188(12):6287-99.

Grochot-Przeczek A, Dulak J, Jozkowicz A. (2012). Haem oxygenase-1: non-canonical roles in physiology and pathology. *Clin Sci (Lond)*. 122(3):93-103.

Harris SG, Padilla J, Koumas L, Ray D, Phipps RP. (2002). Prostaglandins as modulators of immunity. *Trends Immunol*. 23(3):144-50.

Hawkins CL, Davies MJ. (1998a). Degradation of hyaluronic acid, poly- and monosaccharides, and model compounds by hypochlorite: evidence for radical intermediates and fragmentation. *Free Radic Biol Med*. 24(9):1396-410.

Hawkins CL, Davies MJ. (1998b). Hypochlorite-induced damage to proteins: formation of nitrogen-centred radicals from lysine residues and their role in protein fragmentation. *Biochem J*. 332 (Pt 3):617-25.

Haynesworth SE, Baber MA, Caplan AI. (1996). Cytokine expression by human marrow-derived mesenchymal progenitor cells in vitro: effects of dexamethasone and IL-1 alpha. *J Cell Physiol*. 166(3):585-92.

Heinecke JW. (1999). Mechanisms of oxidative damage by myeloperoxidase in atherosclerosis and other inflammatory disorders. *Journal of Laboratory and Clinical Medicine*. 133:321-5.

Huang L, Zhao A, Wong F, Ayala JM, Struthers M, Ujjainwalla F, Wright SD, Springer MS, Evans J, Cui J. (2004). Leukotriene B4 strongly increases monocyte chemoattractant protein-1 in human monocytes. *Arterioscler Thromb Vasc Biol*. 24(10):1783-8.

Huber C, Stingl G. (1981). Macrophages in the regulation of immunity. *Haematol Blood Transfus*. 27:31-7.

Hurst SM, Wilkinson TS, McLoughlin RM, Jones S, Horiuchi S, Yamamoto N, Rose-John S, Fuller GM, Topley N, Jones SA. (2001). IL-6 and its soluble receptor orchestrate a temporal switch in the pattern of leukocyte recruitment seen during acute inflammation. *Immunity*. 14(6):705-14.

In't Anker PS, Scherjon SA, Kleijburg-van der Keur C, Noort WA, Claas FH, Willemze R, Fibbe WE, Kanhai HH. (2003). Amniotic fluid as a novel source of mesenchymal stem cells for therapeutic transplantation. *Blood*. 102(4):1548-9.

Ivanova-Todorova E, Bochev I, Mourdjeva M, Dimitrov R, Bukarev D, Kyurkchiev S, Tivchev P, Altunkova I, Kyurkchiev DS. (2009). Adipose tissue-derived mesenchymal stem cells are more potent suppressors of dendritic cells differentiation compared to bone marrow-derived mesenchymal stem cells. *Immunology Letters*. 126:37-42.

Ivanova-Todorova E, Bochev I, Dimitrov R, Belemezova K, Mourdjeva M, Kyurkchiev S, Kinov P, Altankova I, Kyurkchiev D. (2012). Conditioned medium from adipose tissue-derived mesenchymal stem cells induces CD4+FOXP3+ cells and increases IL-10 secretion. *J Biomed Biotechnol*. 2012:295167.

Jame AJ, Lackie PM, Cazaly AM, Sayers I, Penrose JF, Holgate ST, Sampson AP. (2007). Human bronchial epithelial cells express an active and inducible biosynthetic pathway for leukotrienes B4 and C4. *Clin Exp Allergy*. 37:880–892.

James AJ, Penrose JF, Cazaly AM, Holgate ST, Sampson AP. (2006). Human bronchial fibroblasts express the 5-lipoxygenase pathway. *Respir Res*. 7:102.

Jiang S, Dupont N, Castillo EF, Deretic V. (2013). Secretory versus degradative autophagy: unconventional secretion of inflammatory mediators. *J Innate Immun*. 5(5):471-9.

Johnstone RM, Adam M, Hammond JR, Orr L, Turbide C. (1987). Vesicle formation during reticulocyte maturation. Association of plasma membrane activities with released vesicles (exosomes). *J Biol Chem*. 262(19):9412-20.

Johnstone B, Hering TM, Caplan AI, Goldberg VM, Yoo JU. (1998). In vitro chondrogenesis of bone marrow-derived mesenchymal progenitor cells. *Exp Cell Res.* 238(1):265-72.

Jurado M, De La Mata C, Ruiz-Garcia A, Lopez-Fernandez E, Espinosa O, Remigia MJ, Moratalla L, Goterris R, García-Martín P, Ruiz-Cabello F, Garzón S, Pascual MJ, Espigado I, Solano C. (2017). Adipose tissue-derived mesenchymal stromal cells as part of therapy for chronic graft-versus-host disease: A phase I/II study. *Cytotherapy*. 19(8):927-936.

Kaczorowski DJ, Mollen KP, Edmonds R, Billiar TR. (2008). Early events in the recognition of danger signals after tissue injury. *J Leukoc Biol*. 83(3):546-52.

Karin M, Delhase M. (2000). The I kappa B kinase (IKK) and NF-kappaB: key elements of proinflammatory signalling. *Semin Immunol*. 12:85-98.

Kawai T, Akira S. (2010). The role of pattern-recognition receptors in innate immunity: update on Toll-like receptors. *Nat Immunol*. 11(5):373-84.

Keane MP, Strieter RM. (2000). Chemokine signaling in inflammation. *Crit Care Med*. 28(4 Suppl):N13-26.

Keeley EC, Mehrad B, Strieter RM. (2008). Chemokines as mediators of neovascularization. *Arterioscler Thromb Vasc Biol*. 28(11):1928-36.

Khatami M. (2008). 'Yin and Yang' in inflammation: duality in innate immune cell function and tumorigenesis. *Expert Opin Biol Ther*. 8:1461-72.

Khubutiya MS, Vagaboy AV, Temnov AA, Sklifas AN. (2014). Paracrine mechanisms of proliferative, anti-apoptotic and anti-inflammatory effects of mesenchymal stromal cells in models of acute organ injury. *Cytotherapy*. 16(5):579-85.

Kilroy GE, Foster SJ, Wu X, Ruiz J, Sherwood S, Heifetz A, Ludlow JW, Stricker DM, Potiny S, Green P, Halvorsen YD, Cheatham B, Storms RW, Gimble JM. (2007). Cytokine profile of human adipose-derived stem cells: expression of angiogenic, hematopoietic, and pro-inflammatory factors. *J Cell Physiol*. 212(3):702-9.

Klinke A, Nussbaum C, Kubala L, Friedrichs K, Rudolph TK, Rudolph V, Paust HJ, Schröder C, Benten D, Lau D, Szocs K, Furtmüller PG, Heeringa P, Sydow K, Duchstein HJ, Ehmke H, Schumacher U, Meinertz T, Sperandio M, Baldus S. (2011). Myeloperoxidase attracts neutrophils by physical forces. *Blood*. 117(4):1350-8.

Konala VB, Mamidi MK, Bhonde R, Das AK, Pochampally R, Pal R. (2016). The current landscape of the mesenchymal stromal cell secretome: A new paradigm for cell-free regeneration. *Cytotherapy*. 18(1):13-24.

Kotobuki N, Hirose M, Takakura Y, Ohgushi H. (2004). Cultured autologous human cells for hard tissue regeneration: preparation and characterization of mesenchymal stem cells from bone marrow. *Artif Organs*. 28(1):33-9.

Kowal J, Arras G, Colombo M, Jouve M, Morath JP, Primdal-Bengtson B, Dingli F, Loew D, Tkach M, Thery C. (2016). Proteomic comparison defines novel markers to characterize heterogeneous populations of extracellular vesicles subtypes. *Proc Natl Acad Sci U S A*. 113(8):E968-77.

Kronlage M, Song J, Sorokin L, Isfort K, Schwerdtle T, Leipziger J, Robaye B, Conley PB, Kim HC, Sargin S, Schön P, Schwab A, Hanley PJ.

(2010). Autocrine Purinergic Receptor Signaling Is Essential for Macrophage Chemotaxis. *Sci Signal*. 3:ra55.

Kuhns DB, Nelson EL, Alvord WG, Gallin JI. (2001). Fibrinogen induces IL-8 synthesis in human neutrophils stimulated with formyl-methionyl-leucyl-phenylalanine or leukotriene B (4). *J Immunol*. 167:2869-78.

Kukulski F, Ben Yebdri F, Lefebvre J, Warny M, Tessier PA, Sevigny J. (2007). Extracellular nucleotides mediate LPS-induced neutrophil migration in vitro and in vivo. *J Leukoc Biol*. 81:1269-75.

Kuraitis D, Giordano C, Ruel M, Musarò A, Suuronen EJ. (2012). Exploiting extracellular matrix-stem cell interactions: a review of natural materials for therapeutic muscle regeneration. *Biomaterials*. 33(2):428-43.

Kyurkchiev D, Bochev I, Ivanova-Todorova E, Mourdjeva M, Oreshkova T, Belemezova K, Kyurkchiev S. (2014). Secretion of immunoregulatory cytokines by mesenchymal stem cells. *World J Stem Cells*. 6(5):552-70.

Lavoie JR, Rosu-Myles M. (2013). Uncovering the secrets of mesenchymal stem cells. *Biochimie*. 95(12):2212-21.

Le Bel M, Brunet A, Gosselin J. (2014). Leukotriene B_4, an endogenous stimulator of the innate immune response against pathogens. *J Innate Immun*. 6(2):159-68.

Le Blanc K, Davies LC. (2015). Mesenchymal stromal cells and the innate immune response. *Immunol Lett*. 168(2):140-6.

Lee MJ, Kim J, Kim MY, Bae YS, Ryu SH, Lee TG, Kim JH. (2010). Proteomic analysis of tumor necrosis factor-alpha-induced secretome of human adipose tissue-derived mesenchymal stem cells. *J Proteome Res*. 9(4):1754-62.

Lee JK, Kim SH, Lewis EC, Azam T, Reznikov LL, Dinarello CA. (2004). Differences in signaling pathways by IL-1β and IL-18. *Proc Natl Acad Sci U S A*. 101(23):8815–20.

Lee RH, Pulin AA, Seo MJ, Kota DJ, Ylostalo J, Larson BL, Semprun-Prieto L, Delafontaine P, Prockop DJ. (2009). Intravenous hMSCs improve myocardial infarction in mice because cells embolized in lung are activated to secrete the anti-inflammatory protein TSG-6. *Cell Stem Cell*. 5:54–63.

Lener T, Gimona M, Aigner L, Börger V, Buzas E, Camussi G, Chaput N, Chatterjee D, Court FA, Del Portillo HA. (2015). Applying extracellular vesicles based therapeutics in clinical trials - an ISEV position paper. *J Extracell Vesicles*. 4:30087.

Leuschner F, Courties G, Dutta P, Mortensen LJ, Gorbatov R, Sena B, Novobrantseva TI, Borodovsky A, Fitzgerald K, Koteliansky V, Iwamoto Y, Bohlender M, Meyer S, Lasitschka F, Meder B, Katus HA, Lin C, Libby P, Swirski FK, Anderson DG, Weissleder R, Nahrendorf M. (2015). Silencing of CCR2 in myocarditis. *Eur Heart J*. 36(23):1478-88.

Li L, Du G, Wang D, Zhou J, Jiang G, Jiang H. (2017). Overexpression of heme oxygenase-1 in mesenchymal stem cells augments their protection on retinal cells in vitro and attenuates retinal ischemia/reperfusion injury in vivo against oxidative stress. *Stem Cells Int*. 2017:4985323.

Liew FY, Xu D, Brint EK, O'Neill LA. (2005). Negative regulation of toll-like receptor-mediated immune responses. *Nat Rev Immunol*. 5:446-58.

Lin J, Kakkar V, Lu X. (2014). Impact of MCP-1 in atherosclerosis. *Curr Pharm Des*. 20(28):4580-8.

Liu Z, Jiang Y, Li Y, Wang J, Fan L, Scott MJ, Xiao G, Li S, Billiar TR, Wilson MA, Fan J. (2013). TLR4 Signaling augments monocyte chemotaxis by regulating G protein-coupled receptor kinase 2 translocation. *J Immunol*. 191:857-64.

Lobb RJ, Becker M, Wen SW, Wong CS, Wiegmans AP, Leimgruber A, Möller A. (2015). Optimized exosome isolation protocol for cell culture supernatant and human plasma. *J Extracell Vesicles*. 4:27031.

Lötvall J, Hill AF, Hochberg F, Buzás EI, Di Vizio D, Gardiner C, Gho YS, Kurochkin IV, Mathivanan S, Quesenberry P, Sahoo S, Tahara H, Wauben MH, Witwer KW, Théry C. (2014). Minimal experimental requirements for definition of extracellular vesicles and their functions: a position statement from the International Society for Extracellular Vesicles. *J Extracell Vesicles*.3:26913.

Lu YC, Yeh WC, Ohashi PS. (2008). LPS/TLR4 signal transduction pathway. *Cytokine*.42(2):145-151.

MacMicking J, Xie QW, Nathan C. (1997). Nitric oxide and macrophage function. *Annu Rev Immunol*. 15:323-50.

Madrigal M, Rao KS, Riordan NH. (2014). A review of therapeutic effects of mesenchymal stem cell secretions and induction of secretory modification by different culture methods. *J Transl Med*. 12:260.

Maguire G. (2013). Stem cell therapy without the cells. *Commun Integr Biol*. 6(6):e26631.

Martínez-Colon GJ, Moore BB. (2018). Prostaglandin E_2 as a regulator of immunity to pathogens. *Pharmacol Ther*. 185:135-46.

Marty V, Medina C, Combe C, Parnet P, Amedee T. (2005). ATP binding cassette transporter ABC1 is required for the release of interleukin-1beta by P2×7-stimulated and lipopolysaccharide-primed mouse Schwann cells. *Glia*. 49(4):511-9.

Matsushima K, Larsen CG, DuBois GC, Oppenheim JJ. (1989). Purification and characterization of a novel monocyte chemotactic and activating factor produced by a human myelomonocytic cell line. *J Exp Med*. 169(4):1485-90.

Matula Z, Nemeth A, Lorincz P, A, Brozik A, Buzas EI, Low P, Nemet K, Uher F, Urban VS. (2016). The role of extracellular vesicle and tunneling nanotube-mediated intercellular cross-talk between mesenchymal stem cells and human peripheral T cells. *Stem Cells Dev*. 25(23):1818-32.

Mehta VB, Hart J, Wewers MD. (2001). ATP-stimulated release of interleukin (IL)-1beta and IL-18 requires priming by lipopolysaccharide and is independent of caspase-1 cleavage. *J Biol Chem*. 276(6):3820-6.

Meng X, Ichim TE, Zhong J, Rogers A, Yin Z, Jackson J, Wang H, Ge W, Bogin V, Chan KW, Thébaud B, Riordan NH. (2007). Endometrial regenerative cells: a novel stem cell population. *J Transl Med*. 5:57.

Milner CM, Day AJ. (2003). TSG-6: a multifunctional protein associated with inflammation. *J Cell Sci*. 116(Pt10):1863-73.

Monsel A, Zhu YG, Gennai S, Hao Q, Hu S, Rouby JJ, Rosenzwajg M, Matthay MA, Lee JW. (2015). Therapeutic effects of human mesenchymal stem cell-derived micro-vesicles in severe pneumonia in mice. *Am J Respir Crit Care Med*. 192(3):324-36.

Moroney MA, Alcaraz MJ, Forder RA, Carey F, Hoult JR. (1988). Selectivity of neutrophil 5-lipoxygenase and cyclo-oxygenase inhibition by an anti-inflammatory flavonoid glycoside and related aglycone flavonoids. *J Pharm Pharmacol*. 40(11):787-92.

Morrison TJ, Jackson MV, Cunningham EK, Kissenpfennig A, McAuley DF, O'Kane CM, Krasnodembskaya AD. (2017). Mesenchymal stromal cells modulate macrophages in clinically relevant lung injury models by

extracellular vesicle mitochondrial transfer. *Am J Respir Crit Care Med*. 196:1275-86.

Mortaz E, Alipoor SD, Varahram M, Jamaati H, Garssen J, Mumby SE, Adcock IM. (2018). Exosomes in severe asthma: Update in their roles and potential in therapy. *Biomed Res Int*. 2018:2862187.

Mosser D, Zhang X. (2008). Interleukin-10: new perspectives on an old cytokine. *Immunol Rev.* 226:205-18.

Moser B, Clark-Lewis I, Zwahlen R, Baggiolini M. (1990). Neutrophil-activating properties of the melanoma growth-stimulatory activity. *J Exp Med*. 171(5):1797-802.

Murray RZ, Kay JG, Sangermani DG, Stow JL. (2005). A role for the phagosome in cytokine secretion. *Science*. 310(5753):1492-5.

Muzio M, Polentarutti N, Bosisio D, Prahladan MK, Mantovani A. (2000). Toll-like receptors: a growing family of immune receptors that are differentially expressed and regulated by different leukocytes. *J Leukoc Biol*. 67(4):450-6.

Netea MG, Van de Veerdonk FL, van der Meer JW, Dinarello CA, Joosten LA. (2015). Inflammasome-Independent Regulation of IL-1-Family Cytokines. *Annu Rev Immunol*. 33:49-77.

Nishimoto N, Kishimoto T. (2004). Inhibition of IL-6 for the treatment of inflammatory diseases. *Curr Opin Pharmacol*. 4(4):386-91.

Nordberg RC, Loboa EG. (2015). Our fat future: Translating adipose stem cell therapy. *Stem Cells Transl Med*. 4(9):974-9.

Nunes KP, de Oliveira AA, Mowry FE, Biancardi VC. (2018). Targeting TLR4 signaling pathways: can therapeutics pay the toll for hypertension? *Br J Pharmacol*. [Epub ahead of print].

Omori K, Kida T, Hori M, Ozaki H, Murata T. (2014). Multiple roles of the PGE_2 -EP receptor signal in vascular permeability. *Br J Pharmacol*. 171(21): 4879-89.

Oswald IP, Wynn TA, Sher A, James SL. (1992). Interleukin 10 inhibits macrophage microbicidal activity by blocking the endogenous production of tumor necrosis factor alpha required as a costimulatory factor for interferon gamma-induced activation. *Proc Natl Acad Sci USA*. 89(18):8676-80.

Pagan JK, Wylie FG, Joseph S, Widberg C, Bryant NJ, James DE, Stow JL. (2003). The t-SNARE syntaxin 4 is regulated during macrophage activation to function in membrane traffic and cytokine secretion. *Curr Biol*. 13(2):156-60.

Pelus LM, Fukuda S. (2006). Peripheral blood stem cell mobilization: the CXCR2 ligand GRObeta rapidly mobilizes hematopoietic stem cells with enhanced engraftment properties. *Exp Hematol*. 34(8):1010-20.

Perregaux DG and Gabel CA. (1998). Post-translational processing of murine IL-1: evidence that ATP-induced release of IL-1 alpha and IL-1 beta occurs via a similar mechanism. *J Immunol*. 160:2469-77.

Posadas I, Terencio MC, Guillen I, Ferrandiz ML, Coloma J, Paya M, Alcaraz MJ. (2000). Co-regulation between cyclo-oxygenase-2 and inducible nitric oxide synthase expression in the time-course of murine inflammation. *Naunyn Schmiedebergs Arch Pharmacol*. 361(1):98-106.

Prince LR, Whyte MK, Sabroe I, Parker LC. (2011). The role of TLRs in neutrophil activation. *Curr Opin Pharmacol*. 11(4):397-403.

Prockop DJ. (2013). Concise review: two negative feedback loops place mesenchymal stem/stromal cells at the center of early regulators of inflammation. *Stem Cells*. 31(10):2042-6.

Prokopowicz Z, Marcinkiewicz J, Katz DR, Chain BM. (2012). Neutrophil myeloperoxidase: soldier and statesman. *Arch Immunol Ther Exp (Warsz)*. 60(1):43-54.

Qu Y, Franchi L, Nunez G, Dubyak GR. (2007). Non-classical IL-1β secretion stimulated by P2×7 receptors is dependent on inflammasome activation and correlated with exosome release in murine macrophages. *J Immunol*. 179(3):1913-25.

Raposo G, Nijman HW, Stoorvogel W, Liejendekker R, Harding CV, Melief CJ, Geuze HJ. (1996). B lymphocytes secrete antigen-presenting vesicles. *J Exp Med*. 183(3):1161-72.

Raposo G, Stoorvogel W. (2013). Extracellular vesicles: exosomes, microvesicles, and friends. *J Cell Biol*. 200(4):373-83.

Ravikumar B, Futter M, Jahreiss L, Korolchuk VI, Lichtenberg M, Luo S, Massey DC, Menzies FM, Narayanan U, Renna M, Jimenez-Sanchez M, Sarkar S, Underwood B, Winslow A, Rubinsztein DC. (2009). Mammalian macroautophagy at a glance. *J Cell Sci*. 122(Pt 11):1707-11.

Riordan NH, Ichim TE, Min WP, Wang H, Solano F, Lara F, Alfaro M, Rodriguez JP, Harman RJ, Patel AN, Murphy MP, Lee RR, Minev B. (2009). Non-expanded adipose stromal vascular fraction cell therapy for multiple sclerosis. *J Transl Med*. 7:29.

Robbins PD, Dorronsoro A, Booker CN. (2016). Regulation of chronic inflammatory and immune processes by extracellular vesicles. *J Clin Invest*. 126:1173-80.

Roddy GW, Oh JY, Lee RH, Bartosh TJ, Ylostalo J, Coble K, Rosa RH Jr, Prockop DJ. (2011). Action at distance: systemactically administered adult stem/progenitor cells (MSCs) reduce inflammatory damage to the cornea without engraftment and primarily by secretion of TNF-α stimulated gene/protein 6. *Stem Cells*. 29(10):1572-9.

Rola-Pleszczynski M, Lemaire I. (1985). Leukotrienes augment interleukin 1 production by human monocytes. *J Immunol*. 135:3958-61.

Rosenblum JM, Shimoda N, Schenk AD, Zhang H, Kish DD, Keslar K, Farber JM, Fairchild RL. (2010). CXC chemokine ligand (CXCL) 9 and CXCL10 are antagonistic costimulation molecules during the priming of alloreactive T cell effectors. *J Immunol*. 184(7):3450-60.

Rousset F, Garcia E, Defrance T, Peronne C, Vezzio N, Hsu DH, Kastelein R, Moore KW, Banchereau J. (1992). Interleukin 10 is a potent growth and differentiation factor for activated human B lymphocytes. *Proc Natl Acad Sci U S A*. 89(5):1890-3

Sadik CD, Kim ND, Luster AD. (2011). Neutrophils cascading their way to inflammation. *Trends Immunol*. 32:452-60.

Samuelsson B, Funk CD. (1989). Enzymes involved in the biosynthesis of leukotriene B4. *J Biol Chem*. 264: 19469-72.

Sanjabi S, Oh SA, Li MO. (2017). Regulation of the immune response by TGF-beta: From conception to autoimmunity and infection. *Cold Spring Harb Perspect Biol*. 9:a022236.

Santos RC, Rico MA, Bartrons R, Pujol FV, Rosa JL, de Oliveira JR. (2011). The transcriptional activation of the cyclooxygenase-2 gene in zymosan-activated macrophages is dependent on NF-kappa B, C/EBP, AP-1, and CRE sites. *Inflammation*. 34:653-8

Scapini P, Lapinet-Vera JA, Gasperini S, Calzetti F, Bazzoni F, Cassatella MA. (2000). The neutrophil as a cellular source of chemokines. *Immunol Rev*. 177:195-203.

Scheller J, Chalaris A, Schmidt-Arras D, Rose-John S. (2011). The pro- and anti-inflammatory properties of the cytokine interleukin-6. *Biochim Biophys Acta*. 1813(5):878-88.

Schettler A, Thorn H, Jockusch BM, Tschesche H. (1991). Release of proteinases from stimulated polymorphonuclear leukocytes. Evidence for subclasses of the main granule types and their association with cytoskeletal components. *Eur J Biochem*. 197(1):197-202.

Schultz J, Kaminker K. (1962). Myeloperoxidase of the leucocyte of normal human blood. I. Content and localization. *Arch Biochem Biophys*. 96:465-7.

Serhan CN and Levy BD. (2018). Resolvins in inflammation: emergence of the pro-resolving superfamily of mediators. *J Clin Invest*. [Epub ahead of print].

Sheng J, Ruedl C, Karjalainen K. (2015). Most tissue-resident macrophages except microglia are derived from fetal hematopoietic stem cells. *Immunity*. 43(2):382-93.

Shevchenko A, Jensen ON, Podtelejnikov AV, Sagliocco F, Wilm M, Vorm O, Mortensen P, Shevchenko A, Boucherie H, Mann M. (1996). Linking genome and proteome by mass spectrometry: large-scale identification of yeast proteins from two dimensional gels. *Proc Natl Acad Sci U S A*. 93(25):14440-5.

Shi D, Liao L, Zhang B, Liu R, Dou X, Li J, Zhu X, Yu L, Chen D, Zhao RC. (2011). Human adipose tissue-derived mesenchymal stem cells facilitate the immunosuppressive effect of cyclosporin A on T lymphocytes through Jagged-1-mediated inhibition of NF-κB signaling. *Exp Hematol*. 39(2):214-224.e1.

Sinclair KA, Yerkovich ST, Hopkins PM, Chambers DC. (2016). Characterization of intercellular communication and mitochondrial donation by mesenchymal stromal cells derived from the human lung. *Stem Cell Res Ther*. 7(1):91.

Singer NG, Caplan AI. (2011). Mesenchymal stem cells: mechanisms of inflammation. *Annu Rev Pathol*. 6:457-78.

Smale ST. (2012). Dimer-specific regulatory mechanisms within the NF-kB family of transcription factors. *Immunol Rev*. 246(1):193-204.

Smith JB, Wadleigh DJ, Xia YR, Mar RA, Herschman HR, Lusis AJ. (2002). Cloning and genomic localization of the murine LPS-induced CXC chemokine (LIX) gene, Scyb5. *Immunogenetics*. 54(8):599-603.

Soehnlein O, Lindbom L, Weber C. (2009). Mechanisms underlying neutrophil-mediated monocyte recruitment. *Blood*. 114(21):4613-23.

Sotiropoulou PA, Perez SA, Salagianni M, Baxevanis CN, Papamichail M. (2006). Characterization of the optimal culture conditions for clinical scale production of human mesenchymal stem cells. *Stem Cells*. 24(2):462-71.

Sozzani S, Abbracchio MP, Annese V, Danese S, De Pita O, De Sarro G, Maione S, Olivieri I, Parodi A, Sarzi-Puttini P. (2014). Chronic inflammatory diseases: do immunological patterns drive the choice of biotechnology drugs? A critical review. *Autoimmunity*. 47(5):287-306.

Sperlagh B, Hasko G, Nemeth Z, Vizi ES. (1998). ATP released by LPS increases nitric oxide production in raw 264.7 macrophage cell line via P2Z/P2X7 receptors. *Neurochem Int*. 33(3):209-15.

Starckx S, Van den Steen PE, Wuyts A, Van Damme J, Opdenakker G. (2002). Neutrophil gelatinase B and chemokines in leukocytosis and stem cell mobilization. *Leuk Lymphoma*. 43(2):233-41.

Stow JL, Murray RZ. (2013). Intracellular trafficking and secretion of inflammatory cytokines. *Cytokine Growth Factor Rev*. 24(3):227-39.

Swirski FK, Nahrendorf M, Etzrodt M, Wildgruber M, Cortez-Retamozo V, Panizzi P, Figueiredo JL, Kohler RH, Chudnovskiy A, Waterman P, Aikawa E, Mempel TR, Libby P, Weissleder R, Pittet MJ. (2009). Identification of splenic reservoir monocytes and their deployment to inflammatory sites. *Science*. 325(5940):612-6.

Szanto S, Bardos T, Gal I, Glant TT, Mikecz K. (2004). Enhanced neutrophil extravasation and rapid progression of proteoglycan-induced arthritis in TSG-6-knockout mice. *Arthritis Rheum*. 50(9):312-22.

Takashima A, Yao Y. (2015). Neutrophil plasticity: acquisition of phenotype and functionality of antigen-presenting cell. *J Leukoc Biol*. 98(4):489-96.

Taylor PR, Martinez-Pomares L, Stacey M, Lin HH, Brown GD, Gordon S. (2005). Macrophage receptors and immune recognition. *Annu Rev Immunol*. 23:901-44.

Théry C, Amigorena S, Raposo G, Clayton A. (2006). Isolation and characterization of exosomes from cell culture supernatants and biological fluids. *Curr Protoc Cell Biol*. Chapter 3: Unit 3.22.

Ti D, Hao H, Tong C, Liu J, Dong L, Zheng J, Zhao Y, Liu H, Fu X, Han W. (2015). LPS-preconditioned mesenchymal stromal cells modify macrophage polarization for resolution of chronic inflammation via exosome-shuttled let-7b. *J Transl Med*. 13:308.

Timmers L, Lim SK, Arslan F, Armstrong JS, Hoefer IE, Doevendans PA, Piek JJ, El Oakley RM, Choo A, Lee CN, Pasterkamp G, de Kleijn DP. (2007). Reduction of myocardial infarct size by human mesenchymal stem cell conditioned medium. *Stem Cell Res*. 1(2):129-37.

Tkach M, Kowal J, Zucchetti AE, Enserink L, Jouve M, Lankar D, Saitakis M, Martin-Jaular L, Théry C. (2017). Qualitative differences in T-cell activation by dendritic cell-derived extracellular vesicle subtypes. *EMBO J*. 36(20):3012-3028.

Tofiño-Vian M, Guillen MI, Perez Del Caz MD, Silvestre A, Alcaraz MJ. (2018). Microvesicles from human adipose tissue-derived mesenchymal stem cells as a new protective strategy in osteoarthritic chondrocytes. *Cell Physiol Biochem*. 47(1):11-25.

Tögel F, Hu Z, Weiss K, Isaac J, Lange C, Westenfelder C. (2005). Administered mesenchymal stem cells protect against ischemic acute renal failure through differentiation-independent mechanisms. *Am J Physiol Renal Physiol*. 289(1):F31-F42.

Uccelli A, Moretta, L, Pistoia V. (2008). Mesenchymal stem cells in health and disease. *Nature Rev. Immunol*. 8(9):726-36.

Ulevitch RJ, Tobias PS. (1995). Receptor-dependent mechanisms of cell stimulation by bacterial endotoxin. *Annu Rev Immunol*. 13:437-57.

Van Coillie E, Van Damme J, Opdenakker G. (1999). The MCP/eotaxin subfamily of CC chemokines. *Cytokine Growth Factor Rev*. 10(1):61-86.

Van Damme J, Struyf S, Opdenakker G. (2004). Chemokine-protease interactions in cancer. *Semin Cancer Biol*. 14(3):201-8.

Van de Veerdonk FL, Netea MG. (2013). New insights in the immunobiology of IL-1 family members. *Front Immunol*. 4:167.

Varma MJ, Breuls RG, Schouten TE, Jurgens WJ, Bontkes HJ, Schuurhuis GJ, van Ham SM, van Milligen FJ. (2007). Phenotypical and functional characterization of freshly isolated adipose tissue-derived stem cells. *Stem Cells Dev*. 16(1):91-104.

Varol C, Mildner A, Jung S. (2015). Macrophages: development and tissue specialization. *Annu Rev Immunol*. 33:643-75.

Varzaneh FN, Keller B, Unger S, Aghamohammadi A, Warnatz K, Rezaei N. (2014). Cytokines in common variable immunodeficiency as signs of immune dysregulation and potential therapeutic targets -a review of the current knowledge. *J Clin Immunol*. 34(5):524-43.

Vicente AM, Guillén MI, Alcaraz MJ. (2001). Modulation of haem oxigenase-1 expression by nitric oxide and leukotrienes in zymosan-activated macrophages. *Br J Pharmacol*. 133(6):920-6.

Vicente AM, Guillen MI, Alcaraz MJ. (2003). Participation of heme oxygenase-1 in a model of acute inflammation. *Exp Biol Med*. 228(5):514-6.

Vieira SM, Lemos HP, Grespan R, Napimoga MH, Dal-Secco D, Freitas A, Cunha TM, Verri WA Jr, Souza-Junior DA, Jamur MC, Fernandes KS, Oliver C, Silva JS, Teixeira MM, Cunha FQ. (2009). A crucial role for TNF-α in mediating neutrophil influx induced by endogenously generated or exogenous chemokines, KC/CXCL1 and LIX/CXCL5. *Br J Pharmacol*. 158(3):779-89.

Wabitsch M, Brenner RE, Melzner I, Braun M, Möller P, Heinze E, Debatin KM, Hauner H. (2001). Characterization of a human preadipocyte cell strain with high capacity for adipose differentiation. *Int J Obes Relat Metab Disord*. 25(1):8-15.

Wang D, Dubois RN. (2010). Eicosanoids and cancer. *Nat Rev Cancer*. 10(3), 181-93.

Watt FM, Hogan BL. (2000). Out of eden: Stem cells and their niches. *Science*. 287:1427-30.

Weiss SJ. (1989). Tissue destruction by neutrophils. *N Engl J Med*. 320(6):365-76.

Willms E, Cabanas C, Mager I, Wood MJA, Vader P. (2018). Extracellular vesicle heterogeneity: Subpopulations, isolation techniques, and diverse functions in cancer progression. *Front Immunol*. 9:738.

Wisniewski HG, Hua JC, Poppers DM, Naime D, Vilcek J, Cronstein BN. (1996). TNF/IL-1-inducible protein TSG-6 potentiates plasmin

inhibition by inter-alpha-inhibitor and exerts a strong anti-inflammatory effect in vivo. *J Immunol*. 156(4):1609-15.

Yang F, Feng C, Zhang X, Lu J, Zhao Y. (2017). The diverse biological functions of neutrophils, beyond the defence against infections. *Inflammation*. 40(1):311-323.

Zent CS, Elliott MR. (2017). Maxed out macs: physiologic cell clearance as a function of macrophage phagocytic capacity. *FEBS J*. 284(7):1021-39.

Zhang L, LiWang PJ. (2014). Chemokine-receptor interactions: solving the puzzle, piece by piece. *Structure*. 22(11):1550-2.

Zhang ZH, Zhu W, Ren HZ, Zhao X, Wang S, Ma HC, Shi XL. (2017). Mesenchymal stem cells increase expression of heme oxygenase-1 leading to anti-inflammatory activity in treatment of acute liver failure. *Stem Cell Res Ther*. 8(1):70.

Zitvogel L, Regnault A, Lozier A, Wolfers J, Flament C, Tenza D, Ricciardi- Castagnoli P, Raposo G, Amigorena S. (1998). Eradication of established murine tumors using a novel cell-free vaccine: dendritic cell-derived exosomes. *Nat Med*. 4:594-600.

Zuk PA, Zhu M, Mizuno H, Huang J, Futrell JW, Katz AJ, Benhaim P, Lorenz HP, Hedrick MH. (2001). Multilineage cells from human adipose tissue: implications for cell-based therapies. *Tissue Eng*. 7:211-228.

Annex

List of figures

Introduction

Material and Methods

Results

VNIVERSITAT
D VALÈNCIA
Vicerectorat d'Investigació i Política Científica

D. Fernando A. Verdú Pascual, Profesor Titular de Medicina Legal y Forense, y Secretario del Comité Ético de Investigación en Humanos de la Comisión de Ética en Investigación Experimental de la Universitat de València,

CERTIFICA:

Que el Comité Ético de Investigación en Humanos, en la reunión celebrada el día 10 de febrero de 2014, una vez estudiado el proyecto de investigación titulado:
"Mecanismos celulares reguladores de la respuesta inflamatoria en patologías articulares crónicas", número de procedimiento H1389967869063,
cuya investigadora responsable es Dña. Mª José Alcaraz Tormo,
ha acordado informar favorablemente el mismo dado que se respetan los principios fundamentales establecidos en la Declaración de Helsinki, en el Convenio del Consejo de Europa relativo a los derechos humanos y cumple los requisitos establecidos en la legislación española en el ámbito de la investigación biomédica, la protección de datos de carácter personal y la bioética.

Y para que conste, se firma el presente certificado en Valencia, a once de febrero de dos mil catorce.

FERNANDO ALEJO|VERDU| PASCUAL
2014.02.11
11:26:13 +01'00'

GENERALITAT VALENCIANA

Unión Europea

DIRECCIÓN GENERAL DE PRODUCCIÓN AGRARIA Y GANADERÍA

Ciutat Administrativa 9 d'Octubre
Castán Tobeñas, 77. Edif. B3 P2 46018 VALENCIA

AUTORIZACION PROCEDIMIENTO 2015/VSC/PEA/00113

Vista la solicitud realizada en fecha **07/04/15** con nº reg. entrada **5773** por D/Dª. **Pilar Campins Falcó**, Vicerrectora de Investigación y Política Científica, centro usuario **ES460780001001**, para realizar el procedimiento:

"Bolsa de aire en ratón inducida por zimosán "

Teniendo en cuenta la documentación aportada, según se indica en el artículo 33, punto 5 y 6, y puesto que dicho procedimiento se halla sujeto a autorización en virtud de lo dispuesto en el artículo 31 del Real Decreto 53/2013, de 1 de febrero,

Vista la propuesta del jefe del servicio de Sanidad y Bienestar Animal.

AUTORIZO:

la realización de dicho procedimiento al que se le asigna el código: **2015/VSC/PEA/00113** tipo **2**, de acuerdo con las características descritas en la propia documentación para el número de animales, especie y periodo de tiempo solicitado. Todo ello sin menoscabo de las autorizaciones pertinentes, por otras Administraciones y entidades, y llevándose a cabo en las siguientes condiciones:

Usuario: **Universidad de Valencia**

Responsable del proyecto: **Mª Luisa Ferrándiz Manglano**

Establecimiento: **Animalario Facultad de Farmacia SCSIE Burjassot**

Necesidad de evaluación restrospectiva:

Condiciones específicas:

Observaciones:

Valencia a, 19 de mayo de 2015

El director general de Producción Agraria y Ganadería

José Miguel Ferrer Arranz

30 anys d'identitat
GENERALITAT VALENCIANA

Unión Europea

DIRECCIÓN GENERAL DE PRODUCCIÓN AGRARIA Y GANADERÍA
Ciutat Administrativa 9 d'Octubre
Castán Tobeñas, 77. Edif. B3 P2 46018 VALENCIA

AUTORIZACION PROCEDIMIENTO 2014 / 020 / UVEG / 031

Vista la solicitud realizada en fecha 21 de febrero de 2014 con nº reg. entrada 2748 por D. Pedro M. Carrasco Sorli Vicerrector de Investigación y Política Científica de la Universidad de Valencia, centro usuario **ES46250 0001010**, para realizar el procedimiento:

"Mecanismos celulares reguladores de la respuesta inflamatoria en patologías articulares crónicas"

Teniendo en cuenta la documentación aportada, según se indica en el artículo 33, punto 5 y 6, y puesto que dicho procedimiento se halla sujeto a autorización en virtud de lo dispuesto en el artículo 31 del Real Decreto 53/2013, de 1 de febrero,

Vista la propuesta del jefe del servicio de Sanidad y Bienestar Animal

AUTORIZO:

la realización de dicho procedimiento al que se le asigna el código: **2014/020/UVEG/031 tipo 2**, de acuerdo con las características descritas en la propia documentación para el número de animales, especie y periodo de tiempo solicitado. Todo ello sin menoscabo de las autorizaciones pertinentes, por otras Administraciones y entidades, y llevándose a cabo en las siguientes condiciones:

Usuario: **Universidad de Valencia-Estudio General**

Responsable del proyecto: **Mª Luisa Ferrándiz Manglano**

Establecimiento: **Animalario de mamífero superior**

Necesidad de evaluación restrospectiva:

Condiciones específicas:

Observaciones:

Valencia a, 14 de marzo de 2014

El director general de Producción Agraria y Ganadería

José Miguel Ferrer Arranz

GENERALITAT VALENCIANA

Unión Europea

DIRECCIÓN GENERAL DE AGRICULTURA, GANADERÍA Y PESCA

AUTORIZACION PROCEDIMIENTO 2015/VSC/PEA/00254

Vista la solicitud realizada en fecha **18/12/15** con nº reg. entrada **28308** por D/Dª. **Pilar Campins Falcó**, Vicerrectora d' Investigació i Política Científica, centro usuario **ES460780001001**, para realizar el procedimiento:

"Obtención y caracterización de células madre mesenquimales en tejido adiposo de ratón "

Teniendo en cuenta la documentación aportada, según se indica en el artículo 33, punto 5 y 6, y puesto que dicho procedimiento se halla sujeto a autorización en virtud de lo dispuesto en el artículo 31 del Real Decreto 53/2013, de 1 de febrero.

Vista la propuesta del jefe del servicio de Ganadería y Sanidad y Bienestar Animal.

AUTORIZO:

la realización de dicho procedimiento al que se le asigna el código: **2015/VSC/PEA/00254** tipo **2**, de acuerdo con las características descritas en la propia documentación para el número de animales, especie y periodo de tiempo solicitado. Todo ello sin menoscabo de las autorizaciones pertinentes, por otras Administraciones y entidades, y llevándose a cabo en las siguientes condiciones:

Usuario: **Universidad de Valencia-Estudio General**

Responsable del proyecto: **M Luisa Ferrándiz Manglano**

Establecimiento: **Animalario Facultad de Farmacia SCSIE Burjassot**

Necesidad de evaluación restrospectiva:

Condiciones específicas:

Observaciones:

Valencia a, 12 de enero de 2016

El director general de Agricultura, Ganadería y Pesca

Rogelio Llanes Ribas

GENERALITAT VALENCIANA

CONSELLERIA DE AGRICULTURA, MEDIO AMBIENTE, CAMBIO CLIMÁTICO Y DESARROLLO RURAL

DIRECCIÓN GENERAL DE AGRICULTURA, GANADERÍA Y PESCA

Unión Europea

AUTORIZACION PROCEDIMIENTO 2015/VSC/PEA/00253

Vista la solicitud realizada en fecha **18/12/15** con nº reg. entrada **28308** por D/Dª. **Pilar Campins Falcó**, Vicerrectora d' Investigació i Política Científica, centro usuario **ES460780001001**, para realizar el procedimiento:

"Modelo de inflamación aguda por bolsa de aire en ratón (MAP) "

Teniendo en cuenta la documentación aportada, según se indica en el artículo 33, punto 5 y 6, y puesto que dicho procedimiento se halla sujeto a autorización en virtud de lo dispuesto en el artículo 31 del Real Decreto 53/2013, de 1 de febrero,

Vista la propuesta del jefe del servicio de Ganadería y Sanidad y Bienestar Animal.

AUTORIZO:

la realización de dicho procedimiento al que se le asigna el código: **2015/VSC/PEA/00253** tipo **2**, de acuerdo con las características descritas en la propia documentación para el número de animales, especie y periodo de tiempo solicitado. Todo ello sin menoscabo de las autorizaciones pertinentes, por otras Administraciones y entidades, y llevándose a cabo en las siguientes condiciones:

Usuario: **Universidad de Valencia-Estudio General**

Responsable del proyecto: **M Luisa Ferrándiz Manglano**

Establecimiento: **Animalario Facultad de Farmacia SCSIE Burjassot**

Necesidad de evaluación restrospectiva:

Condiciones específicas:

Observaciones:

Valencia a, 12 de enero de 2016

El director general de Agricultura, Ganadería y Pesca

Rogelio Llanes Ribas